DOKUZ EYLÜL UNIVERSITY
GRADUATE SCHOOL OF NATURAL AND APPLIED SCIENCES

SYNTHESIS AND CHARACTERIZATION OF NANOSTRUCTURES FOR ASSAY OF PHYSIOLOGICALLY IMPORTANT BIOLOGICAL MOLECULES

by
Tülden İNANAN

January, 2015
İZMİR

SYNTHESIS AND CHARACTERIZATION OF NANOSTRUCTURES FOR ASSAY OF PHYSIOLOGICALLY IMPORTANT BIOLOGICAL MOLECULES

A Thesis Submitted to the
Graduate School of Natural and Applied Sciences of Dokuz Eylül University
In Partial Fulfillment of the Requirements for the Degree of Doctor of Philosophy in Chemistry

by
Tülden İNANAN

January, 2015
İZMİR

Ph.D. THESIS EXAMINATION RESULT FORM

We have read the thesis entitled **"SYNTHESIS AND CHARACTERIZATION OF NANOSTRUCTURES FOR ASSAY OF PHYSIOLOGICALLY IMPORTANT BIOLOGICAL MOLECULES"** completed by **TÜLDEN İNANAN** under supervision of **PROF. DR. M. NALAN TÜZMEN** and we certify that in our opinion it is fully adequate, in scope and in quality, as a thesis for the degree of Doctor of Philosophy.

Prof. Dr. M. Nalan TÜZMEN

Supervisor

Prof. Dr. Sinan AKGÖL

Thesis Committee Member

Assoc. Prof. Serap SEYHAN BOZKURT

Thesis Committee Member

Prof. Dr. Adil DENİZLİ

Examining Committee Member

Assist. Prof. Dr. Aylin ALBAYRAK

Examining Committee Member

Prof.Dr. Ayşe OKUR

Director

Graduate School of Natural and Applied Sciences

ACKNOWLEDGEMENTS

First, I offer my sincerest gratitude to my supervisor, Prof. Dr. M. Nalan TÜZMEN, for her excellent guidance, support and caring both for my thesis and about life.

Besides my supervisor, I would like to thank the rest of my thesis committee: Prof. Dr. Melek MERDİVAN, Prof. Dr. Sinan AKGÖL, and Assoc. Prof. Dr. Serap Seyhan BOZKURT, for their helps, encouragement, insightful comments. I also would like to thank Prof. Dr. Adil DENİZLİ for his valuable guidance and suggestion.

This thesis was financially supported by the Scientific Research Projects Coordination of Dokuz Eylul University with project number: 2012-KBFEN-107.

Many thanks also goes to my friends from Biorege Research group. I have many friends, supported and helped me during my Thesis, that I cannot order their names here.

Also, I am grateful to all my family for their encouragement and understanding. I offer my foremost gratefulness to my mother, Tülin KALBURCU. I wish she could stand by me in these days. Finally, I offer my heartfelt thanks to my husband, Burak Evren İNANAN. He was always there cheering me up and stood by me through the good and bad times.

Tülden İNANAN

SYNTHESIS AND CHARACTERIZATION OF NANOSTRUCTURES FOR ASSAY OF PHYSIOLOGICALLY IMPORTANT BIOLOGICAL MOLECULES

ABSTRACT

Molecular imprinted polymeric (MIP) nanospheres specific to cholesterol were prepared by surfactant free emulsion polymerization of 2-hydroxyethyl methacrylate (HEMA) and pre-polymerization complexes. Pre-polymerization complexes were prepared using cholesterol and N-methacryloyl-(L)-phenyl alanine (MAPA) with 1:1, 1:3 and 3:1 monomer:template ratios. Pre-polymerization complexes and synthesized MIP-nanospheres were characterized with several characterization methods such as UV-vis, FTIR spectroscopies and NMR, SEM and Zeta size analyses. Template removal was efficiently succeeded by washing with methanol and tetrahydrofuran (THF). Adsorption performances of cholesterol imprinted polymeric nanospheres were compared in methanol and gastrointestinal mimicking solution (GIMS). It was determined that cholesterol imprinted polymeric nanospheres with monomer:template ratio 1:1 (CP) was more convenient for cholesterol imprinting. Optimization of cholesterol adsorption was performed with CP nanospheres by determining the effects of parameters such as time, polymer amount, initial cholesterol concentration, temperature, and ionic strength. Maximum adsorption capacity of CP nanospheres (714.17 mg per g nanospheres) was determined higher than the one of MIPs in the previous studies. Desorption of cholesterol from CP nanospheres were performed with methanol:acetic acid (80:20) by 86 percentage. Cholesterol removal percentage of CP nanospheres from hypercholesterolemic plasma was determined to be relatively high. Finally, selectivity coefficient and relative selectivity values indicated that imprinted polymeric nanospheres adsorbed cholesterol selectively compared to its analogues and adsorbed cholesterol selectively as regards to non-imprinted polymeric nanospheres.

Keywords: Cholesterol, molecular imprinting, nanostructures, adsorption, GIMS, human plasma, selectivity

FİZYOLOJİK ÖNEMİ OLAN BİYOLOJİK MOLEKÜLLERİN TAYİNİ AMAÇLI NANOYAPILARIN SENTEZİ VE KARAKTERİZASYONU

ÖZ

Kolesterole özgül moleküler baskılanmış polimerik (MIP) nanoyapılar, 2-hidroksietil metakrilat (HEMA) ve ön-polimerizasyon komplekslerinin yüzey aktif madde içermeyen emülsiyon polimerizasyonu ile hazırlanmıştır. Ön-polimerizasyon kompleksleri, kolesterol ve N-metakriloil-(L)-fenil alanin (MAPA) kullanılarak 1:1, 1:3 ve 3:1 monomer:kalıp oranlarıyla hazırlanmıştır. Ön-polimerizasyon kompleksleri ve sentezlenen MIP-nanoyapıları, UV-vis, FTIR spektroskopileri ve SEM, NMR, Zeta boyut analizleri gibi çeşitli karakterizasyon yöntemleri kullanılarak karakterize edilmiştir. Kalıp uzaklaştırma, metanol ve tetrahidrofuran (THF) yıkamaları ile verimli bir şekilde başarılmıştır. Kolesterol baskılanmış polimerik nanoyapıların adsorpsiyon etkinlikleri metanol ve yapay gastrointestinal sıvısı (GIMS) içerisinde karşılaştırılmıştır. Monomer:kalıp 1:1 oranına sahip kolesterol baskılanmış polimerik nanoyapıların (CP), kolesterol baskılanması için daha uygun olduğu belirlenmiştir. CP nanoyapıları ile kolesterol adsorpsiyonunun optimizasyonu, süre, polimer miktarı, başlangıç kolesterol derişimi, sıcaklık ve iyonik şiddet gibi parametrelerin etkisi incelenerek gerçekleştirilmiştir. CP nanoyapılarının maksimum adsorpsiyon kapasitesinin (g nanoyapı başına 714.17 mg), daha önceki çalışmalardaki MIP'lerinkinden daha yüksek olduğu belirlenmiştir. CP nanoyapılarından kolesterol desorpsiyonu metanol:asetik asit (80:20) ile yüzde 86 oranında gerçekleştirilmiştir. CP nanoyapılarının hiperkolesterolemik plazmadan kolesterol uzaklaştırma yüzdesinin oldukça yüksek olduğu belirlenmiştir. Son olarak, seçicilik katsayıları ve bağıl seçicilik değerleri, baskılanmış polimerik nanoyapıların kolesterolü analoglarına göre ve baskılanmış polimerik nanoyapıların baskılanmamış polimerik nanoyapılara göre daha seçici adsorpladığını kanıtlamaktadır.

Anahtar Kelimeler: Kolesterol, moleküler baskılama, nanoyapılar, adsorpsiyon, GIMS, insan plazması, seçicilik

CONTENT

Page

LIST OF FIGURES

Page

LIST OF TABLES

Page

CHAPTER ONE
INTRODUCTION

1.1 Cholesterol: One of Most Important Physiological Biomolecules

Cholesterol [(3β)-cholest-5-en-3-ol] is the major sterol in animal tissues. It is amphipathic, waxy metabolite containing 27 carbons. It is a sterol molecule with the hydroxyl group at C-3 (polar head group) and also has non-polar hydrocarbon chain as long as 16-C fatty acid.

Figure 1.1 Chemical structure of cholesterol

Although cholesterol is the most notorious lipid due to strong correlation between its high levels in blood and the impacts on human cardiovascular diseases, it has a crucial role in many physiological progresses.

Cholesterol is basically found in animal fats at varying amounts with triglycerides and phospholipids. Cheese, egg yolks, beef, pork, poultry, and shrimp are major dietary sources of cholesterol. Also, human breast milk contains significant amounts of cholesterol.

1.1.1 Functions and Transport in the Cell

Cholesterol is an essential structural component of mammalian cell membranes and necessary for creation and maintenance of membranes. It is required to establish proper membrane permeability and fluidity over the range of physiological

temperatures. The polar head group on cholesterol interacts with the polar head groups of the membrane phospholipids and sphingolipids, while the bulky steroid and the hydrocarbon chain are embedded in the membrane, alongside the nonpolar fatty acid chain of the other lipids. Through the interaction with the phospholipid fatty acid chains, it increases membrane packing, which reduces membrane fluidity (Sadava et al., 2011). With these structural roles of cholesterol, the permeability of the plasma membrane to neutral solutes (Yeagle, 1991), protons and sodium ions (Haines, 2001) is being reduced.

Cholesterol functions in intracellular transport within the cell membrane. It assists to formation of lipid rafts in plasma membrane during the cell signaling process (Incardona & Eaton, 2000). In many neurons, a myelin sheath, rich in cholesterol, provides insulation for more efficient conduction of impulses. Thus, cholesterol participates indirectly to nerve signaling (Pawlina & Ross, 2005).

Most important function of cholesterol is as the precursor molecule for a variety of products with specific biological activities within the cell (Hanukoglu, 1992). Mineralocorticoids and glucocorticoids are synthesized in the cortex of adrenal gland. Sex hormones (progestogens, androgens and estrogens) are produced in male and female gonads and placenta. Biosynthetic relations of classes of steroid hormones derived from cholesterol are given in Figure 1.2.

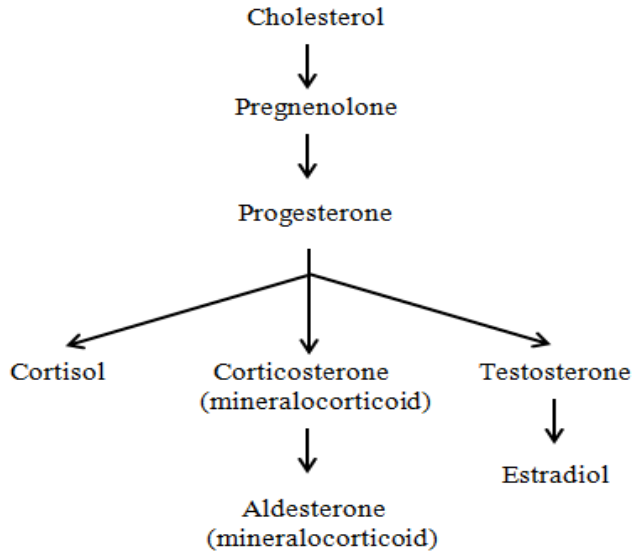

Figure 1.2 Biosynthetic relations of classes of steroid hormones derived from cholesterol

Bile acids are polar derivatives of cholesterol and act as highly effective detergents with containing both polar and nonpolar regions. They emulsify dietary fats and fat-soluble vitamins in the intestine. Bile salts, the major constituent of bile, are synthesized in liver and major breakdown products of cholesterol. Also, cholesterol is the precursor of vitamin D.

Transport of cholesterol and triacylglycerol in body fluids is in the form of lipoprotein particles due to their insolubility in water. A hydrophobic lipid in core surrounded by a shell of more-polar lipids or proteins generates lipoproteins. Apolipoproteins, protein component of macromolecular lipoprotein aggregates, combine with lipids to form different classes of lipoproteins. Different lipoproteins with different densities changing from chylomicrons to high-density lipoproteins are produced with different combinations lipids and proteins and have specific function. Apolipoproteins, synthesized and secreted from liver and intestine, act as signals, targeting lipoproteins to specific tissues or activate the enzymes (Nelson & Cox, 2004).

Triacylglycerols, cholesterol and other lipids from diet form large chylomicrons and are carried out of intestine. Triacylglycerols that constitute about 90% of chylomicrons are released through the hydrolysis by lipoprotein lipases. Then, chylomicron remnants, cholesterol-rich residues, are taken by liver. Lipoprotein particles are crucial for the transport of lipids from liver to other tissues.

Lipoproteins are classified as chylomicrons, chylomicron remnants, very low-density lipoproteins (VLDLs), intermediate-density lipoproteins (IDLs), low-density lipoproteins (LDLs) and high-density lipoproteins (HDLs) according to increasing density. These lipoproteins can shift between classes, thereby changing their density (Berg et al., 2011). Some properties belong to some plasma proteins are summarized in Table 1.1.

Table 1.1 Properties of some plasma lipoproteins

Plasma			**Composition (%)**				
Lipoprotiens	**Density (g/mL)**	**Physiological Role**	**TAG**	**CE**	**FC**	**PL**	**P**
Chylomicrons	< 0.95	Dietary fat transport	86	3	1	8	2
VLDLs	0.95 – 1.006	Endogenous fat transport	52	14	7	18	8
IDLs	1.006 – 1.019	LDL precursor	38	30	8	23	11
LDLs	1.019 – 1.063	Cholesterol transport	10	38	8	22	21
HDLs	1.063 – 1.210	Reverse cholesterol transport	5-10	14-21	3-7	19-29	33-57

TAG: triacylglycerol; CE: cholesteryl ester; FC: free cholesterol; PL: phospholipid; P: protein

Cholesterol is majorly carried by LDLs in blood to peripheral tissues. Cholesterol must be used biochemically in the cell or excreted by the liver due to undegradable steroid nucleus. Lipoprotein particles function not only in transporting cholesterol from sites of synthesis to sites of use but also in transporting to liver for excretion and homeostasis. Liver exports the excess of triacylglycerols and cholesterol into blood in the form of VLDLs. This excess cholesterol in the form of LDL is known as bad cholesterol. HDL is known as good cholesterol due to its function to move cholesterol throughout the body. Cholesterol released from macrophages and peripheral tissues is esterified by HDL and these cholesteryl esters are transferred to tissues for the synthesis of steroid hormones and to the liver for bile salts conversion and excretion (Berg et al., 2011).

1.1.2 Biosynthesis and Regulation

In spite of an essential molecule for many animals including humans, cholesterol is not required in the mammalians diet. Cholesterol can be synthesized from simple precursors in all cells. A single precursor molecule, acetate, provides all carbon atoms for the complex biosynthesis pathway of cholesterol. The other intermediate from acetate to cholesterol is isoprene which is also precursor to other natural lipids.

Cholesterol synthesis takes place in four stages:

1. Three acetate units associate to form six-carbon intermediate, mevalonate.
2. Mevalonate converts to activate isoprene units.
3. Six 5-C isoprene units polymerize to form the 30-C linear squalene.
4. Squalene cyclizes to form the steroid nucleus and further changes (removal of three methyl groups and reduction of one double bond) to form cholesterol. The four stages of cholesterol synthesize is summarized in Figure 1.2 (Nelson & Cox, 2004).

Cholesterol biosynthesis is a complex and energy-expensive process and rates may vary several hundredfold, depending on the complement dietary cholesterol intake. An adult with a low-cholesterol diet typically synthesize about 800 mg cholesterol per day.

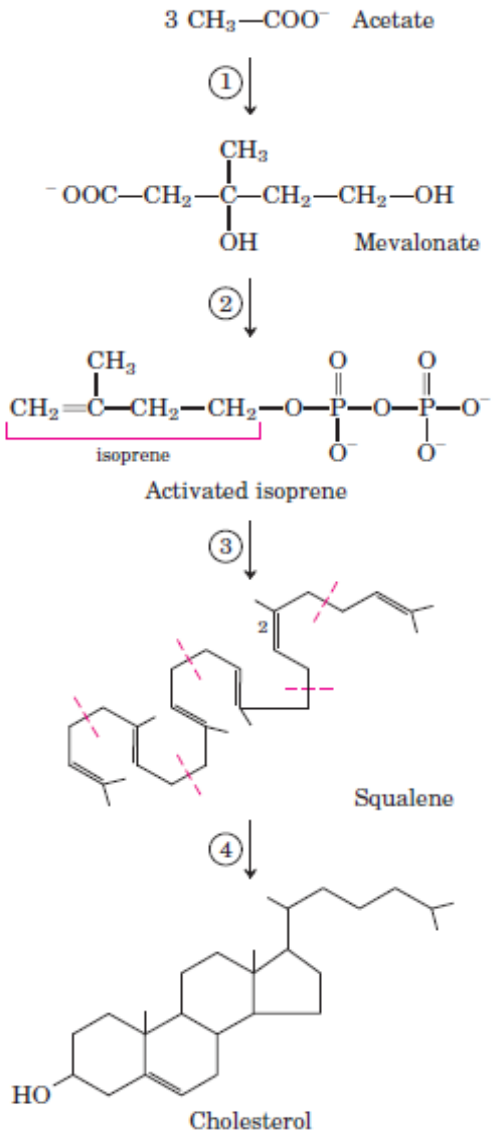

Figure 1.3 Summary for four stages of cholesterol synthesis (Nelson & Cox, 2004)

Although a significant amount of cholesterol is formed in intestine, the major site of cholesterol synthesis in mammals is liver. In mammals, intracellular cholesterol concentration and glucagon and insulin hormones regulate cholesterol synthesis. The feed-back regulation is mediated primarily by the changes in the amount and the activity of 3-hydroxy-3-methylglutaryl (HMG-CoA) CoA reductase that catalyzes the formation of mevalonate. Covalent modification of HMG-CoA reductase provides the hormonal control. Phosphorylated (inactive) form is stimulated by glucagon and insulin stimulates dephosphorylated form and favors the cholesterol

synthesis. In liver, dietary cholesterol affects the cholesterol synthesis by reducing the activity and the amount of this enzyme. In nonhepatic cells, cholesterol is obtained by LDLs from the plasma rather than synthesizing it de novo.

Regulation of energy-expensive process of cholesterol biosynthesis according to complement dietary intake is an advantageous to an organism. Uncontrolled production of cholesterol can lead to accumulation in blood vessels and serious human disease. Therefore, cholesterol biosynthesis is one of most highly regulated metabolic pathway known to prevent these diseases, especially atherosclerosis (Berg et al., 2011).

1.1.3 Hypercholesterolemia and Treatment Methods

Hypercholesterolemia, or high cholesterol, occurs when the sum of cholesterol synthesized and obtained in the diet exceeds the required amounts for the synthesis of membranes, bile salts and steroids. Atherosclerosis is correlated with high levels cholesterol in the form of LDL while a negative correlation between HDL form and arterial disease. The ratio of LDL to HDL can be used for the evaluation of probability to arterial disease. For a healthy person, this ratio cannot be above 3.5. HDL acts as antiatherogenic agent via removal of cholesterol from cells, especially from macrophages and inhibition of LDL oxidation. HDL carries the cholesterol from tissues to liver for excretion. This transport, called reverse cholesterol transport, is important to decrease the development of foam cells. Thus, development of drugs that enhance the levels of HDL in the blood is underway (Berg et al., 2011).

Familial hypercholesterolemia (FH), the most common and severe monogenic form of hypercholesterolemia, is characterized by an increased plasma LDL-cholesterol concentration due to a decrease in the clearance of LDL particles by dysfunctional LDL-receptors in the liver (Goldstein & Brown, 2009). FH is an autosomal co-dominant condition caused primarily by mutations in the LDL-receptor (LDLR) gene (Soutar & Naoumova, 2007). Over 1200 mutations causing FH have been reported that span the entire LDLR gene (Usifo et al., 2012).

Blood cholesterol levels are extremely high due to a defect in LDL receptor and lack receptor-mediated uptake of cholesterol carried by LDL. Excess blood LDL is oxidized and oxidized LDL (oxLDL) is taken up by macrophages. The foam cells, formed by macrophages by becoming engorged, accumulate in the blood vessel walls and lead to formation of arteriosclerotic plaques. Intracellular cholesterol synthesis continues due to inability of cholesterol transport into the cell. Furthermore, IDL input to cells is procured by the LDL receptors, so they stay longer in the blood and are converted into LDL. Thus, absence of LDL receptor ensures the elevated levels of LDL cholesterol in blood (Berg et al., 2011).

Homozygous FH (HoFH) patients die of coronary heart diseases in childhood, due to absence of functional LDL receptors. Heterozygous FH (HeFH) patients have about half of the normal number of LDL receptor hence, they have more variable clinical course. Untreated patients with HeFH usually have plasma LDL-cholesterol concentrations in the 5–12 mmol/L range. The classical physical stigma in adults with HoFH is the presence of tendon xanthomata, characteristically in the Achilles. Less specific features of FH include arcus corneae and xanthelasma palpebrarum (Page et al., 2014). HoFH, a more extreme form of the disorder, is associated with severe hypercholesterolemia (plasma LDL-cholesterol typically in excess of 13 mmol/L untreated; with an LDL-cholesterol >7 mmol/L on treatment) (Khachadurian & Uthman, 1973). In HeFH, atherosclerotic coronary heart disease (CHD) develops by age 50 years in 50% of males and in 30% of women by age 60 (Marks et al., 2003). Clinical diagnosis of FH is based on a personal and family history, physical examination findings and plasma cholesterol concentrations. The diagnostic criteria for HoFH are based on the presence of xanthomata before the age of 10 years and an untreated LDL-cholesterol in the excess of 13.0 mmol/L (Raal & Santos, 2003). Cholesterol-lowering therapies have been shown to reduce both mortality and major adverse cardiovascular events in individuals with FH (Harada-Shiba et al., 2012).

The cornerstone of treatment for FH is diet and lifestyle modifications along with pharmacotherapy, with HMG-CoA reductase inhibitors (statins) the most common and effective drugs to treat FH (Harada-Shiba et al., 2012; Ito et al., 2011; Watts et

al., 2011). Statins have hydrophobic groups covalently linked to HMG-like moieties. On the basis of chemical nature, statins are classified into hydrophilic (pravastatin, fluvastatin, rosuvastatin) or lipophilic (lovastatin, cerivastatin, simvastatin) or combined (atorvastatin) and most recently approved, pitavastatin. Average LDL cholesterol-lowering effects of statins are 63% for rosuvastatin, 57% for atorvastatin, 46% for simvastatin, 41% for pitavastatin, 40% for lovastatin, 34% for pravastatin, and 31% for fluvastatin at their highest approved doses. However, statins require some residual LDL receptor function, thus they are not effective in receptor-negative HoFH.

Other anti-hypercholesterolemia drugs are fibrates, bile acid sequestrants, omega-3 fatty acids, and niacin. Fibrates increase the transcription of peroxisomal fatty acid β-oxidation genes in liver and also regulate the expression of genes involved in lipoprotein metabolism. In clinical trials, fibrate alone causes a significant decrease in triglycerides (20–50%) and in LDL-cholesterol (5–15%) and also an increase in plasma HDL-cholesterol (14–20%). Bile acid sequestrants disturb enterohepatic circulation of cholesterol-rich bile acids and increase their fecal excretion leading to up regulation of 7α-dehydroxylase that catalysis the rate-limiting step of bile acid synthesis. This results in increased flux of intrahepatic cholesterol for production of bile acids and increase in the removal of LDL, IDL and VLDL from the circulation.

Niacin is a lipid-modulating agent and produces beneficial effects on dyslipidemia by decreasing plasma levels of all atherogenic apoB-containing lipoproteins, and inhibiting the release of free fatty acids from adipose tissue by raising those of cardio protective HDL. Niacin reduces LDL-C levels by 25% and causes the inhibition of fat breakdown in adipose tissue. Statin/fibrate or niacin/fibrate combined therapies can be used for patients with mixed hyperlipidemia who are resistant or intolerant to statins (Tiwari and Khokhar, 2014). Ezetimibe is a selective cholesterol absorption inhibitor and reduces cholesterol levels by blocking the absorption of sterols in the small intestine without affecting absorption of fat-soluble vitamins or triglycerides. Combination of ezetimibe with statin reduces both intestinal and hepatic sources of cholesterol and provides greater reductions in LDL-C levels than those achieved with

either drug alone (Brautbar & Ballantyne, 2011). Omega-3 fatty acids administered at pharmaceutical dosages (3–12g/day) reduce elevated triglyceride levels and have modest effects on non-HDL-C and apoB levels, but they do not reduce LDL-C levels. Therefore, patients with mixed dyslipidemia, omega-3 fatty acids have been useful when given with statin (Barter & Ginsberg, 2008). All these inhibitors can be prepared with adding edible resin to increase the effectiveness of the drug by prohibiting the reabsorption. Thus, 50 % decrease in the plasma cholesterol levels can be obtained (Nelson & Cox, 2004; Berg et al., 2011).

The word apheresis, derived from the Greek, means ‘taking away’. The successful use of plasmapheresis, or plasma exchange, to treat severe hypercholesterolaemia was first described in 1975 (Thompson et al., 1975). The first attempt to selectively remove low density lipoprotein (LDL) from plasma involved serial venesection, with ex vivo admixture of batches of blood with heparin-linked agarose beads prior to re-infusion (Lupien et al., 1976). The group of Stoffel combined these two approaches by using a cell separator to perfuse plasma through a sepharose column containing anti-LDL antibodies, a procedure they termed LDL apheresis (Stoffel et al., 1981).

LDL apheresis is used as long-term therapy to rapidly produce marked reductions in circulating lipids and lipoproteins in patients who are intolerant or not sufficiently responsive to diet and pharmacologic lipid therapy (Mabuchi et al., 1998).

An LDL apheresis session typically requires 3–4 h. Whole blood is removed and circulated extracorporeally. Approximately 3 liters of blood (one plasma volume) are treated during the procedure. With regular apheresis treatments, long-term decreases are produced in both the pretreatment and post-treatment LDL levels (Lane et al., 1995). Moreover, LDL apheresis provides an alternative to lipid-lowering surgical procedures such as portacaval shunt, partial ileal bypass surgery, and liver transplantation (Thompsen & Thompson, 2006). Several plasma apheresis methods for the reduction of LDL levels were used.

1.1.3.1 Double Filtration Plasmapheresis (DFPP) and Thermofiltration Plasmapheresis

Plasma is separated from blood cells by a hollow fibre filter. Useful plasma components are selectively retained by a second filter and returned to the patient (with necessary systematic anticoagulation). LDL is discarded by size-exclusion principle. DFPP has the advantage of non-requirement of costly albumin infusion that performed in single plasmapheresis. Thermofiltration involves warming plasma to 38°C prior to DFPP, which increases the amount of LDL removed and reduces the amount of HDL lost (Thomsen & Thomson, 2006; Thomson, 2008).

1.1.3.2 Immunoadsorption (IA)

The commercially available system consists of a continuous flow cell separator which pumps plasma through twin columns containing polyclonal sheep antibodies to human apoB100 coupled with sepharose 4B gel (Richter, 1993). Columns are regenerated with glycine buffer and flushed with saline by means of an automated adsorption-desorption device. Each patient has 2 columns dedicated to their sole use, which are stored in sodium azide between procedures (Thompson, 2008).

1.1.3.3 Dextran Sulfate Adsorption (DSA)

In dextran sulfate adsorption apheresis, the plasma is separated from red blood cells and passed over columns containing dextran sulfate covalently bound to cellulose beads which binds apolipoprotein B (apo-B) by a highly selective electrostatic binding mechanism. Since LDL, VLDL, and lipoprotein (A) (Lp(A)) all contain apo-B, dextran sulfate adsorption apheresis selectively reduces these lipoproteins while having little effect on the non-apo-B containing HDL particles. The dextran sulfate procedure requires heparin to prevent extracorporeal clotting of blood (Thompsen & Thompson, 2006). There are no limits to the amount of LDL that can be adsorbed from plasma using this system. The presence of significant numbers of platelets in the plasma during centrifugal separation can lead to blockage

of the affinity column, which is why membrane filtration is preferred (Thompson, 2003). Dextran sulfate direct perfusion method is similar to dextran sulfate adsorption except performed on whole blood (Page et al., 2014).

1.1.3.4 Heparin Extracorporeal LDL Precipitation (HELP)

HELP is an entirely different approach to LDL apheresis involves on-line precipitation of LDL through the addition of heparin to plasma (Eisenhauer et al., 1987). Plasma is passed through a heparin buffer and acidified to a pH of 5.2 after separation from whole blood. At this pH heparin is predominately negatively charged whereas LDL is predominately positively charged. The resultant electrostatic attraction forms heparin–LDL complexes that precipitate and are removed by filtration. Residual heparin is removed from the LDL-free plasma by a heparin adsorber and the plasma returned to the patient (Thompsen & Thomson, 2006). Side effects were mild and infrequent and hemorrhagic complications were not observed (Thompsen, 2003). Proteins such as apoA, albumin or immunoglobulins do not significantly bind to heparin at low pH and are not precipitated in the system (Blessing et al., 2004).

1.1.3.5 Direct Adsorption of Lipoprotein (DALI) Using Haemoperfusion

The development of a novel, non-haemolytic polyacrylate-based LDL adsorber enables LDL apheresis to be undertaken without preliminary separation of plasma from blood cells. Anti-coagulation is initiated by heparin and maintained by anticoagulant citrate dextrose (ACD) (Bosch et al., 1997). The pore size of the polyacrylate-coated polyacrylamide beads is sufficiently small to exclude red cells and platelets. In patients with homozygous or severe heterozygous FH, it was necessary to use larger capacity adsorbers. The ease of use and rapidity of direct adsorption of lipoprotein (DALI) offer major advantages over plasma-based apheresis techniques and release of microparticles into the circulation is less than during DSA procedures (Thompson, 2003).

All currently available lipoprotein apheresis methods acutely lower total cholesterol and LDL cholesterol by > 60%. The data suggest that IMA, DSA and HELP have similar efficacy in lowering LDL cholesterol, with mean reductions of 61.9, 63.7 and 59.4%, respectively (Schmaldienst et al., 2000). Similar reductions were observed in Lp(A) but IA and DFPP (but not thermofiltration) decrease HDL cholesterol more than other methods. More plasma needs to be treated by IA than DSA to achieve an equivalent reduction in LDL cholesterol but this is offset by the faster flow rate of the centrifugal cell separator used in IA. There is no limit to the volume of plasma which can be treated by IA, DSA and DFPP whereas the maximum which can be treated by the HELP system is effectively 4 liters, reflecting its limited capacity to filter out precipitated LDL and the extent to which it reduces fibrinogen. Haemoperfusion systems are the easiest to use but, like HELP and DSA, are less economical than IA with its re-usable columns although these have the disadvantage of needing to be kept sterile between procedures (Thompson, 2008).

Chemically and/or biologically modified specific sorbents are being searched instead of sorbents used in plasma apheresis. Novel sorbents specifically bind the LDL-cholesterol can be useful to avoid the formation of adverse effects of plasma apheresis methods. For this purpose, molecular imprinting technology can be used for the development of novel sorbents that can be used in plasma apheresis.

1.2 Molecularly Imprinted Polymers

Molecular imprinting is a polymerization technique that creates tailor-made synthetic materials that include specific cavities for a target molecule (Bui & Haupt, 2010). Molecular imprinted polymers (MIP) present favored affinity to target molecule compared to other molecules, and this property is the essential driving force for applications of this techniques.

MIPs are synthesized in a reaction mixture composed of a target molecule (template), a functional monomer (or two), a cross-linking monomer (or two), a polymerization initiator in a proper solvent (Cheong et al., 2013). Firstly, functional

monomers are arranged around the template molecule and complexed with using several molecular interactions between the template and the functional monomers. This arrangement can be accomplished by non-covalent interactions, reversible covalent interactions or metal ion mediated interactions (Andersson, 2000). These possible non-covalent interactions are as hydrophobic interactions, hydrogen bonds, ion-pair interactions, van der Waals and electrostatic interactions.

The pre-complex is polymerized by adding cross-linker to the reaction mixture. This spatial arrangement is fixed by polymerization of pre-polymerization complex and cross-linker (Verheyen et al., 2011). The imprinting effectiveness attributed to two factors demonstrates the fundamental mechanisms for molecular recognition. These factors:

(a) Formation of pre-polymerization complex between supplementary functional monomer with the target molecule.
(b) Cavitation with size and structure selectivity for the target molecule (Spivak, 2005).

Template molecule is removed from polymer by deterioration of molecular interactions between polymer and template molecule. Removal of the template creates chemically and sterically complementary sites within the polymer. These sites are named as “memory sites”. Polymer can bind the target molecule selectively by the way of these memory sites from complex samples. Many studies have repeatedly demonstrated that basic advantage of molecular imprinting is the possibility for the production of adsorbents with selectivity pre-specified for a defined molecule (Andersson, 2000). A typical molecular imprinting process is shown in Figure 1.4.

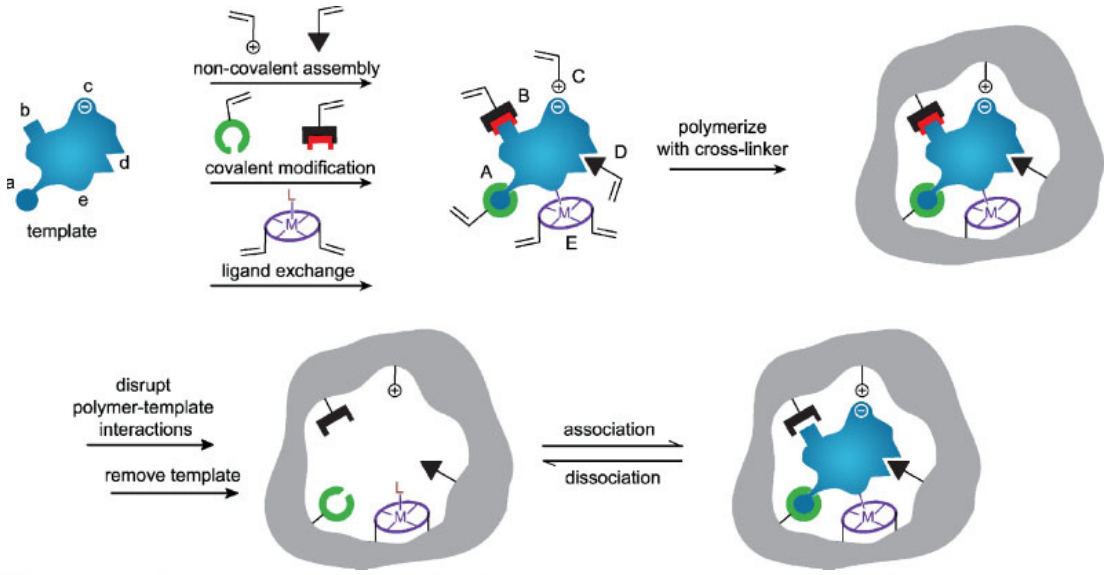

Figure 1.4 Schematic representation of molecular imprinting process (Alexander et al., 2006)

MIPs show higher physical strength, robustness, resistance to elevated pressure and temperature and inertness against organic solvents, acids, bases, and metal ions compared to biological media such as proteins and nucleic acids. Also, they can be produced with low costs and can be stay several years at room temperature (Cheong et al., 2013).

1.2.1 Molecular Imprinting Methods

Molecular imprinting process can be practiced by different approaches. These are covalent, non-covalent, semi-covalent and metal-ion mediated imprinting approaches. These approaches are based on the interactions types between template and monomers.

1.2.1.1 Covalent Imprinting Approach

The basis of covalent imprinting is the polymerization of monomers that can covalently bind templates. Monomer-template complex is formed by a reversible covalent linkage independent of polymer production. Template removal is achieved by chemical cleavage and binding of analyte occurs via the covalent interactions same with the complexation interactions. Covalent imprinting approach uses

reversible condensation reactions to form boronate esters, ketal/acetal and Schiff's bases for monomer-template complex. These incorporations require mild aqueous conditions for template removal (Bui & Haupt, 2010; Mayes & Whitcombe, 2005).

The distinct advantage of covalent approach is the stoichiometric complexation between template and monomer. Thus, more homogeneous population of binding sites occurs within the polymer. Due to stoichiometric complexation and similar binding sties, non-specific binding may be enormously reduced. Nevertheless, this approach is less adaptable because all targets cannot simply complex with monomers for covalent imprinting. Furthermore, re-organization of covalent bonds for template binding may cause to slow binding kinetics (Bui & Haupt, 2010).

1.2.1.2 Non-Covalent Imprinting Approach

Non-covalent imprinting approach uses non-covalent interactions such as hydrogen bonds, ion-pairs, dipole-dipole interactions and van der Waals forces for monomer-template interactions. These monomer-template interactions provide functionality and are same in both pre-polymer complexation step and in re-binding step. Pre-polymerization complexation step do not require synthesis. Thus, pre-polymerization complex is formed easily in the reaction mixture. Removal of template can be achieved easily, usually with continuous extraction (Spivak, 2005).

In stoichiometric non-covalent imprinting, monomer-template complex is strong enough to procure the equilibrium that go towards to the side of the complex. The association constant (K_a) for the monomer-template interaction must be $\geq 10^3\ M^{-1}$ to achieve this equilibrium (Alexander et al., 2006). Unlike covalent imprinting, monomer-template complex is unstable and dynamically re-organize on a time scale relevant to the imprinting process. Instability causes to implications in designing polymers with non-covalent imprinting approach. Production of much more stable complexes that can lead to a greater yield of more uniform receptor sites is the requirement for this approach. It seems like that a little part of polymer structure develops multiple functional groups during polymerization. This leads to produce a

cooperative affect due to the multiple interactions with much higher affinity (Mayes and Whitcombe, 2005). Non-covalent and covalent imprinting approaches are shown in Figure 1.5.

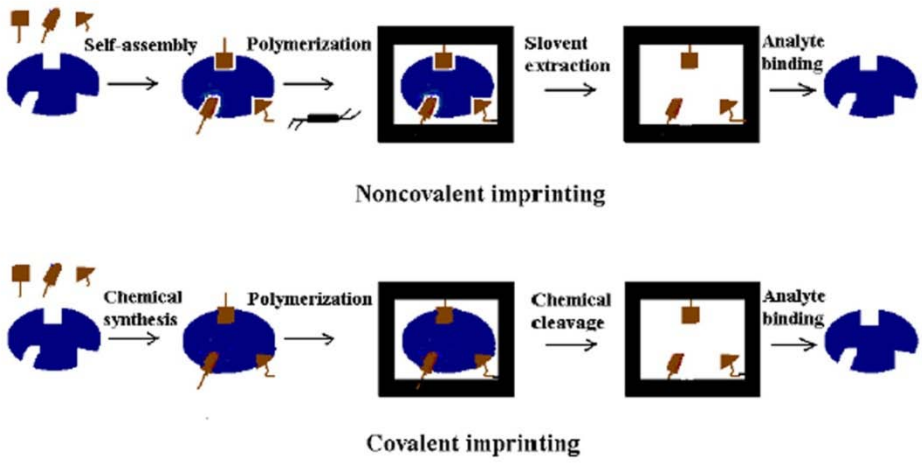

Figure 1.5 Schematic representation of covalent and non-covalent molecular imprinting (Yan & Row, 2006)

The clearest advantage is that non-covalent imprinting process is very simple. Disadvantages of the approach can be listed as:

(i) Heterogeneity of binding sites

(ii) Non-specific interactions can be shown up due to disperse of excess functional monomer in the binding reaction mixture

(iii) Template amount in the pre-polymerization complex can yield to decreased amount of selective binding sites with high-affinity (Mayes & Whitcombe, 2005).

1.2.1.3 Semi-Covalent Imprinting Approach

Semi-covalent imprinting approach combines the advantages of the covalent and the non-covalent approaches. A covalent or partly covalent incorporated template complex is used in the polymerization step, but binding is completely non-covalent in nature.

Two variations for semi-covalent imprinting approach that can be applied are:

(i) Direct connection of the template and the monomer

(ii) Connection of the monomer with the template through a spacer group

Covalent binding in the polymerization steps ensures more homogenous binding site affinities. Non-covalent interactions in the rebinding steps encounter with no kinetic limitations except diffusion. In contrast with the simplicity of the method, method has some disadvantages. Template removal is often not easy and some steric requirements influence the approach (Alexander et al., 2006).

1.2.1.4 Metal-Ion Mediated Imprinting Approach

Metal ions have the ability to bind to a wide range of functional groups through the donation of electrons from the heteroatoms of ligands to the unfilled orbitals of the outer coordination sphere of the metal. The strength of interaction can vary enormously from weak, readily exchangeable bonds to strong bonds which behave like covalent links, depending on the metal, its oxidation state and ligand characteristics. Consequently metal coordination has been employed as an alternative means of association between template and functional monomer in the construction of imprinted polymers. The complex used for imprinting generally consists of polymerizable ligand(s) to complex the metal ion (generally a transition metal ion) which in turn coordinates to the template (Alexander et al., 2006).

1.2.2 Polymerization Components

The design and synthesis of MIPs vary with experimental conditions. Nature and levels of template, cross-linkers, functional monomers, initiator and solvents, initiation method and polymerization period affect the imprinting process.

1.2.2.1 Template

The template has the central importance in all imprinting approaches. Template manages the orientation of functional groups towards monomers (Cormark & Elorza, 2004). Functional chemical groups of template must interact with the monomers adequately for a stable complex formation (Martin-Esteban A., 2001). Selectivity of recognition sites is specified by the strength of the interaction. If the interaction is stronger, more stable complex and a higher binding capacity is obtained. Thus, it is very important to select functional monomers correctly (Li et al., 2011).

An ideal template should provide these requirements:

(i) Template should not contain any polymerizable groups that can participate or prevent to polymerization.

(ii) Template should have functional groups to interact with functional monomers.

(iii) Template should be stable under polymerization conditions such as moderately high temperatures or UV irradiation (Li et al., 2011).

1.2.2.2 Functional Monomers

Functional monomers provide interactions in the binding sites of imprinted polymers. The functionality of the template must match with the functionality of monomer such as H-bond donor and H-bond acceptor. This complementary interaction is required to enhance the complexation between template and functional monomer and, thus imprinting effect. In copolymerization methods, two or more functional monomers can be used concurrently. The reactivities of monomers must be checked to confirm that copolymerization is practicable. Functional monomers with different chemical structures and polarities are commercially available.

Bronsted basic functional monomers such as 2- or 4-vinylpyridine (VPy), diethylaminoethylmethacrylate (DEAEMA) are used for acidic templates and acidic functional monomers such as methacrylic acid (MAA), trifluoromethylacrylic acid

(TFM), itaconic acid (ITA) are used for Bronsted base templates. Primary amide containing monomer such as methacrylamide (MAAM) presents high selectivities for carboxylic acids and amides. *N*-vinylpyrrolidone (NVP) and 2-hydroxyethylmethacrylate (HEMA) are the neutral solvating monomers that improve the imprinting effect (Sellergen et al., 2009). MAA, acrylic acid (AA), Vpy, TFM, acrylamide and HEMA are ordinarily used monomers for molecular imprinting. MAA creates ionic interactions and hydrogen bonds with amines, amides, carbamates and carboxylic acids. Furthermore, MAA has unique characteristics and thus, it is used as universal functional monomer (Li et al., 2011).

When templates are poorly polar to apolar with few polar interaction sites, amphiphilic monomers may be useful to stabilize the monomer-template interactions by hydrophobic and van der Waals forces; or in the case of extended π-systems, monomer-template interaction is stabilized through charge transfer.

Many complementary interactions are needed to improve the strength and suitability of recognition similarly to biological systems. Therefore, it is a beneficial strategy to use comonomers that target different subunits of complex template (Sellergen et al., 2009).

Functional monomers commonly used at the preparation of molecular imprinting polymers are demonstrated in Figure 1.6.

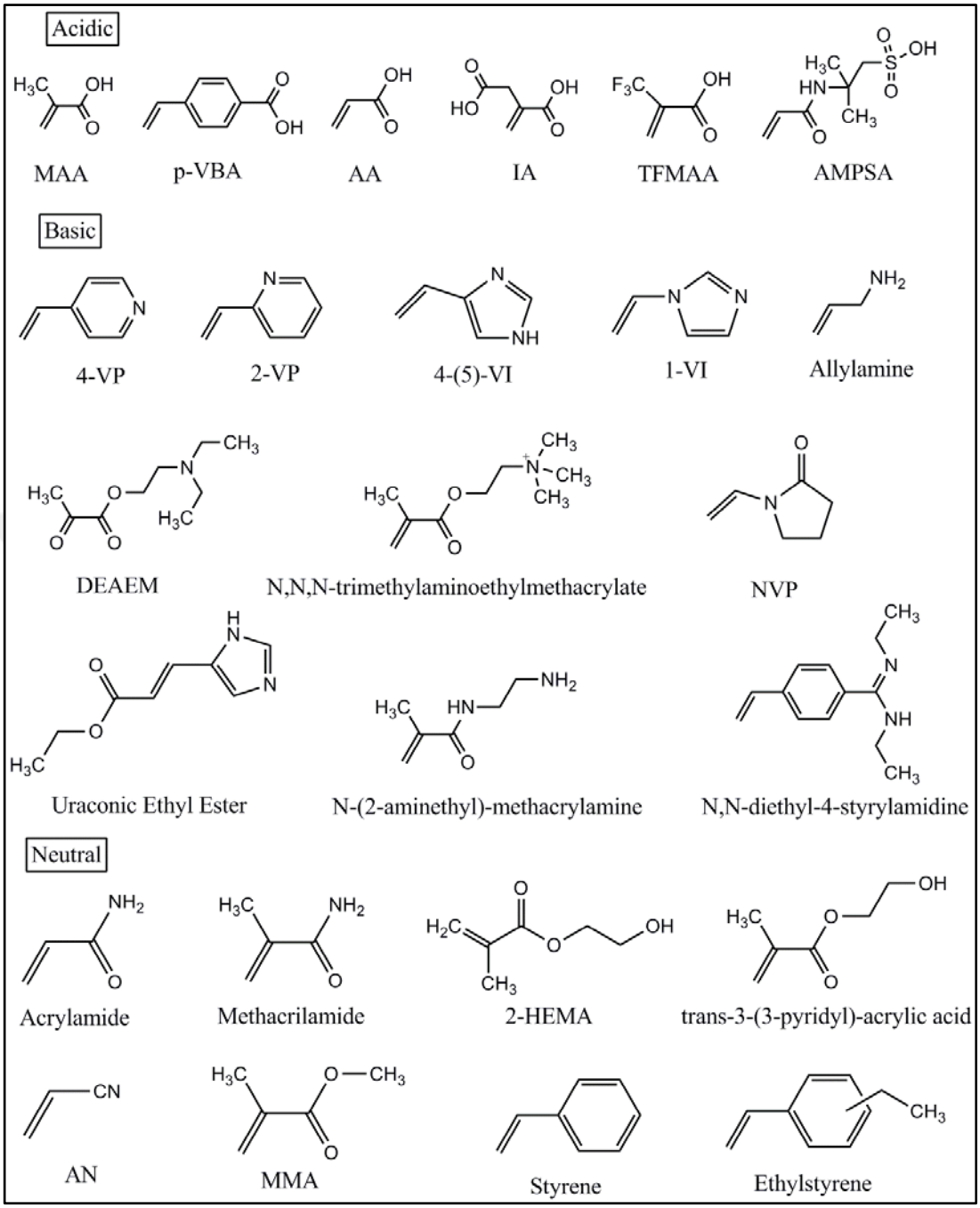

Figure 1.6 Functional monomers used in polymer preparation

Acidic: MAA: methacrylic acid, p-VBA: p-vinylbenzoic acid, AA: acrylic acid, IA: itaconic acid, TFMAA: 2-(trifluoromethyl)-acrylic acid, AMPSA: 21 crylamide-(2-methyl)-propane sulfonic acid. Basic: 4-VP: 4-vinylpyridine, 2-VP: 2-vinylpyridine, 4-(5)-VI: 4-(5)-vinylimidazole, 1-VI: 1-vinylimidazole, DEAEM: N,N-diethyl aminoethyl methacrylamide, NVP: N-vinylpyrrolidone. Neutral: MAA: methacrylamide, 2-HEMA: 2-hydroxyethyl methacrylate, AN: acrylonitrile, MMA: methyl methacrylate

1.2.2.3 Cross-linkers

Cross-linker substantially impacts on chemical and physical properties of molecularly imprinted polymers. Major functions of cross-linker are:

(i) To control the morphology of polymer matrix

(ii) To stabilize the imprinting binding site

(iii) To increase mechanical stability of polymer

For these reasons, high cross-link ratios are commonly needed for the production of porous materials with proper mechanical stability. To achieve this mechanical stability, more than 80 % of cross-liker is used mostly. Furthermore, reactivities of functional monomers should be similar to those of cross-linkers. But, chemically different functional groups in multi-functional monomers may be incorporated at different reactivity ratios.

Divinylbenzene (DVB) and ethylene glycol dimethacrylate (EGDMA) are the most widely used cross-linkers. Wulff and coworkers compared commercial and custom-made styrenic and methacrylate cross-linkers (Wulf & Akelah, 1978; Wulff et al., 1982; Wulff et al., 1987). It was determined that EGDMA was superior to DVB and its tetramethylene analogue in terms of the separation factor (α), shown by the MIPs. This was attributed to the combination of a short flexible linker and the rigidity and prochiral character of the methacrylate groups of EGDMA.

Disulphide-linked bis-acrylamides used as reversible cross-linkers and the dimethacrylate-derived cross-linkers as flexible cross-linkers has been reported (Alexander et al., 2006).

A large number of cross-linkers used for production of molecular imprinted polymers are given in Figure 1.7.

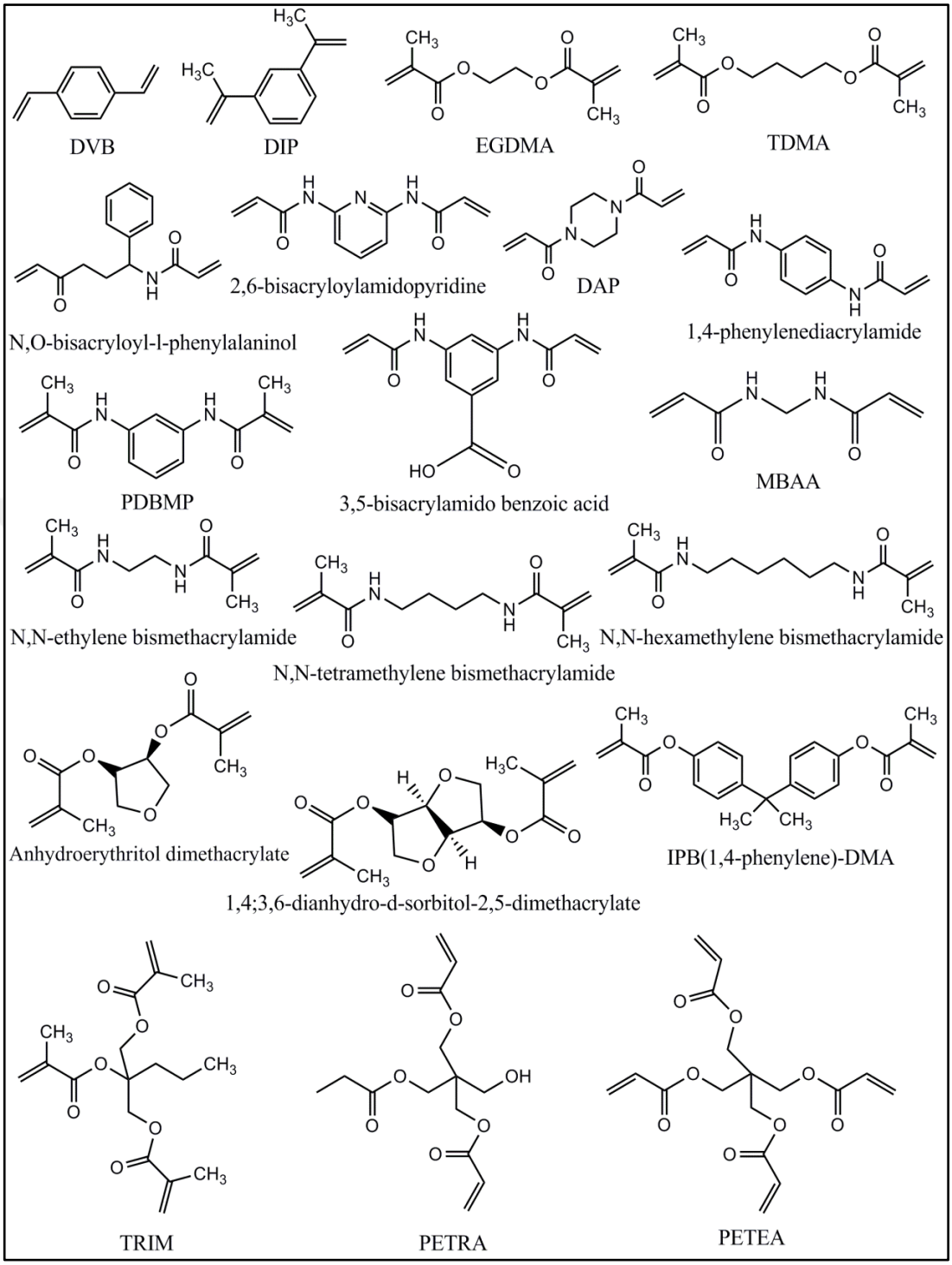

Figure 1.7 Cross-linkers used in molecular imprinting

PVB: p-divinylbenzene, DIP: 1,3-diisopropenyl benzene EGDMA: ethylene glycol dimethacrylate, TDMA: tetramethylene dimethacrylate, PDBMP: N,N-1,3-phenylenebis(2-methyl-2-propenamide), DAP: 1,4-diacryloyl piperazine, MDAA: N,N-methylene bisacrylamide, IPB(1,4-phenylene)-DMA: isopropylenebis(1,4-phenylene)dimethacrylate, TIRM: trimethylpropane trimethacrylate PETRA: pentaerythritol triacrylate, PETEA: pentaerythritol tetraacrylate

1.2.2.4 Initiators

Initiators are used at lower amounts in comparison with monomers; at the amount of 1% (weight) or 1 mol % of total polymerizable double bonds. Decompositions of initiator into radicals can be initiated by heat, light and chemical and electrochemical ways. Thermal and redox initiation and γ-irridation can be used. The rate and the mode of decomposition can be controlled according to the chemical structure of initiator. Oxygen hinders the free radical polymerization. Thus, dissolved oxygen in monomer solution should be removed by ultrasonication or by sparging with nitrogen or argon to accelerate the polymerization (Yan & Row, 2006).

Azo-initiators by thermal decomposition are ordinarily used for production of DVB- and (met)acrylate-based polymers. Azobisisobutyronitrile (AIBN), the most common azo-initiator, provides the production of molecular imprinted polymers at low temperatures with higher separation efficiency. 2,2'-azo-bis-(2,4-dimethylvaleronitrile) (ABDV) and 2,2'-azo-bis-(cyclohexylcarbonitrile) (ABCHC) are the initiators used against to temperature limit and solubility problems. Benzoyl peroxide and lauryl peroxide are organic thermal initiators. Water-soluble inorganic initiators, used either alone or with N,N,N',N'-tetramethylenediamine (TEMED), are ammonium and potassium persulphate (Alexander et al., 2006).

Initiators with different chemical structure used as a source of free radicals are given in Figure 1.8.

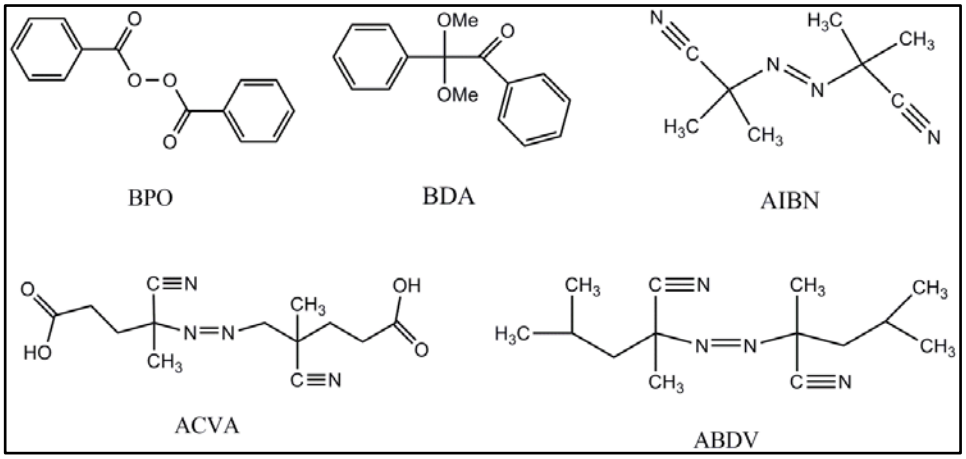

Figure 1.8 Some initiators used in molecular imprinting

BPO: benzoylperoxide, BDA: benzyl dimethyl acetal, AIBN: azobisisobutyronitrile, ACVA: 4,4'-azo(4-cyanovaleric acid), ABDV: azobisdimethylvaleronitrile

1.2.2.5 Solvents (Porogens)

The accessibility for rebinding is crucial as well as rigidity for efficiency of MIPs. Thus, MIPs should be porous. This is practiced by solvation of polymerization components in a porogenic solvent (Sellergen, 2003). An ideal porogen should provide these requirements:

(i) Template, monomers, cross-linker and initiator must be soluble in porogen.

(ii) Porogens should provide large pores to achieve good flow-through properties of MIPS.

(iii) Porogens should have relatively low polarity to decrease interferences between template and monomer (Yan & Row, 2006).

Pore size, pore distribution, swellability and morphology of MIPs are influenced by the amount and choice of porogenic solvent (Alexander et al., 2006). More specifically, well matured pore structures and high specific surface areas are achieved by the use of thermodynamically good solvents, whereas poorly pore structures and low specific surface areas are achieved by the use of thermodynamically poor solvents (Cormark & Elorza, 2004). Although molecular recognition weakens with increasing polarity of porogen, strong monomer-template interactions can occur in quite polar solvents such as methanol/water. In addition to

the role of porogen as solvent and pore former, porogen affects the strength of pre-polymerization complex. Generally, apolar, protic solvents such as toluene are used to stabilize hydrogen bonds whereas water could be best solvent for hydrophobic interactions (Yan & Row, 2006).

1.2.2.6 Other Conditions

Some physical conditions such as temperature and pressure also affect the imprinting process. In some cases, lower initiation temperatures can help polymerization. Generally, exothermal nature of the polymerization process cause to higher temperature within a monolith than the surroundings. There are some reports about MIPs prepared at temperatures over 200°C. This situation is the result of MIPs to withstand extreme temperatures and pHs. Effect of high pressure on MIP synthesis has been examined that it may approve related processes such as pre-polymerization complex formation (Alexander et al., 2006).

1.2.3 Parameters Effecting the Performance of MIPs

1.2.3.1 Template Size and Template Analogues

Template size has an important effect on the selectivity of imprinted polymers. Martin-Esteban et al. has investigated the selectivity of the fenuron and isoproturan imprinted polymers for the target molecules. It is shown that fenuron imprinted polymers present high selectivity for fenuron. Steric interactions inhibit the access of the other phenylurea herbicides into the cavities for fenuron. In the case of isoproturon imprinted polymers, herbicides related to isoproturon can enter into the cavities for isoproturon and demonstrate cross reactivity (Martin-Esteban et al., 2001).

Template leakage is one of the important problems of molecular imprinting technique. Dummy templates can be used to overcome this problem (Li et al., 2013). Hydrophobic template analogues can be used if the template is not water-soluble.

Ion-pairs may be useful in this situation. Imprinting biological macromolecules such as proteins is a challenging process due to their large structure. Protein fragments can be used as a template based on the antibody-antigen interaction mechanism to ease imprinting large molecules (Li et al., 2011).

1.2.3.2 Intramolecular H-bonds

In the study of Zhang et al. (2001), it was demonstrated that hydrogen bond interactions between the functional monomer and the template played a major role in the recognition process. This group has investigated the effect of intramolecular hydrogen bonds on recognition properties of MIPs. In order to determine the effect of intramolecular hydrogen bonding of templates on imprinting, different templates which can form intramolecular hydrogen bond, were used as templates to prepare MIPs. The results showed that the molecular recognition ability of the MIP decrease when the template form intramolecular hydrogen bonding itself in the case of hydrogen bonding are the major interaction in molecular recognition of the imprinted polymer. The intramolecular hydrogen bond interactions within the template reduce the formation of monomer-template complex. As a conclusion of the study, formation of a stable complex between template and functional monomer in MIP production is a pre-requirement for the achievement of MIPs with high molecular recognition property (Zhang et al., 2001).

1.2.3.3 Monomer-Template Ratio

The molar ratio of monomer to template has very important effect on the number and quality of MIP recognition sites (Andersson et al., 1996). Low monomer/template ratio induces to less than optimal complexation due to insufficient functional monomer. Too high an M/T ratio yields non-imprinted polymer and so non-specific binding (Nicholls, 1995).

Initial amount of template required for polymerization is a common consideration for MIPs. Based on the molecular weight of template, several hundred mg template are required for the production of five gram batch of MIP with using the commonly applied M:T ratios of 4:1 to 10:1. For chromatographic applications where MIPs used as stationary phases, maximum template must be used for imprinting due to high load capacity requirement. Nevertheless, it is not same for equilibrium binding applications. Only labelled analyte ≤ 1 pmol, related to label, is used for 1 mg polymer in a typical competitive assay protocol. Yılmaz et al. (1999) had demonstrated the possibility of reducing template amount in polymerization scheme to decrease imprint preparation costs. So, they investigated the amount of template needed for creation of a sufficient amount of binding sites in another study. Imprinted polymers with different monomer/template ratios ranging from 4:1 to 5000:1 were prepared and tested. They have demonstrated that adsorption capacity of imprinted polymers are higher than of the non-imprinted polymers at M:T ratio as high as 500:1. Also it was detected that at ratios between 4:1 and 100:1, the amount of polymers needed did not change significantly where polymer shows the highest binding capacity at 12:1 ratio. The required amount of polymer increased largely at higher ratio of 5000:1 and this demonstrates that amount of imprinted sites increase with using more templates. However, binding sites with high affinity is fewer due to simultaneously association and dissociation processes of the pre-polymerization complex in non-covalent imprinting method. On the other hand, equilibrium shifts toward complex formation with large excess of monomer at higher M/T ratios. Thus, amount of produced binding sites are small but they show high affinity. Another advantageous of using high M:T ratio is the avoidance of solubility problems (Yılmaz et al., 1999).

1.2.3.4 Degree of Cross-linking

Highly cross-linked imprinted polymers are required to acquire good separations for chromatographic applications. Polymers must be mechanically stable enough for chromatographic applications such as HPLC. Furthermore, stable rigidity is necessary for the protection of imprint memory. Imprinted polymers used in sensors

expose to less mechanical stress than in HPLC. Change in the recognition properties of polymer with decreasing cross-linking degree was investigated in the study of Yılmaz et al. Polymers can get more flexible structure with low cross-linking degree. Flexibility could be an advantage for some applications using imprinted films and membranes. A higher binding capacity can be obtained with the incorporation of more functional monomer and template. Different cross-linker amount was studied with constant monomer:template ratio and monomer concentration in the study. It was demonstrated that recognition properties of low cross-linked imprinted polymers were similar with the high cross-linked and amount of high affinity binding sites decreased with increasing cross-linking degree. Results showed that specifity and non-specific binding capacity are independent from cross-linking degree. Binding sites with molecular memory were successfully obtained with low cross-linked imprinted polymer (Yılmaz et al., 1999).

1.2.4 Polymerization Methods for MIPs

1.2.4.1 Bulk Polymerization

The most popular and general method for the production of MIPs is bulk polymerization. This method has challenging properties such as fastness and simplicity. Advanced and expensive instruments are not required for preparation (Li et al., 2011). Bulk polymerization is a simple solution polymerization method and imprinting conditions can be optimized directly. After polymerization, mechanical granulation is applied to obtain small particles (Yan & Row, 2006). Acquired particles are irregular in size and shape, and typically 5-50 μm sized (Poma et al., 2010). Particles, sized < 25 μm may be used as chromatographic support materials such as conventional high performance liquid chromatography (HPLC) columns, immobilized thin layer chromatography (TLC) plates, and entrapped capillary columns. Creation of 3-D binding sites for template may be advantages for imprinting. Oppositely, it is difficult to remove template from bulk polymer (Kryscio & Peppas, 2012). Moreover, grinding can cause the detriment of some interaction sites and this lead to decrease in chromatographic performance and binding capacity.

Grinding and sieving step is unfavorable, time-consuming, and induce to waste of polymer (50-75 % of acquired polymer is usable) (Yan & Row, 2006). Furthermore, bulk polymerization is an exothermic process, thus sample overheating is a danger when scaling-up the bulk polymerization (Li et al., 2011). Heterogeneous binding sites and remarkable requirement of template limit the use of MIPs synthesized by bulk polymerization as chromatographic adsorbents (Yan & Row, 2006).

The main difference between bulk and suspension, emulsion polymerization techniques is the no usage of stabilizers/surfactants in bulk polymerization. Monomer and template are used at a lower concentration in suspension and emulsion polymerization compared to bulk polymerization (Kryscio & Peppas, 2012).

1.2.4.2 Suspension Polymerization

Suspension polymerization creates aggregates of spherical particles without requirement of any granulation. Regularly sized microspheres can be obtained when the polymerization solution is diluted enough (Yan and Row, 2006). This method needs the use of stabilizer or surfactant. Pre-polymerization mixture droplets are suspended in continuous phase containing stabilizer or surfactant (Li et al., 2011). Size distribution of polymer particles is polydisperse. In conventional suspension polymerization, water is used as the continuous phase. Particle diameter of particles obtained by conventional suspension polymerization method is between 5µm and 2 mm (Pérez-Moral & Mayes, 2002). However, these polymers mostly demonstrate poor recognition. Non-covalent interactions between functional monomers and template may decrease due to the use of water as solvent. Furthermore, stabilizers or surfactants can disrupt the template-functional monomer interactions. Resulting from these disadvantages, monomer droplets are formed in liquid perfluorocarbon or in liquid paraffin (Li et al., 2011).

Uniform imprinted particles can be obtained with liquid perfluorocarbon and they present superior chromatographic efficiency and good selectivity at high flow rates. However, applicability and practicability of the method decrease due to requirement of specific fluorinated solvent and surfactant (Yan & Row, 2006).

1.2.4.3 Emulsion Polymerization

Emulsion polymerization is an effective method for the production of high-yield, monodispersed polymeric particles. Protein imprinting is successfully practiced by emulsion polymerization. However, remnants of surfactant complicate the emulsion polymerization (Li et al., 2011).

Mini-emulsion polymerization is a method for the production of MIP nanoparticles with high-yield. High-shear homogenization and the use of co-surfactant are required to synthesize 50-500 nm sized particles (Poma et al., 2010). Mini-emulsion polymer particles are polydisperse in size (Pérez-Moral & Mayes, 2002). Very small particles in the size of 30-220 nm can be obtained by this method however; surfactants or stabilizers in the polymerization mixture might block the binding sites. Wide distribution of high affinity binding sites is resulted from these components. Semi-covalent imprinting approach can be used to avoid this problem.

Core-shell emulsion polymerization is a two-phased method to obtain core-shell MIP nanoparticles. Preparation of monodisperse seed latex sized between 30 nm and 1 μm is continued with imprinting shell formation using emulsion polymerization. Magnetic cores can be used to obtain core-shell particles with high yield and binding capacity MIP nanoparticles with superparamagnetic structure. Porogen must be chosen carefully due to its effect on porosity and binding capacity. Secondary nucleation reaction can be prohibited by the optimization of synthesis conditions. Method has the advantage of applicability for large-scale industry. Nevertheless, surfactants and aqueous phase in polymerization mixture can disrupt the method and thus, particle size and imprinting effect (Poma et al., 2010).

1.2.4.4 Precipitation Polymerization

Precipitation polymerization ensures the obtainment of more uniform spherical imprinted particles with higher active surface area. Particles grow orderly after the coagulation of nano-gel beads with taking oligomers from solution. Thus, similar monodispersed beads are obtained and; size and porosity can be adjusted delicately by the change in polymerization conditions (Yan & Row, 2006). Particles prepared by precipitation polymerization method have particle size between 100nm and 10µm (Pérez-Moral & Mayes, 2002) and can be applied in chromatographic applications such as electrochromatography. Obtainment uniform polymers with high yield by precipitation polymerization are favorable for fabrication of MIP. Although, a large amount of template is required due to highly diluted polymerization solution, pH effect on template can be ignored in the diluted system. Particles prepared by this method present more excellent recognition binding properties compared to traditional bulk polymerization (Yan & Row, 2006). Beside binding advantage, precipitation polymerization bears the advantage of synthesis in a single step without using surfactant (Li et al., 2011). Disuse of surfactants ensures the applicability of method to various substances such as peptides (Poma et al., 2010).

1.2.4.5 Dispersion Polymerization

Dispersion polymerization begins with the homogeneous mixture of monomers, solvents, initiators and surfactants (dispensable) in contradiction to suspension polymerization. As the polymer is being formed, insoluble polymer and aggregates occur. The surfactant used in polymerization and surface rigidity stabilizes the polymer particles sterically (Perez-Moral & Mayes, 2002).

1.2.4.6 Free-Radical Polymerization

Free radical polymerization, also called chain growth polymerization, is one of important polymer synthesis methods. It is extensively used in industry, especially for the production of commercially significant plastics. Free radical polymerization

uses various vinyl monomers such as styrene, ethylene, and methyl methacrylate; and produces high yielded polymers efficiently. Controlled/living free radical polymerization (CLRP) methods are extensively studied methods and newly applied for the production of MIPs. These are reversible-addition fragmentation chain transfer (RAFT), metal-catalyzed atom transfer radical (ATRP) and nitroxide-mediated (NMP) polymerization methods. CLRP methods are applied to obtain well-established polymers with limited molecular weight distribution. Polymers obtained by CLRP methods have low polydispersity. Composition and functionality of these polymers can be controlled. Also, these methods are thermodynamically controllable. Chain termination reaction is negligible and chain grow rate is slow. These provides similar chain growth and relaxation rates. Thus, polymers produced by CLRP methods have the advantage of homogenous polymer network. Moreover, CLRP methods present superior advantages over conventional free radical polymerization and thus, these methods are valuable for the production of MIPs (Perez-Moral & Mayes, 2002).

1.2.4.7 Surface Imprinting

Surface imprinting, location of imprinted binding sites on or very near to surface of polymer, is very extensive method for protein imprinting. Surface imprinting is achieved by modification of polymer films or membranes synthesized by traditional methods or attaching the template on the surface of material with subsequent polymerization (Kryscio & Peppas, 2012). There are some advantageous for using surface imprinting method. Imprinted templates are located at the surface or in the proximity of surface. Thus, template removal is easier compared to highly cross-linked materials and this is the most promising advantageous of the method. Incomplete template removal, small binding capacity and slow mass transfer problems can be overcome by using this method. Additionally, surface imprinted polymers have higher binding capacity, faster mass transfer and binding kinetics compared to traditional MIPs (Li et al., 2011).

Chromatographic grade imprinted materials can be obtained by surface imprinting of MIPs onto pre-produced materials attractively. Thin imprinted layers have been coated onto chromatography grade silica at the surface of the beads with different method applications (Ruckert et al., 2002; Sellergen et al., 2002). Sreenivasan produced an imprinted layer selective to specific molecules at the surface of commonly utilized polymers without changing the bulk properties. Modified surfaces, can be prepared by this method simply, find application area for separation, sensor and medical purposes (Sreenivasan, 2006).

1.2.4.8 Epitope Imprinting

Antibody-antigen interactions in nature occur between antibody and antigenic site of protein. The epitope is a short amino acid sequence that matches antibody binding site (Bossi et al., 2007). The group of Rachkov (2000, 2001) proposed a new method to produce MIPs with protein recognition properties with the epitope approach (Rachkov & Minoura, 2000; Rachkov & Minoura, 2001). This method has been used for the preparation of MIPs for peptides, hormones and DNA (Bossi et al., 2007).

A short polypeptide, usually present on the protein surface, is used as a template instead of a larger polypeptide or protein which is the real target. The method is based on the mimicking specific interactions between an antibody and antigen (Kryscio & Peppas, 2012). After polymerization, imprinted site can recognize and bind the target (Bossi et al., 2007).

The epitope approach combines the terms of surface and bulk imprinting approaches. This method has advantages over bulk and surface imprinting methods towards the major problems for successful protein imprinting. Advantageous of epitope imprinting can be listed as:

i) High cross-linked and structured binding sites are obtained by the use of small template without concerning template removal.

ii) Small molecular weighted molecules, used as template, supplies analogous to natural recognition pathway imprint. The use of small imprints minimizes the complexity of template and limits the non-specific interactions. Thus, binding affinity and selectivity of MIPs are increased theoretically.

iii) Polypeptides are more resistant to environment conditions compared to secondary and tertiary structures. Also, aprotic organic solvents can be used for solubility or conformational change concerns.

iv) Using short peptides of a protein instead of expensive protein markers is cost-effective (Kryscio & Peppas, 2012).

On the other hand, evaluation of true efficiency for protein imprinting by epitope approach is not very simple. Epitope method has been applied with a few amino acids long and targets were just small peptides with 8-10 amino acids long and non-three-dimensionally structured. Application for a protein with sequences more than 200 amino acids, three-dimensional structure of protein must be considered due to its significant role in recognition (Bossi et al., 2007).

1.2.5 Challenges of MIPs

1.2.5.1 Imprinting Large Groups

Imprinting water-soluble biomacromolecules such as proteins is very difficult. These molecules should be imprinted in the media similar to natural environments to promise conformational integrity. Large biomacromolecules cannot move within highly cross-linked polymer and this results poor rebinding efficiency.

Methods for imprinting biomacromolecules are surface imprinting, epitope-iimprinting, micro-contact imprinting, metal coordination procedure and protein imprinted hydrogels. Surface imprinting is already the most popular and general method against to diffusion limitation problem. Imprinting template molecules covalently onto the surface of solid material has some advantages. This method can be used for templates insoluble in pre-polymerization mixture. Thus, template

aggregation can be minimized and more homogeneous binding sites can be produced. The disadvantage of surface imprinting is the requirement of multistep procedure of the support before attaching the template.

Epitope-imprinting, directed with similar mechanism wit antibody-antigen interactions, uses protein fragments such as short peptides or amino acid residues as template. These polymers, having recognition ability for peptide or amino residue, exhibit selective recognition for the corresponding protein. Epitope imprinting enables template removal after polymerization and decreases the production cost due to no requirement to notably pure protein. Preparation of protein imprinted polymers with recognition properties in aqueous media is inestimable due to water-soluble property of biomacromolecules. Sufficient selectivity toward template can be procured by hydrophobic interactions together with shape recognition.

1.2.5.2 Heterogeneous Binding Sites

Non-covalent interactions for designing MIPs usually tend to heterogeneous binding sites. Non-well specified process of pre-polymerization step induces complexation with improper ratios of template to monomer. Moreover, excess monomers are used for complex formation. These may cause to creation of different and non-selective binding sites. These troubles can be overcome by applying semi-covalent approach. Furthermore, semi-covalent approach can prevent template bleeding. It is difficult to remove the left template with organic solvent elution due to strong interactions between template and polymer. Homogeneous binding sites can be obtained by the combination of molecular micelles with molecular imprinting technology. This method relies on the substitution of monomer with a surfactant monomer by mini-emulsion polymerization. Micelle formation tends to location of all binding sites homogeneously onto surface of MIPs. Other succeeding approaches such as selective chemical modification of low affinity sites, stoichiometric non-covalent imprinting can be performed for reduction of heterogeneous binding sites and improvement of binding homogeneity (Li et al., 2011).

1.2.5.3 Incompatibility with Aqueous Media

MIPs show good recognition properties in the environments where they have been synthesized. Polar solvents can disturb hydrogen bond formation between template and polymer that is synthesized in organic solvent. Several methodologies have been developed to work in polar solvents such as aqueous media. One of these is two-step extraction. MIPs' extraction and micro-liquid-liquid extraction (MLLE) methods are combined in two-step extraction. Template is extracted from aqueous phase into organic phase and incorporated to the solid phase of MIPs. Two-phase solvents extraction system improves the specificity and presents extreme potential for MIP applications in biological and environmental samples.

Hydrophilic monomers such as HEMA, β-cyclodextrins (β-CPs) can be used for the production of water-compatible MIPs. Another approach is restricted access material MIPs (RAM-MIPs) synthesis. MIPs' surface is modified hydrophilicly in two-step polymerization for recognition in aqueous media. Furthermore, water can be used as porogen to take the advantage of solvent memory.

Metal-ion mediated method is another useful strategy to produce water-compatible MIPs specifically (Li et al., 2011).

1.2.5.4 Template Leakage

Template leakage (or named as template bleeding) is one of drawbacks of molecular imprinting. It was observed that a bit of template used in imprinting can remain in the polymer after washings for template removal (Tamayo et al., 2007). Recognition properties of MIPs can be influenced by the slow leakage of template especially in the analysis of trace amounts (Kryscio & Peppas, 2012). Template leakage problem usually show up in case of solvent or volume changes of polymers (Bui & Haupt, 2010). In the studies with low concentration of template, template leakage was not detected. Furthermore, template leakage is not a problem in some situations.

An analogue of the target molecule can be used as template to prevent template leakage (Tamayo et al., 2007). In this manner, template leaked from polymer is not inhibitive for the target analysis. Andersson et al. originally suggested this approach for selective extraction of target with using template analogue in imprinting process (Andersson et al., 1997). Unfortunately, template-analogue imprinted polymers can show inferior molecular recognition properties considering to polymers prepared with original analyte as template. Use of template analogue with very similar shape and functionality can enhance the recognition ability (Tamayo et al., 2007).

Template leakage causes to some problems in analytical separations with MIPs such as peak broadening in liquid chromatography. Template leakage during elution leads to error in quantification. Consequently, interference arising from template leakage must be checked for method developments (Andersson, 2000).

In the study of Ellwanger et al. (2001), different methods were tested for template removal. Generally, methanol/acetic acid mixture (9:1, v/v) is used in Soxhlet extraction or in batch mode for template removal. Removal efficiency can be increased by using trifluoroacetic acid or acetic acid as pure with combining thermal treatment, ultrasonication or microwaveassisted extraction. Nevertheless, the use of harsh solvents for template removal cause to decrease in binding affinity or selectivity (Ellwanger et al., 2001).

1.2.5.5 Imprinting Hydrophilic Compounds

Water-soluble hydrophilic compounds such as alkaloids cannot be imprinted in apolar organic solvents due to solubility problems. Hydrophilic template can be converted to hydrophobic by alkyl chain attachment to overcome solubility problems. Chemical modification and separation of template molecule is time-consuming. Furthermore, this approach limits the applications due to exhaustion of functional groups during chemical reactions. Hydrophobic analogue of hydrophilic target molecule can be used as an alternative to original molecules. However, it is not

easy to find an appropriate analogue to hydrophilic molecule. Use of ion-pairs as template for water-soluble molecular imprinting is the simplest method practiced until now (Li et al., 2011).

1.2.6 Characterization of MIPs

Polymeric materials with macroscopic or microscopic network system, including MIPs, cannot be characterized easily due to their insoluble and compelling structure. Chemical, morphological and molecular recognition features of MIPs must be investigated for detailed characterization. Molecular recognition features of MIPs are examined in different experimental conditions such as pH, temperature, initial concentration of analyte and absent of competitive agents. Several methodologies can be used for chemical and morphological characterizations.

1.2.6.1 Chemical Characterization

Solution state techniques cannot be applied to insoluble MIP structures. Thus, elemental micro-analysis, FTIR, solid-state NMR techniques are used for chemical characterization of MIPs. For the characterization of pre-polymerization complexes, FTIR, NMR and UV spectroscopic techniques should be performed.

Elemental micro-analysis is used to determine carbon, hydrogen, nitrogen, chlorine percentages within the polymers. It is usually used in the case of copolymerization. Co-monomer composition of the polymer can be obtained if one of the co-monomers contains a heteroatom such as nitrogen in 4-vinylpyridine monomer in poly(4-vinylpyridine-co-divinylbenzene). It should be paid attention to template remnants due to sensivity of detection.

FTIR spectra of MIPs can be applied for quantitative consideration about polymer composition. This method is valuable when signals belonging to different functional groups of polymerization components are procured with high resolution. The method

has potential to analyze the non-covalent interactions between MIP and template such as H-bonds.

NMR spectra of insoluble, challenging MIP structures can be obtained by solid-state NMR. It provides the comprehending different chemical environments and the chemical formula of reticular MIPs.

1.2.6.2 Morphological Characterization

Morphological characterization of MIPs can be performed with similar methods for porous solid materials. Specific pore volumes, pore sizes and size distributions, and specific surface areas of materials can be analyzed by several morphological analysis methods such as SEM, inverse size exclusion chromatography (ISEC) and nitrogen sorption porosimetry.

Cross-linked insoluble polymers adsorb some quantity of solvent and swell. Steady state swelling ratio is the direct function of crosslinking degree. Measuring the amount of solvent uptake to micro- and macropores gives information about specific pore volume of polymer (mL/g). These experiments are simple and low-cost method for the morphological characterization.

In nitrogen sorption porosimetry analysis, a gas (usually nitrogen) is passed through the fixed mass of dried polymer. The amount of gas adsorbed by polymer is measured at several fixed pressures. Adsorption isotherms by Brunauer–Emmett–Teller (BET) theory and mathematical models provide information about specific surface area (m^2/g), specific pore volume (mL/g), average pore diameter and pore size distribution. This method is more convenient for the analysis of meso- and micropores.

In mercury intrusion porosimetry analysis, mercury is forced through the fixed mass of dried polymer. Similar information about morphological features as similar

as nitrogen sorption porosimetry analysis can be obtained although this method investigates macropores more sensitively.

ISEC examines the pore structure of polymer in wet-state in contrast to nitrogen sorption and mercury intrusion porosimetry methods. The porous solid is used as stationary phase in a flow-through column set-up in a typical ISEC experiment. Soluble polymer standards of known molar mass are eluted from the column at a fixed flow rate. The time taken is measured and suitable mathematical models are applied to get information about pore structure.

Microscopy analysis is used to specify length scales of polymers by several ways. Light microscopy can be used to demonstrate structural integrity of polymer beads while macropores imaging is usually performed by SEM (Cormark &Elorza, 2004).

1.2.7 Applications of MIPs

1.2.7.1 Purification and Separation

Separation of enantiomers and other molecules purely is one of the most interested and needed aims for pharmaceutical industry. MIPs have been used as stationary phases in HPLC and capillary electrochromatography (Schweitz et al., 1998) to separate compounds (Remcho & Tan, 1999) and racemates (Kempe & Mosbach, 1995) from several complex mixtures. The advantage of intrinsic stability, low cost and simple production of MIPs is practiced on in the chromatographic applications of MIPs. Furthermore, stereoselectivity and enantioselectivity for amino acids and their derivatives (Andersson et al., 1990), peptides (Kempe, 1996), and anti-inflammatory agents (Kempe and Mosbach, 1995) are the excellent feature of MIPs.

Extraction and concentration of biologically important molecules from complex samples such as milk, serum and urine are difficult and time consuming processes with limited accuracy.

Specific and stable synthetic receptors are suitable and have several advantages in the purification and separation of molecules from complex samples. MIPS are focused materials as purification and separation matrixes from food and biologic samples. There are several studies with MIPs for separation, isolation of pesticides, environmental pollutants, enantiomers, steroids, antibiotic and several biological active molecules.

1.2.7.2 Separation of Bioactive Compounds Using MIPs

There are many studies for isolation of pharmacophoric compounds from herbs using MIPs, directly. One of the highly active biomolecules in flavonoid family, quercetin, was imprinted and used for extraction of its analogues from Chinese gingko leaves. These quercetin extracted MIPs used for inhibition of protein kinase that can be inhibited by quercetin (Zhu & Xu, 2003; Zhu et al., 2003). These studies indicated that MIPs could be efficiently used instead of traditional isolation methods for drug discovery and biomolecule screening.

1.2.7.3 Screening of Bioactive Molecules Using MIPs

The group of Mosbach (2001) performed MIPS to an ‘‘anti-idiotypic’’ approach to produce biologically active molecules with template guidance. This group also imprinted kallikrein inhibitor and applied these MIPs to enable new inhibitor production. It was detected that kallikrein imprints act as the active site tissue kallikrein enzyme. These MIPs compared with synthetically produced inhibitors to monitor drugs (Mosbach et al., 2001). More inhibitors or active enzyme sites can be designed with MIPs to screen drugs in the future studies.

1.2.7.4 Sensors

Biological recognition molecules such as enzymes, antibodies, and receptors have been widely employed as affinity recognition molecules for the preparation of biosensors. Artificial receptors such as MIPs are currently under investigation in

numerous applications owing to their stability and advantageous features (Plietsky et al., 2001).

A molecular imprinting screen-printed electrode-based biomimitic sensor for the detection of 2,4-dichlorophenoxyacetic acid (2,4-D) using differential pulse voltammetry was reported by Kröger et al (1999). The screen-printed electrodes were coated with a homogeneous thin layer of polymer and covered with an agarose layer to protect the molecular imprint layer from the washing steps (Kröger et al., 1999).

A highly sensitive piezoelectric sensor incorporating a MIP as the recognition element has been reported for the detection of 2-methylisoborneol (MIB). MIB and geosmin are off-flavor compounds produced by a variety of microorganisms, which cause odor problems in drinking water and in fish. Highly sensitive detection limits down to 10 ng mL^{-1} were obtained. The sensitivity of these devices has been improved by 20-fold while maintaining selectivity (Ji et al., 2000).

The group of Dickert and Hayden (2001, 2003) reported some MIPs for the detection of microbial cells in aqueous samples using quartz crystal microbalance (QCM) (Dickert et al., 2003; Hayden & Dickert, 2001; Hayden et al., 2003). Also this group (2003) published a review on sensor strategies for microorganism detection (Dickert et al., 2003). Biological recognition materials like antibodies showed promising sensitivity towards the detection of cells. But the main limitation was the limited stability of the resulting sensor layers.

Say et al. (2009) applied molecularly imprinted polymers to sensor systems and developed a (QCM) hybrid sensor for 8-hydroxy-2'-deoxyguanosine. 8-Hydoxylated guanine derivatives, such as 8-oxoguanine (8-oxoG) and 8-hydroxy-2'-deoxyguanosine (8-OHdG), are known as biomarkers for oxidative stress. It was determined that environmental agents such as benzene, mineral powders or smoking, cancer and chemotherapy caused to 8-OHdG formation in human. Several methods such as gas chromatography-mass spectroscopy (GC-MS), high performance capillary electrochromatography (HPCE), and HPLC and immunoaffinity

chromatography are used for OHdG assay but these are not favored due to being expensive and requirement of pre-processing. However, QCM is a simple and cheap method and effectively sensitive to mass alteration but don't have specific selectivity. Modification of QCM surface with several chemicals and biomaterials can provide selectivity. 8-OHdG specific QCM electrode was obtained by using 8-OHdG as template and metal-chelate interaction. This MIP-QCM electrode was applied for 8-OHdG assay in blood samples (Say et al., 2009).

Another example to molecularly imprinted polymer-sensor application is the study of Prasad and his group (2009). Dopamine amounts in Parkinson patients decrease and vary in the range of 1.22-1.81 ng/mL. Dopamine levels in serum samples provide extra information for the treatments of Alzheimer disease and schizophrenia. In the study, trace amounts of dopamine in real samples were assigned with MIP-sensor. Hanging mercury drop electrode (HMDE) modified with MIP was developed for direct dopamine assay in serum, cerebrospinal fluid and drug samples. HMDE was modified with poly(mel-co-chl) synthesized from melamine and chloranil precursors. Selectivity experiments were performed with using molecules including functional groups or having zwitter ions. For this purpose, ascorbic acid, uric acid, caffeine, glucose, urea, citric acid, glycine, histidine, cysteine, tyrosine, creatine and epinephrine structures were applied. MIP-modified sensor proposed for dopamine assay performed high performance with poly(mel-co-chl) having zwitter ion binding sites. It was specified that this method notably simple, rapid and re-usable method which measures by increasing the interaction between analyte and MIP-modified HMDE sensor (Prasad et al., 2009).

1.2.7.5 Catalysis

In many cases, enzymes exhibit low catalytic activities due to the presence of organic solvents, inhibitors, and/or complex mixtures and perturbations in the temperature and solution pH. These problems may be avoided by employing synthetic biomimetic catalytic counterparts instead of biomolecules such as enzymes and catalytic antibodies. The catalytic counterparts can be synthesized by tuning the

enzyme active site through molecular imprinting with substrates or their transition state analogues (TSAs). For the preparation of catalytically active MIPs, a cavity has to first be made with a defined shape corresponding to the shape of the substrate or, even better, to the shape of the transition state of the reaction. At the same time, functional groups are incorporated that act as binding sites, coenzyme analogs, or catalytic sites within the cavity and in a defined stereo-chemical manner. These artificial polymeric catalysts are more durable and more resistant to harsh environments than biomolecules, thus they may be highly advantageous for industrial continuous transformation and/or conversion reactions (Kandimalla & Ju, 2004).

1.2.8 MIP Studies with Cholesterol

In the study of Hwang and Lee (2002), cholesterol-imprinted polymers were prepared by bulk polymerization with covalent and non-covalent imprinting methods. Firstly, template-containing monomer, cholesteryl (4-vinyl)phenyl carbonate was used in polymerization. Then, methacrylic acid and 4-vinylpyridine functional monomers were complexed with template and used in polymerization. Columns were packed with these MIPs and used for the separation of cholesterol from other steroids. It was determined that cholesterol adsorption capacities of MIPs was significantly depend on functional monomers used in polymerization. MIP prepared by covalent imprinting adsorbs more cholesterol. Specific binding of cholesterol onto MIPs lead to slightly different selectivity factors such as 2.9 and 3.2. The capacity factors for cholesterol were determined to be 3.5, 4.0 and 3.1, for covalently imprinted, 4-vinylpyridine-based, and methacrylic acid-based non-covalently imprinted polymers, respectively. Consequently, recognition sites formed by template significantly affect the adsorption capacity. Also, insignificant difference between selectivity factors of MIPs against to β-estradiol shows the specific cholesterol binding to recognition sites (Hwang & Lee, 2002).

Srenivasan (1997) used molecular imprinting method to create cholesterol recognition sites in synthetic polymers. Cholesterol imprinted polymers were prepared with using 2-hydroxyethyl methacrylate by γ-irradiation. Preliminary

studies using a mixture of cholesterol and testosterone demonstrated the high degree of selectivity of the polymer towards cholesterol. Chromatographic results clearly suggest that the molecularly imprinted poly(HEMA) has a high degree of selectivity in its interaction with cholesterol (k' (CHO/testosteron): 26.13) (Sreenivasan, 1997).

In the study of group of Whitcombe (1995), recognition site functionality inserted into highly cross-linked polymeric matrices via molecular imprinting. These polymer matrices were prepared for compounds with single (or multiple, spatially separated) hydroxyl groups. Method depends on the use of the 4-vinylphenyl carbonate ester which is a covalently bound template monomer. This template monomer was procured easily and efficiently by cleavage of CO_2 hydrolytically. This preparation method of template monomer leads to noncovalent recognition site formation, bearing a phenolic residue. This residue can interact with the template through hydrogen bonding. The polymers obtained by this method were shown to bind cholesterol with a single dissociation constant, thus displaying characteristics similar to a true biological receptor or synthetic host (Whitcombe et al., 1995).

In the study of Asanuma et al. (1998), synthetic receptors for cholesterol were prepared with using cholesterol as template. MIPs were prepared by cross-linking of β-cyclodextrin with hexamethylene diisocyanate (HDMI) or toluene 2,4-diisocyanate (TDI) in dimethyl sulfoxide. Binding experiments were performed in a water/THF mixture (5/6, v/v) due to solubility problem of cholesterol in water. The molecularly imprinted polymer synthesized in presence of TDI as a cross-linker showed a better rebinding capacity than the one prepared with HDMI; probably TDI is more adequate to regulate the positions of β-CyD residues. Also, 60 % of the initial cholesterol adsorbed rapidly onto TDI-MIP within 1 min. But, non-imprinted polymers prepared with the same method adsorb much smaller amount of cholesterol. Stigmasterol and phenols were used to test the selectivity of MIPs. Stigmasterol, very close chemical analogue of cholesterol, was adsorbed by the polymeric receptor with a similar amount. The selectivity ratio for cholesterol against phenol was enormously high. These MIPs indicates a strong potential for practical

applications due to removing all adsorbed cholesterol from the polymers by treating with ethanol (Asanuma et al., 1998).

Ciardelli et al. (2006) produced advanced polymeric systems by molecular imprinting technology and applied these polymers in extracorporeal blood purification. Membranes were prepared with using MMA and AA by phase inversion method. Three polymeric systems in form of nanoparticles were prepared differing in the polymerization solvent (a mixture of acetonitrile and ethanol (1:1) or pure ethanol), and the molar ratio between the functional monomer and the cross-linker (2.3:1 and 1:1) with cholesterol as template. Two out of three of the prepared polymers showed a very good template rebinding capacity both in phosphate buffer solution (pH 6.9) and in ethanol. In particular the nanoparticles rebound 115.4 mg cholesterol/g polymer in buffer solution, and 57 mg cholesterol/g polymer in ethanol. These nanoparticles were embedded into membrane prepared by phase inversion method to provide specific binding sites for cholesterol. These membranes were prepared for the aim of selectively cholesterol removal from blood. Cholesterol removal is based on the interactions between membrane/nanoparticles and cholesterol at a molecular level. The deposition of the nanoparticles on the surface of the phase inversion membranes produced devices with interesting rebinding performances towards cholesterol in buffer solution: a specific recognition of 14.09 mg cholesterol/g system (membrane and nanoparticles) was detected, indicating maintained binding capacity of supported particles as well (Ciardelli et al., 2006).

The group of Aghaei (2010) has prepared a novel cholesterol biosensor based on capacitive detection using molecular imprinting technology. Cholesterol was used as a template molecule in the electro-polymerization and the sensitive layer was prepared by of 2-mercaptobenzimidazole (2-MBI) on a gold electrode. Cyclic voltammetry and capacitive measurements were used to monitor the process of electro-polymerization. Surface uncovered areas were plugged with 1-dodecanethiol to make the layer dense, and the insulating properties of the layer were studied in the presence of $K_3Fe(CN)_6/K_4Fe(CN)_6$ redox couples and also by the use of AC impedance measurements. The template molecules and the non-bound thiol were

removed from the modified electrode surface by washing with an alkaline solution of ethanol. The proposed molecularly imprinted polymer capacitive (MIPC) sensor exhibited good selectivity for cholesterol. The reproducibility and repeatability of the MIPC sensor were all found to be satisfactory. The results from sample analysis confirmed the applicability of the MIPC sensor to quantitative analysis (Aghaei et al., 2010).

A hybrid method of covalent imprinting and non-covalent imprinting was used to prepare cholesterol-imprinted polymer by Wang et al. (2005). This approach involves the copolymerization of a template containing monomer, cholesteryl 2-hydroxyethyl methacrylate carbonate, and a cross-linker, followed by hydrolysis to afford a flexible guest-binding site accompanied with the easy and efficient removal of a “sacrificial spacer”. The effect of solvent on the binding capacity of cholesterol-imprinted polymer towards cholesterol was studied, indicating that a good binding capacity towards cholesterol could be achieved in a less-polar solvent. Batch rebinding tests showed this new cholesterol-imprinted polymer to have a large adsorption capacity with a high dissociation constant and a low median binding affinity to cholesterol. The increase of binding capacity is mainly due to a higher template/cross-linker ratio. However, a higher dissociation constant may be ascribed to its more flexible binding sites and weaker binding affinity between template and MIPs. The binding experiments of cholesterol-imprinted polymer towards a series of structural analogues of cholesterol, including cholesterol acetate, progesterone and stigmasterol, were carried out in hexane. The results showed that cholesterol-imprinted polymer almost did not bind cholesterol acetate at all because the hydrogen-bonding site is blocked. It exhibited a similar binding towards both cholesterol and stigmasterol, but much higher binding towards progesterone (Wang et al., 2005).

A sol–gel method was used to fabricate a cholesterol MIP for application in polar solutions by Hsu and Yang (2008). In this study, (cholesteryl propylcarbamate) triethoxysilane and tetraethyl ortho-silicate were used as the hydrophobic monomer and cross linker, respectively. The MIP had a larger pore volume when formation of

the polymer was catalyzed at a higher pH than when it was formed at lower pH values. Both pore volumes were greater than those found for the respective control polymers formed without template. However, only the polymers formed at low pH values showed an imprinting effect. Nevertheless, the sol–gel procedure gave only a small amount of non-specific binding for both the MIP and NIP when synthesized at low pH values. The MIP showed high selectivity towards cholesterol in comparison with other steroid hormones, and also to a lesser extent recognized vitamin D3 in methanol solution containing 5 vol.% water. The recognition sites of MIPs formed at lower pH appear to show that each recognition site was formed from a single cholesterol molecule. At higher pH values, the porous network of silica showed more non-specific adsorption and a reduced imprinting effect (Hsu & Yang, 2008).

Sellergen et al. (1998) prepared imprinted polymers for selective adsorption of cholesterol from gastrointestinal fluids. A series of highly cross-linked terpolymers of methacryloylated cholesterol or bile acid methyl esters, methacrylic acid, and ethyleneglycol dimethacrylate were prepared in the presence or absence of cholesterol acting as a template molecule. The polymers were freed from cholesterol by washing and the resulting adsorbents tested for cholesterol rebinding in the chromatographic mode using methanol-water as mobile phase or in the batch mode using an intestinal mimicking fluid of concentrated bile acids in water. The polymers prepared in polar solvents, favoring the apolar association of the template and the apolar face of the amphiphilic monomers, exhibited selective rebinding of cholesterol as compared to a non-imprinted blank polymer prepared identically but without cholesterol. The strongest rebinding was seen for the polymer prepared using 3β-methacryloyl-cholesterol as the functional monomer. Using a physiologically relevant intestinal-mimicking solution of cholesterol, these polymers adsorbed circa 17 mg cholesterol per gram dry adsorbent, whereas a non-imprinted blank polymer adsorbed circa 13 mg. The adsorptive capacity seems to be due to binding sites induced by the presence of steroid units in the polymer backbone and the presence of cholesterol during formation of the adsorbent. The templating effect of cholesterol probably involves apolar interactions with the apolar parts of the monomers during polymerization. This may result in hydrophobic binding pockets capable of

accommodating cholesterol in the subsequent rebinding experiment. The imprinted polymers showed the highest uptake of cholesterol as compared to other adsorbents (<13 mg/g) that were expected to show high affinity for cholesterol. The adsorptive capacity exhibited by the cholesterol imprinted polymers, as well as their low cost and ease of preparation, appears promising for their future therapeutic use in the prevention of diet-cholesterol related diseases. The adsorbents may also be useful in other applications relying on strong and selective binding of steroids in aqueous media (Sellergren et al., 1998).

Boonpangrak, Prachayasittikul et al. (2006) prepared molecularly imprinted polymer microspheres by precipitation polymerization using a sacrificial covalent bond. In the study, cholesteryl (4-vinyl)phenyl carbonate was used as a template monomer. The imprinted microspheres were prepared using ethylene glycol dimethacrylate (EDMA) and divinylbenzene (DVB) as crosslinker. The base-labile carbonate ester bond was easily hydrolyzed to leave imprinted cavities in the resulting polymers. Radio ligand binding analysis, elemental analysis, and scanning electron microscopy were used to characterize the imprinted materials. Imprinted microspheres prepared from DVB cross linker had larger and more defined spherical shape, and displayed better imprinting effect than did the EDMA-based microparticles. For comparison, imprinted bulk polymers were also prepared in the same solvent used in precipitation polymerization. Elemental analysis results indicated that imprinted microspheres contained more template monomer units than bulk materials. The efficiency of template removal by hydrolysis treatment for microspheres was also higher than that for bulk polymers. For DVB-based polymers, imprinted microspheres displayed higher specific cholesterol uptake than did the corresponding bulk polymer. The present study demonstrated that precipitation polymerization method can be used to prepare covalently imprinted polymer microspheres (Boonpangrak, Prachayasittikul et al., 2006).

Molecularly imprinted hydrophobic monolayers were fabricated by the group of Plietsky (1999). They were produced by spontaneous self-assembly of hexadecyl mercaptan in the presence of cholesterol on gold surfaces. The lypophilic layer of

long chain hexadecan was formed around the template molecules adsorbed on gold surface. The extraction of cholesterol resulted in formation of sites in the layer of hexadecyl mercaptan which could selectively re-bind the template molecules. The imprinting cavities were used as channels for potassium ferricyanide which was reduced at the electrode surface. It was shown, that the molecular recognition process running inside of these channels diminished the mass-transport of potassium ferricyanide to the electrode surface and consequently reduced an electrochemical signal. The change of potassium ferricyanide reduction peak was related to the cholesterol concentration. The formation of the cholesterol-specific monolayers, their specificity and stability were studied and detected that imprinted monolayer was able to discriminate between hydrophobic and more polar substances having similar structure. Also, the sensor gived a possibility of cholesterol detection in the 15–60 μM ranges (Plietsky et al., 1999).

Tong et al. (2011), synthesized a novel chitin derivative, cholesteryl chitin carbonate (Chitin-Chol), from chitin and cholesteryl chloroformate. This product was used as a covalently bound template precursor for imprinting cholesterol. After cross-linking with toluene 2,4-diisocyanate, it was efficiently cleaved hydrolytically to afford a guest-binding site accompanying the easy and efficient removal of a sacrificial spacer. The selectivity and efficacy of a chitin-based imprinting polymer for steroid binding were assessed by a chromatographic screening process. The results of binding experiments showed that this MIP had a high binding capacity with cholesterol. The target discrimination towards cholesterol over its close structural analogue suggested that the polymer recognition site was possible on the basis of the inversion of configuration of a single hydroxyl group. In addition, noncovalent imprinting was done using chitin as a precursor and its binding properties for cholesterol were also evaluated (Tong et al., 2011).

Steroid-selective polymers were prepared by Kugimiya et al (2001). The molecular imprinting technique was applied by using 2-(methacryloyloxy)ethyl phosphate as functional monomer. The retentivity and selectivity of the obtained imprinted polymers were evaluated by liquid chromatography. The cholesterol-

imprinted polymer showed higher affinity for cholesterol than that for cholesterol derivatives. The selectivity of the imprinted polymer was superior to the imprinted polymer prepared with the conventional functional monomer, 2-(trifluoromethyl)acrylic acid (Kugimiya et al., 2001).

In the study of Gupta and Kumar (2011), hybrid sol–gel MIPs were synthesized in the form of crushed powder (CP) by both non-hydrolytic and hydrolytic method for cholesterol recognition. The template molecule was extracted by means of soxhlet extraction and calcination method. The cholesterol adsorption experiments were performed by using non-imprinted (NICP) and extracted crushed powder (ExCP) and the percentage of adsorption was determined by measuring the residual quantity in the analyte solution using Liebermann-Burchard (L-B) reagent. The adsorption studies with NICP showed interference with L-B reagent as well as non-specific binding between analyte molecules and silica matrix. The percentage of adsorption or rebinding was found to be higher for phenyl triethoxysilane (PhTEOS)-derived ExCP (composition 3) which was synthesized by the aqueous sol–gel processing method at low pH as compared to PhTEOS-derived (composition 1) and 3-aminopropyltriethoxysilane (APTES)-derived ExCP (composition 2) prepared by nonhydrolytic method. The reusability of used ExCP after reextraction was also investigated. The various factors affecting rebinding of template molecules were discussed along with interference study. The study provided information on molecular imprinting of cholesterol in sol–gel matrix and highlighted the importance of characterization of MIPs before applying it for sensing applications (Gupta & Kumar, 2011).

Yavuz et al. (2007) prepared cholesterol-imprinted polymeric particles with using N-Methacryloyl-(L)-tyrosinemethylester (MAT) as the complexing monomer. Pre-polymerization of cholesterol was prepared with MAT and then polymerized with 2-hydroxyethyl methacrylate by bulk polymerization. The template molecules were removed from the polymer structure in the ratio of 76–84% of the initial concentration using chloroform. MIP particles were characterized by elemental analysis, FTIR, SEM, swelling tests and surface area measurements. Cholesterol

adsorption experiments were performed in a batch experimental set-up. Adsorption medium was methanol or intestinal mimicking solution. Stigmasterol and estradiol were used as competing molecules in selectivity tests. MIP particles prepared using higher amounts of cholesterol exhibit significantly higher capacity to the NIP particles. MIP particles were 3.09 and 3.60 times selective with respect to the stigmasterol and estradiol, respectively. It was detected that MIP particles showed negligible loss in the cholesterol adsorption capacity after five adsorption–desorption cycles with the same adsorbent (Yavuz et al., 2007).

Monodispersed molecularly imprinted polymer particles selective for cholesterol were prepared by Kitahara et al (2010). Styrene and divinylbenzene were copolymerized in the presence of template silica gel particles (particle size: 5μm; pore size: 10 nm) functionalized with cholesterol on the surface, followed by dissolution of the cholesterol-bonded silica gel with NaOH aqueous solution. Transmission and scanning electron micrographs of the molecularly imprinted polymer (MIP) particles revealed good monodispersity and porous structure. The MIP particles were packed into a high performance liquid chromatographic column, and its recognition ability of cholesterol was evaluated using cholesterol, cholesterol esters and fatty acid methyl esters by comparison with the non-imprinted polymer (NIP) particles prepared from styrene and divinylbenzene without cholesterol. It was detected in the study, The MIP particles showed a high affinity for cholesterol and cholesterol esters ($K'_{MIP}/K'_{NIP} > 5.7$). The polymer particles showed a high affinity for cholesterol and cholesterol esters, but showed no affinity for fatty acid methyl esters. These results indicate that the MIP column recognizes the cholesterol moiety. As a result, the templating polymerization method in the porous silica gel particles will be useful for preparing monodispersed MIP particles (Kitahara et al., 2010).

Boonpangrak, Whitcombe et al. (2006) applied nitroxide-mediated living radical polymerization for the first time to prepare molecularly imprinted polymers. The unique chain propagation mechanism in the living system resulted in different binding characteristics for the final MIPs synthesized. MIPs using cholesterol as template and non-imprinted polymers (NIP) were prepared using either the NMP

reagent or benzoyl peroxide (BPO) as initiator. The covalently linked cholesterol was removed by basic hydrolysis. For comparison, NIPs were subjected to the same hydrolysis treatment. Compared to MIPs prepared under the same condition using a traditional radical initiator, template cleavage from the covalently imprinted NMP polymer was much more efficient. The imprinted hydrolyzed polymer prepared by NMP also displayed an imprinting effect that was clearly superior to that obtained using traditional radical polymerization, particularly for the high affinity sites that were easily characterized by radioligand binding analysis. It was clearly indicated that the increased cholesterol binding by MIP prepared with NMP reagent was due to the different imprinting process, rather than any non-specific effect such as the altered surface area. Although the present NMP reagent requires a high temperature to maintain the activity of the growing polymer radical, the NMP-based MIP displayed cholesterol affinity and capacity similar to MIPs that were synthesized at a more conventional temperature (Boonpangrak, Whitcombe et al., 2006).

1.3 Nanostructures

One of the great scientific and technical achievements at the end of the 20^{th} century is the creation of nanomaterials and nanotechnology. The prefix “nano” derives from the Greek word “nanos” meaning dwarf. It matches one thousand millionth of a particular unit and pertains to a length of 10^{-9} m (1 nm). It is predicted by experts that the scientific and technological advance in the present century will be much determined by achievements associated with nanomaterials, nanotechnology, and their application in various fields of natural science and technology and in other fields of human activity.

The most likely trends in nanotechnology are (i) molecular nanotechnology, (ii) nanomaterials and nanopowders, (iii) nanoelectronics, (iv) nanooptics and nanophotonics, and (v) nanobiometrics (Guz & Rushchitskii, 2003).

Nanotechnology term usually serves as a general heading for all manner of analyses and material investigations at nanoscale. American Nanoscale Science, Engineering and Technology (NSET) Subcommittee of the U.S. National Science and Technology Council, which coordinates the National Nanotechnology Initiative (NNI) describes nanotechnology such as “Research and technology development at the atomic, molecular or macromolecular levels, in the length scale of approximately 1-100 nanometer range, to provide a fundamental understanding of phenomena and materials at the nanoscale and to create and use structures, devices and systems that have novel properties and functions because of their small and/or intermediate size. The novel and differentiating properties and functions are developed at a critical length scale of matter typically under 100 nm. Nanotechnology research and development includes manipulation under control of the nanoscale structures and their integration into larger material components, systems and architectures”. Furthermore, German Federal Ministry of Education and Research (BMBF) summarises nanotechnology as follows: "Nanotechnology refers to the creation, investigation and application of structures, molecular materials, internal interfaces or surfaces with at least one critical dimension or with manufacturing tolerances of (typically) less than 100 nanometres (Leydecker, 2008).

Nanomaterials are at the leading edge of the rapidly developing field of nanotechnology. Their unique size-dependent properties make these materials superior and indispensable in many areas of human activity (Salata, 2004).

In some particular cases, the critical length scale of nanomaterials for novel properties and phenomena may be under 1 nm (e.g., manipulation of atoms at ~0.1 nm) or be larger than 100 nm (e.g., nanoparticle reinforced polymers have the unique feature at ~200–300 nm as a function of the local bridges or bonds between the nanoparticles and the polymer) (Guz & Rushchitskii, 2003).

The wavelength range of visible light is approximately 400 to 800 nm and as the wavelength of light scattered by smaller particles reduces significantly. Nanoparticles are invisible due to the fact that they are smaller than the wavelength

of visible light and therefore unable to scatter light. For this reason, a solution that contains a 60% proportion of solids in the form of nanoparticles can still be transparent (Leydecker, 2008). Electronic microscopes, such as scanning electronic microscope, scanning atomic-force microscope and the scanning tunneling microscope, are used to study nanomaterials (Guz & Rushchitskii, 2003).

Nanomaterials as materials whose internal structure has nanoscale dimensions are described hardly something new to science by many authors. However, it was relatively recently realized that some formations of oxides, metals, ceramics, and other substances are nanomaterials. Particles constituting ordinary (black) carbon, fumed silica powder are of nanoscale dimensions. Examples of natural nanomaterials used in nanotechnology are zeolites (aluminosilicates) and sheet silicates (phyllosilicates). Titania (TiO_2), zirconia (ZrO2), alumina (AlO_4), and aluminum titanate ($AlTiO_3$) are examples of natural nanoparticles used in nanotechnology and nanobiotechnology. Carbon particles are a well-studied class of nanoparticles. Fullerenes, a spherical form, with carbon atoms on the surface and contains 60 atoms in five-atom rings separated by six-atom rings, may deposit onto a surface, forming a monolayer. Fullerene molecules form carbon nanotubes, which may be considered relatives of graphite. Graphite lattices rolled up into a tube, with a very large number of atoms, are called nanotubes. Nanotubes differ in diameter, length, and the way they are rolled.

It should be noted that the particle size is not the only characteristic of a nanoparticle or nanomaterial. It is pointed out by the authors that one quite important and specific property of many nanomaterials is the majority of their atoms localize on the surface of a particle, in contrast to ordinary materials where atoms are distributed over the volume of a particle (Guz & Rushchitskii, 2003).

Understanding of biological processes on the nanoscale level is a strong driving force behind development of nanotechnology (Whitesides, 2003). Out of plethora of size-dependent physical properties available to someone who is interested in the practical side of nanomaterials, optical (Parak et al., 2003) and magnetic (Pankhurst

et al., 2003) effects are the most used for biological applications. Nanoparticles are applied in biology and medicine (Salata, 2004). They are used for fluorescent biological labeling (Bruchez et al., 1998; Chan & Nie, 1998; Wang et al., 2002), drug and gene delivery (Mah et al., 2000; Panatarotto et al., 2003), biodetection of pathogens (Edelstein et al., 2000), detection of proteins (Nam et al., 2003), probing of DNA structure (Mahtab et al., 1995), tissue engineering (Isla et al., 2003; Ma et al., 2003), tumor destruction via heating (hyperthermia) (Yoshida & Kobayashi, 1999) separation and purification of biological molecules and cells (Molday & MacKenzie, 1982), MRI contrast enhancement (Weissleder et al., 1990) and phagokinetic studies (Parak et al., 2002). Nanoparticles are nowadays developing for tissue engineering, cancer therapy, multicolour optical coding for biological assays (Han et al., 2001), manipulation of cells and biomolecules (Reich et al., 2003), and protein detection (Cao et al., 2003).

The fact that nanoparticles exist in the same size domain as proteins makes nanomaterials suitable for bio tagging or labelling. However, size is just one of many characteristics of nanoparticles that it is rarely sufficient if one is to use nanoparticles as biological tags. In order to interact with biological target, a biological or molecular coating or layer acting as a bioinorganic interface should be attached to the nanoparticle. Examples of biological coatings may include antibodies, biopolymers like collagen (Sinani et al., 2003), or monolayers of small molecules that make the nanoparticles biocompatible (Zhang et al., 2002). In addition, as optical detection techniques are widespread in biological research, nanoparticles should either fluoresce or change their optical properties. Nanoparticles usually form the core of nanobiomaterials. It can be used as a convenient surface for molecular assembly, and may be composed of inorganic or polymeric materials. It can also be in the form of nano-vesicle surrounded by a membrane or a layer. The shape is more often spherical but cylindrical, plate-like and other shapes are possible. The size and size distribution might be important in some cases.

1.4 Aim of the Study

In the current study, it was aimed to prepare and characterize nanostructures for the determination of cholesterol that one of physiologically important biological molecules. Nanostructures were prepared on the basis of molecular imprinting technology. Three different monomer:template ratios were used in the preparation of pre-polymerization complexes of MAPA and cholesterol to determine the effect of monomer:template ratio onto imprinting efficacy. Several characterization methods were performed during the pre-polymerization and polymerization processes. Template removal that one of important requirements for MIPs was successfully performed from imprinted polymeric nanospheres. In the second stage of the study, it was aimed to optimize cholesterol adsorption in methanol using the imprinted polymeric nanospheres having the most efficient monomer:template ratio and to exhibit the selectivity of the imprinted polymeric nanospheres to the analogues of cholesterol. The final purpose of the study was to compare cholesterol adsorption efficiencies of polymeric nanospheres from different media such as gastrointestinal mimicking solution and human plasma.

CHAPTER TWO
MATERIALS AND METHOD

2.1 Materials

2-hydroxyethylmethacrylate (99%) was supplied from Fluka. Ethylene glycol dimethacrylate (EGDMA), sodium desoxycholate (NaDC) and cholesterol were supplied from Sigma. Poly(vinyl alcohol) (PVA, high molecular weight, more than 99%) and potassium persulphate (KPS) were purchased from Merck. Sodium cholate (NaC) was supplied from Applichem. Methanol, acetonitrile, tetrahydofuran (THF) and other organic solvents were chromatographic grade. All other chemicals were analytical grade with high purity and no purification was applied before use. All water used in the adsorption experiments was purified using a Millipore S.A.S 67120 Molsheim-France facility. Before use the laboratory glassware was rinsed with deionised water and dried in a dust-free environment.

2.2 Synthesis of Methacryloylamidophenylalanine (MAPA) Comonomer

The synthesis of methacryloylamidophenylalanine (MAPA) comonomer was performed in accordance with the method of Say et al. (2003). 30 mL of 5% (w/v) K_2CO_3 solution was prepared and 5.0 g phenylalanine, 0.2 g sodium nitrite was added to this solution. 4 mL of methacyloyl chloride was added dribbly into the solution cooled down to 0°C under N_2 and leaved to stirring at 100 rpm for 2h at room temperature. After chemical reaction finished, solution pH was adjusted to 7.0. Extraction was performed with ethyl acetate and rotary evaporator was used to remove aqueous phase. After ether and cyclohexane crystallization, the obtained residue was MAPA (Say et al., 2003). Molecular structures of phenylalanine, methacyloyl chloride and MAPA were given in Figure 2.1.

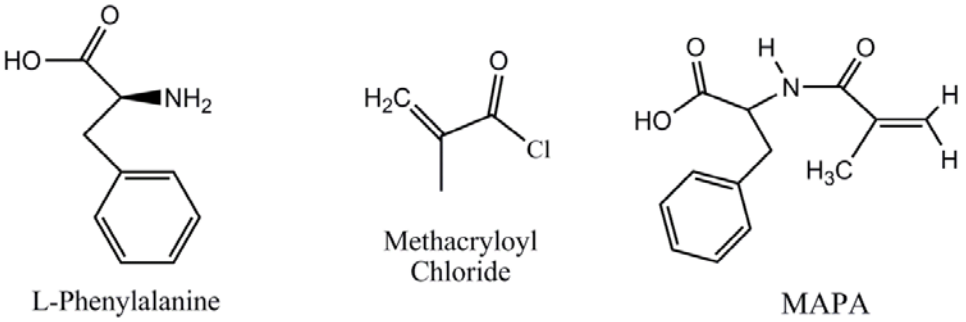

Figure 2.1 Molecular structures of L-phenylalanine, methacryloyl chloride and MAPA

2.3 Preparation and Characterization of Pre-polymerization Complexes of MAPA with Cholesterol

Template:monomer ratios chosen as 1:1, 1:3 and 3:1 were used to prepare pre-polymerization complexes of cholesterol with MAPA and these called as CP, CP3 and C3P pre-polymerization complexes, respectively. To prepare pre-polymerization complexes, first of all the solubility of cholesterol was studied with methanol, ethanol, acetonitrile, dichloromethane and THF. The highest solubility result with THF as 30 mg/mL, so it was choosen as pre-polymerization solvent because of the requirement of minimum solvent usage in pre-polymerization. Required amount of cholesterol solutions were mixed with stoichiometrically needed amount of MAPA and preparation procedures were summarized in Table 2.1.

Table 2.1 Preparation procedure for pre-polymerization complexes

	CP (1:1)	**CP3 (1:3)**	**C3P (3:1)**
CHO	4.950×10^{-5} mol	4.950×10^{-5} mol	1.485×10^{-4} mol
(MW:386.7 g/mol-30mg/mL)	638 µL	638 µL	1914 µL
MAPA	4.950×10^{-5} mol	1.485×10^{-4} mol	4.950×10^{-5} mol
(MW: 234 g/mol-0.34 g/mL)	34 µL	102.2 µL	34 µL

Characterization of pre-polymerization complexes was carried out with using ultra-violet (UV), nuclear magnetic resonance (NMR), and Fourier transform infra-red (FTIR) spectroscopies. Cholesterol and MAPA co-monomer, pre-polymerization complex were scanned to determine maximum wavelengths with UV-

spectrophotometer (Schimadzu 1601, Japan). H-NMR spectrums of pre-polymerization complexes were taken by liquid MERCURYplus-AS 400 with 400 mHz operation frequency. FTIR spectrums of cholesterol, MAPA and pre-polymerization complexes were recorded with FTIR spectrophotometer (Perkin Elmer spectrum 100 FT-IR spectrometer) with a universal ATR sampling accessory.

2.4 Preparation of Cholesterol Imprinted Polymeric Nanospheres

Molecularly imprinted polymeric nanospheres were synthesized using 2-hydroxyethylmethacrylate (HEMA) and pre-polymerization complexes (CP, CP3 and C3P) in accordance with the method in the study group of Akgöl (2009). 0.2775 g polyvinyl alcohol (PVA) was dissolved in 25 mL distillated hot water by stirring and this solution was used as stabilizer. Each synthesized pre-polymerization complexes were added into polyvinyl alcohol solutions and sonicated for 5 min to ensure the dispersion. 300 µL ethylene glycol dimethacrylate (EGDMA) as cross-linker and 600 µL HEMA as functional monomer were added to polymerization solutions and mixed. Molecular structures of 2-HEMA and EGDMA are shown in Figure 2.2. Finally, 0.0198 g potassium persulphate (KPS) was dissolved in 45 mL distillated water and added to polymerization solution as initiator. Polymerization mixtures were sonicated and mixed to homogenate the solutions. N_2 gas was passed through the polymerization solution for 5 min to remove dissolved oxygen from solution. Polymerization reaction was started at 70°C and was shacked at 65 rpm for 24 h in a temperature controlled water bath shaker (GFL 1092) .

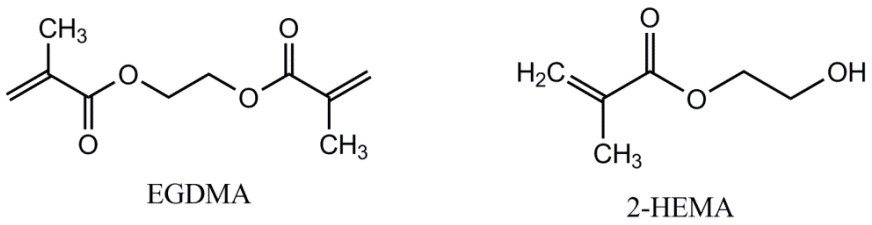

Figure 2.2 Molecular structures of HEMA and EGDMA

Non-imprinted polymeric nanospheres were synthesized using the same method with imprinted polymeric nanospheres synthesis without template into polymerization solution (Akgöl et al. 2009).

The synthesized polymeric nanospheres were leaved in ultrasonic batch for 1h for homogenization. Cholesterol imprinted and non-imprinted polymeric nanospheres were washed with water and methanol to remove unreacted monomers and cross-linker. All polymers were centrifuged at 12000 rpm for 30 min and supernatants were kept for cholesterol quantification with HPLC. Polymer precipitates were resuspended in water by ultrasonic bath application and homogenized by vortex. Polymers were centrifuged again and polymer precipitate was washed with methanol with the same method. Finally, polymer precipitates were resuspended in water with the same volume in initial.

2.5 Cholesterol Quantification with HPLC

Chromatographic analysis of cholesterol was performed according to the procedure by the group of Sánchez-Machado (2004) with some modifications (Sánchez-Machado et al, 2004). HPLC analyses were performed using Agilent 1100 HPLC system and Thermo LC systems with especial calibrations for both. Hewlett Packard Agilent 1100 series HPLC system (HP Corporation, Germany) consisted of an online vacuum degasser (G1322A), a column oven (G1316A), a quaternary pump (G1311A), diode array detector (G1315B), and manual injector (G1328B) with a PC system control program. Thermo Scientific Dionex Ultimate 3000 series LC system was equipped with diode array detector, pump, autosampler, degasser and column oven. A Phenomenex Gemini C18 column (5.0 cm x 0.3 cm; pore diameter: 5 µm; equipped with a guard column: drop-in guard cartridge holder for 4 mm stacking rings, 3 mm bore, ODS C 18; Phenomenex Inc., CA, USA) was used as a stationary phase. 30:70 methanol-acetonitrile was used as mobile phase and passed through the column at 1.2 mL/min at 30°C. Cholesterol peaks were followed at 205 nm.

Cholesterol standards were prepared in mobile phase from 1 ppm to 10 ppm. Areas belong to these solutions were used to generate calibration curve. HPLC chromatogram of cholesterol collected at 205 nm was seen in Figure 2.3.

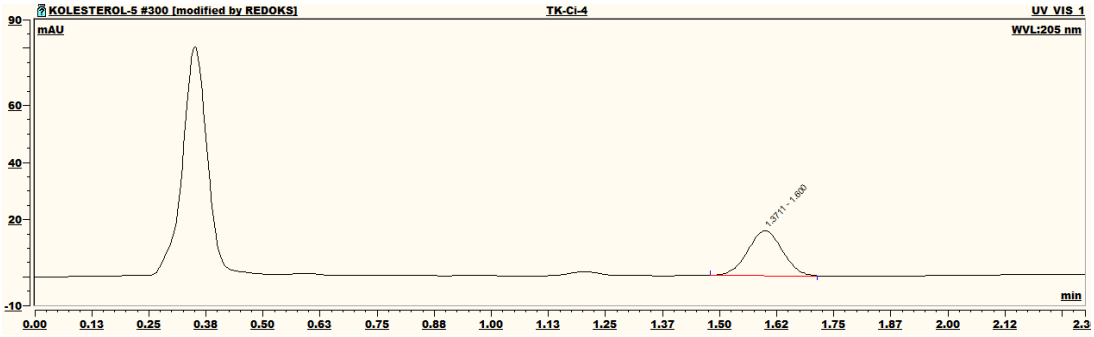

Figure 2.3 HPLC chromatogram of cholesterol

2.6 Template Removal Studies

Various template removal solutions were studied for the determination of most efficient one. Cetryl trimethylammonium bromide (CTAB) as a cationic surfactant, sodium dodecyl sulfate (SDS) as an anionic surfactant, triton X-100 as a nonionic surfactant were used in the concentration of 0.00001 %. Also, 0.1 M $(NH_4)_2SO_4$ solution and tetrahydrofuran (THF) were tested for template removal. Different template removal mediums were added to a small volume of imprinted polymeric nanospheres and template removal studies were performed for 2 h at 225 rpm shaking at room temperature. After removal period, imprinted polymers were centrifuged at 12000 rpm for 30 min. Supernatants were evaporated under N_2 stream at 40°C. Residues were resolved in mobile phase and cholesterol concentrations of the solutions were analyzed with HPLC. Also, template removal supernatants were concentrated under N_2 stream and were analyzed with FTIR spectrophotometer (Perkin Elmer spectrum 100 FT-IR spectrometer) to demonstrate that the molecule removed from imprinted polymers is cholesterol.

2.7 Characterization of Cholesterol Imprinted Polymers

Mass of imprinted polymeric nanospheres and non-imprinted nanospheres per 1 mL must be identified. For this purpose, different volumes of polymeric nanospheres were taken into microtubes which have weighed before. Polymers were centrifuged at 12000 rpm and precipitates were dried in oven at 60°C until stable weighs were obtained. Polymeric nanospheres weights were calculated as g per mL.

FTIR spectrum of cholesterol imprinted polymeric nanospheres after template removal and washings were recorded using spectrophotometer (Perkin Elmer spectrum 100 FT-IR spectrometer) with a universal ATR sampling accessory.

The surface morphology of the polymeric nanospheres was examined using scanning electron microscope (SEM). The sample was initially dried in air at 25°C for 7 days before being analyzed. A fragment of the dried bead was mounted on a SEM sample mount and was sputtered coated for 2 min. The sample was then mounted in a SEM (Phillips, XL-30S FEG, Germany). The surface of the sample was then scanned at the desired magnification to study the morphology of the nanospheres.

The particle size of cholesterol imprinted and non-imprinted were determined by Zeta Sizer (Malvern Instruments, Model 3000 HSA, England).

To calculate the specific surface area of cholesterol imprinted polymeric nanospheres, the equation which gives the particle count in 1 mL suspension was used (Bangs, 1987).

$$N = 6 \cdot 10^{10} S / \pi \rho_s d^3 \qquad (2.1)$$

Where; N is the nanoparticle count in 1 mL suspension; S is the percentage of solid part (S=10 for 5 mL suspension, 0.5 g); d is the particle diameter (μm) and ρ_s is the polymer density (g/mL).

Surface area of one nanosphere calculated from the equation for surface area of spheres.

$$\text{Surface area of sphere} = 4 \pi r^2 \quad (2.2)$$

Where, r is the nanosphere diameter (m)

Specific surface areas of imprinted nanospheres were calculated with using surface area of one nanosphere and N value.

The thermal gravimetric (TG) and derivated thermal gravimetric (DTG) curves at the thermal degradation of cholesterol imprinted polymeric nanospheres were evaluated by an EXSTAR S11 7300 at a heating rate of 10°C/min.

2.8 Adsorption Studies onto Molecularly Imprinted and Non-Imprinted Polymeric Nanospheres

Effects of different parameters on the adsorption capacity of imprinted polymeric nanospheres were tested. Adsorption experiments were performed with using temperature controlled shaker (Max Q 4000). 100 µL imprinted polymeric nanospheres were mixed with cholesterol solutions prepared in methanol (100 ppm concentration mostly) and shacked at 225 rpm. At the end of the adsorption period, adsorption media was centrifuged at 12000 rpm for 30 min to remove imprinted polymeric nanospheres. Supernatants were diluted 10 times with mobile phase and injected to HPLC for quantification of cholesterol.

Initially, adsorption capacities of CP, CP3 and C3P nanospheres were determined to identify the effect of template:monomer ratio and compared with the adsorption capacity of NIP nanospheres. Effects of adsorption time, polymer amount, initial cholesterol concentration, temperature, ionic strength, salt type on the adsorption capacity of imprinted polymeric nanospheres were investigated.

The amount of cholesterol adsorbed per unit mass of the nanospheres was calculated by using the following expression:

$$q = \frac{C_0 - C_e}{V M} \tag{2.3}$$

Where q is adsorption capacity (mg/g nanospheres), C_0 and C_e are cholesterol concentrations (ppm) of initial and equilibrium solution, V is the volume of adsorption media (L) and M is the amount of nanospheres used (g).

2.8.1 Comparison of Adsorption Capacities of Imprinted Polymeric Nanospheres with Different Template:Monomer Ratio

Adsorption capacities of CP, CP3 and C3P nanospheres were determined to specify the effect of template:monomer ratio with using 100 ppm cholesterol solution in methanol. 100 µL of each nanospheres were used in comparison experiments at 25°C. By the results of comparison, CP nanospheres were used in further adsorption studies.

2.8.2 Effect of Time

Adsorption equilibrium time was determined by the time effect studies. Adsorption capacities of CP nanospheres were identified from 2 min to 4 h time period. Adsorption experiments were performed with 100 ppm cholesterol solution with 100 µL nanospheres at 25°C in separate microtubes.

Adsorption kinetics was calculated from the data acquired from the results of time effect studies.

Adsorption kinetics, that controls the equilibrium time, was applied to these data to describe the rate of cholesterol uptake. The pseudo-first-order kinetic model has

been widely used to predict adsorption kinetics. The model given by Langergren and Svenska (1898) is defined as:

$$\ln (q_e - q_t) = \ln q_e - k_1 t \quad (2.4)$$

Where q_e and q_t (mg/g) are the amounts of cholesterol adsorbed at equilibrium and at any time, t (h), and k_1 (1/h) is the adsorption rate constant. When $\ln (q_e - q_t)$ is graphed against t, a straight line with slope of k_1 and intercept of $\ln q_e$ is obtained (Langergren & Svenska, 1898).

The pseudo-second-order equation based on equilibrium adsorption is expressed as:

$$\frac{t}{q_t} = \frac{1}{k_2 q_e} + \frac{1}{q_e} \quad (2.5)$$

Where k_2 (g/mg h) is the rate constant. The linear plot of t/qt versus t gave $1/q_e$ as the slope and $1/k^2q^2_e$ as the intercept. This procedure is more likely to predict the behavior over the whole range of adsorption (Ho & McKay, 1998).

The Elovich equation, analyzed for applicability of adsorption data, is expressed as:

$$q_t = \left(\frac{1}{\beta}\right) \ln (\alpha\beta) + \frac{1}{\beta} \ln t \quad (2.6)$$

Where α (mg/g h) is the initial adsorption rate and β (g/mg) is related to the extent of surface coverage. The parameters $(1/\beta)$ and $(1/\beta)$ $\ln(\alpha\beta)$ can be obtained from the slope and intercept of the linear plot of q_t versus $\ln t$ (Ozacar & Sengil, 2005).

The value of $(1/\beta)$ is indicative of the number of sites available for adsorption while the $(1/\beta)$ $\ln (\alpha\beta)$ is the adsorption quantity when $\ln t$ is equal to zero. This value

is helpful in understanding the adsorption behavior of the first step (Tseng, 2006). The q_e values calculated from Elovich equation agreed quite well with the experimental values.

The above kinetic models were not able to identify the diffusion mechanism, thus intraparticle diffusion model based on the theory proposed by Weber and Morris (1962) was tested. It is an empirically found functional relationship, common to the most adsorption processes, where uptake varies almost proportionally with $t^{1/2}$ rather than with the contact time. According to this theory:

$$q_t = k_{pi}\, t^{1/2} + Ci \qquad (2.7)$$

Where k_{pi} (mg/g $h^{1/2}$), the rate parameter of stage *i*, is obtained from the slope of the straight line of *qt* versus $t^{1/2}$. *Ci*, the intercept of stage *i*, gives an idea about the thickness of boundary layer, i.e., the larger the intercept, the greater the boundary layer effect (Weber & Morris, 1962).

2.8.3 Effect of Polymer Amount

To determine the convenient polymer amount, volumes of CP nanospheres used in adsorption experiments were ranged from 25 µL to 250 µL. Volume of cholesterol solutions were constant while studying with different polymer amounts. 100 ppm cholesterol solution in methanol was used at 25°C in adsorption experiments.

2.8.4 Effect of Initial Cholesterol Concentration

So as to determine maximum cholesterol adsorption capacity of CP nanospheres, initial cholesterol concentration was increased up to 3000 ppm cholesterol concentration. Effect of initial concentration was investigated from 0.5 ppm to 3000 ppm cholesterol concentration with 100 µL nanospheres at 25°C in separate micro-tubes. Cholesterol solutions up to 1000 ppm were prepared in methanol. Cholesterol

solution concentrations from 1000 ppm to 3000 ppm were prepared in THF due to solubility problems.

Adsorption isotherms are used to define the interactions between adsorbant and adsorbate in the equilibrium state. Langmuir isotherm assumes monolayer adsorption onto a surface containing a finite number of adsorption sites of uniform strategies of adsorption with no transmigration of adsorbate in the plane of surface. The linear form of Langmuir isotherm equation is given as:

$$C_e/qe = 1/(Lq_m) + (C_e/q_m) \quad (2.8)$$

Where, q_e is the amount of cholesterol adsorbed per unit weight of nanostructure at equilibrium (mg/g) and C_e is the equilibrium concentration of cholesterol in solution (ppm). q_m is the monolayer adsorption capacity (mg/g) and L is related with the adsorption energy (L/mg). When C_e/q_e is plotted against C_e, a straight line with slope of $1/q_m$ and intercept of $1/L\ q_m$ is obtained (Weber & Chakkravorti, 1974).

The essential characteristics of Langmuir isotherm can be expressed by a dimensionless constant called equilibrium parameter, R_L, defined by Weber and Chakkravorti (1974) as:

$$R_L = \frac{1}{1 + L\ C_0} \quad (2.9)$$

Where, L is the Langmuir constant and C_0 is the highest initial cholesterol concentration (ppm) (Weber and Chakkravorti, 1974). Adsorption type can be commented as favorable at batch adsorption conditions due to R_L values (Table 2.2) calculated between 0 and 1.

Table 2.2. R_L values for Langmuir isotherm

R_L Value	Type of Adsorption
$R_L > 1.0$	Unfavorable
$R_L = 1.0$	Linear
$0 < R_L < 1$	Favorable
$R_L = 0$	Irreversible

Freundlich model is an empirical equation based on adsorption on a heterogeneous surfaces or surfaces supporting sites of varied affinities. It is assumed that the stronger binding sites are occupied first and the binding strength decreases with the increasing degree of site occupation. A linear form of the Freundlich expression can be presented as below:

$$\log q_e = \log K_f + n_f \log C_e \tag{2.10}$$

Where, K_F is the Freundlich constants giving the adsorption capacity and n_f is the Freundlich constants indicating favorability of the adsorption process. The plot of log q_e versus log C_e gave a straight line with slope of n_f and intercept of log K_f (Freundlich, 1906). The slope of n_f ranging between 0 and 1 is a measure of surface heterogeneity. The value of n_f below one indicates a normal Langmuir isotherm while n_f above one is indicative of cooperative adsorption (Altınısık et al., 2010).

Temkin isotherm contains a factor that explicitly takes into account the adsorbent–adsorbate interactions. The adsorption is characterized by a uniform distribution of binding energies, up to some maximum binding energy. The Temkin isotherm is expressed as:

$$q_e = \left(\frac{RT}{b_T}\right) \ln (A\, C_e) \tag{2.11}$$

Where, $RT/b_T = B$ (J/mol), which is the Temkin constant related to heat of adsorption whereas A (L/g) is the equilibrium binding constant corresponding to the maximum binding energy. R (8.314 J/mol K) is the universal gas constant and T (K) is the absolute solution temperature (Temkin & Pyzhev, 1940).

In order to calculate the mean free energy value of adsorption, Dubinin–Radushkevich (DR) isotherm has also been applied. The DR equation can be defined by the following equation:

$$\ln q_e = \ln X_m - \beta\varepsilon^2 \tag{2.12}$$

Where, β is the constant related to sorption energy (mol^2/J^2), X_m is the Dubinin–Radushkevich monolayer capacity (mol/g), q_e is the amount of adsorbed cholesterol (mg/g), ε is the Polanyi potential which can be obtained as follows:

$$\varepsilon = R\,T \ln\left(1 + \frac{1}{C_e}\right) \tag{2.13}$$

Where, C_e is the equilibrium concentration of cholesterol (mg/mL), R gas constant (8.314 J/mol K) and T the temperature (K). By plotting ln q_e versus ε^2, β can be determined from the slope and X_m from the intercept (Dubinin &Radushkevich, 1947). The mean free energy E (kJ/mol) of adsorption can be estimated by using β values in the following equation:

$$E = \frac{1}{(2\beta)^{½}} \tag{2.14}$$

Results of initial concentration effect were used to specify adsorption isotherm.

2.8.5 Effect of Temperature

Temperature is an important impact on adsorption behavior of polymeric materials. To determine the effect of temperature on adsorption behavior, adsorption studies were performed over a range of temperatures from 5 to 35°C at 100 ppm cholesterol concentration in methanol with using 100 µL CP nanospheres.

Using the data obtained from temperature effect studies, thermodynamic parameters such as Gibbs free energy change (ΔG°), enthalpy change (ΔH°), and entropy change (ΔS°) were estimated for cholesterol adsorption.

ΔG° values at different temperatures were calculated from the following equations:

$$\Delta G^\circ = - RT \ln K_d \tag{2.15}$$

$$K_d = \frac{q_e}{C_e} \tag{2.16}$$

Where q_e is the amount of cholesterol adsorbed at equilibrium (mg/g), C_e is the equilibrium cholesterol concentration (ppm), K_d is the distribution coefficient. ΔH° is obtained from Van't Hoff equation:

$$\ln K_d = \frac{-\Delta H^\circ}{RT} + \frac{\Delta S^\circ}{R} \tag{2.17}$$

Where T is the absolute temperature, R is gas constant (8.314 J/mol K).ΔH° and ΔS° values were calculated from the slope and the intercept of the plot of ln K_d versus 1/T.

2.8.6 Effect of Ionic Strength

Effect of ionic strength on adsorption capacity of CP nanospheres was investigated with different salt concentrations ranging from 0 to 3000 ppm both in methanol and in gastrointestinal mimicking solution (GIMS). GIMS was prepared as follows: 12.5 mL 0.2 M KH_2PO_4, 9.5 mL 0.2 M NaOH and 20 mL distillated water were mixed. Sodium desoxycholate (Na-DC) and sodium cholate (NaC) were used as bile salts. 2.45 g Na-DC and 1.65 g NaC were dissolved in solution mixture and pH of the final solution was adjusted to 7.5 with 0.2 M NaOH. Final volume was adjusted to 50 mL. N_2 was passed through the solution for 15-20 min.

NaCl solutions were prepared in methanol and mixed with cholesterol solution so as to get 100 ppm cholesterol and the requested salt concentration in the methanol. In the same manner, NaCl was dissolved in GIMS and mixed with cholesterol solution prepared in GIMS. Adsorption experiments were performed at 25°C with 100 µL CP nanospheres in separate microtubes. After centrifugation at the end of adsorption period, supernatants were filtered through 0.2 µm Sartorius filter to avoid salt contamination to HPLC system.

2.8.7 Effect of Salt Type

Effect of salt type was studied with using NaCl, NH_4Cl, $CaCl_2$ and $AlCl_3$ at 100 ppm concentrations. Monovalent monoatomic, monovalent polyatomic, divalent and trivalent salts prepared in methanol were mixed with cholesterol solution so as to get 100 ppm cholesterol and 100 ppm salt in the solution. Adsorption experiments were performed at 25°C with 100 µL CP nanospheres in separate microtubes. After centrifugation at the end of adsorption period, supernatants were filtered through 0.2 µm Sartorius filter to avoid salt contamination to HPLC system.

Na_2SO_4, NH_4SO_4 and Na_3PO_4 salts could not be used due to solubility problems.

2.9 Desorption and Repeated Usage

Desorption of cholesterol from imprinted polymeric nanospheres were studied with using MeOH:THF (70:30) mixture and 20% acetic acid in methanol (HAc:MeOH (20:80)). At the end of adsorption period, adsorption media was centrifuged at 12000 rpm for 30 min and supernatant was used for HPLC cholesterol analysis. Precipitated nanospheres were resuspended in water with the same volume of initial polymer amount (1 mg). Desorption solutions were added to these nanospheres and shacked at 225 rpm for 2 h at 25°C. This period was repeated 2 times with fresh desorption solution. After desorption studies, polymeric nanospheres were washed with water many times to remove solvent remnants and finally resuspended in water for a new adsorption period.

Cholesterol amount in the desorption solution was determined with Zak method spectrophotometrically (Zlatkis et al., 1953). HPLC cholesterol analysis cannot be practiced under acidic condition due to presence of acetic acid. Zak method is usually used to determine serum cholesterol amounts. Protein-free sample solution is treated with concentrated sulphuric acid. Cholesterol in the presence of sulphuric acid undergoes to dehydration to form cholesterol-3,5-diene. A red colored complex is formed by the catalytic action of Fe^{3+} ions. Ferric chloride acetic acid reagent is prepared by solving $FeCl_3$ in glacial acetic acid as 0.05 % (w/v). Cholesterol stock solution was prepared as 100 ppm in glacial acetic acid and diluted with glacial acetic acid for a series of solution. Standard cholesterol solutions and desorption solutions were performed in the same way. 250 µL of the standards or samples were mixed with 250 µL ferric chloride acetic acid reagent and 250 µL concentrated sulphuric acid. Homogenized mixture of samples was incubated for 20 minutes. Blank was prepared by mixing 500 µL glacial acetic acid and 250 µL ferric chloride acetic acid reagent. Intensities of samples were measured against blank at 560 nm. Cholesterol amounts can be determined by using cholesterol standard curve obtained by a series of cholesterol standard solution.

Desorption media consist of 20% acetic acid in methanol were used directly in Zak method. However, desorption media consist of MeOH:THF mixture were dried under N_2 stream at 40°C. Residues were solved in glacial acetic acid and applied to Zak method.

Re-usability is an important advantage of adsorbents. To determine re-usability of imprinted polymeric nanospheres, adsorption process was pursued with desorption process. Imprinted polymeric nanospheres were washed with deionized water many times after great amount of adsorbed cholesterol was desorbed from imprinted polymeric nanospheres. Then, same imprinted polymeric nanospheres were used in another adsorption-desorption cycle. Adsorption-desorption cycle was repeated 5 times for repeated usage studies.

2.10 Cholesterol Adsorption Studies from Gastrointestinal Solution (GIMS)

There are many studies about cholesterol adsorption from GIMS. Thus, cholesterol adsorption studies were performed from GIMS with CP, CP3, C3P and NIP nanospheres. Cholesterol solution at 100 ppm concentration in GIMS was prepared by ultra-sonication the solution at least 30 min at 40°C. GIMS solution and cholesterol solution in GIMS were prepared freshly and protected from day light.

Adsorption studies from GIMS were performed with using 100 µL nanospheres at 25°C. After centrifugation at the end of adsorption period, supernatants were filtered through 0.2 µm Sartorius filter to avoid salt contamination to HPLC system.

2.11 Cholesterol Adsorption Studies from Healthy Plasma and Hypercholesterolemic Plasma

Cholesterol adsorption studies were performed with commercial human plasma purchased from Sigma. Different dilution ratios were tested for matrix effect determinations and dilutions were performed with pH 7.4 buffer and methanol to specify the most appropriate solvent for plasma dilution. Plasma was diluted at 1:1,

1:2, 1:5 and 1:10 dilution ratios with both dilution solvents. Plasma samples diluted with methanol were centrifuged to remove protein aggregates formed due to decreased solubility in methanol. All diluted plasma solutions were used in cholesterol adsorption with 100 µL imprinted polymeric nanospheres and shacking at 225 rpm at 25°C for 30 min. After removal of imprinted polymeric nanospheres by centrifugation, supernatant was diluted with mobile phase and filtered (0.2 µm Sartorius filter) and then cholesterol concentrations were determined by HPLC analysis. Cholesterol concentration of initial plasma solution was also tested by Trinder reaction with using BT 3000 autoanalyzer equipment for comparison with HPLC method (Trinder & Webster, 1984).

After the most appropriate dilution solvent and dilution ratio were specified, cholesterol adsorption from plasma were studied with CP, CP3 and C3P nanospheres as mentioned above.

For cholesterol adsorption from hypercholesterolemic plasma, plasma was diluted with methanol including high concentration of cholesterol and then, performed adsorption experiment.

2.12 Selectivity Experiments

In order to show the specificity of cholesterol imprinted nanostructures for cholesterol, competitive adsorption of progesterone, testosterone, estrone and estradiol must also studied. The structures of cholesterol analogues are given in Figure 2.4.

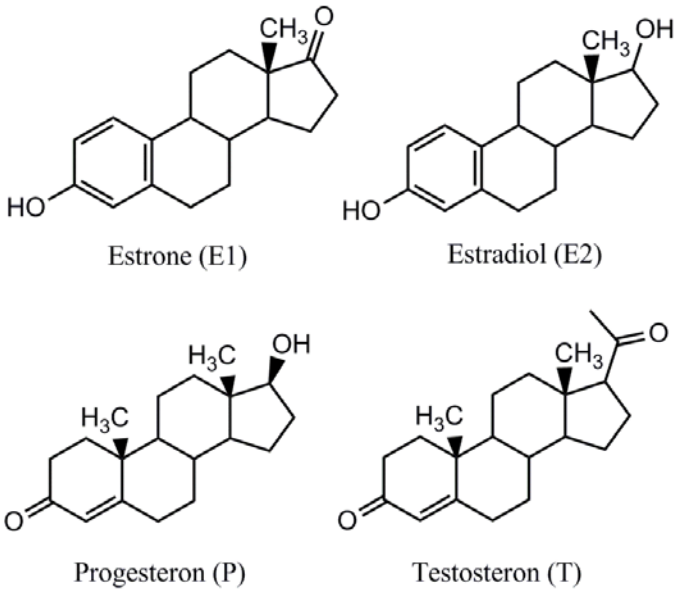

Figure 2.4 Molecular structures of cholesterol analogues

Quantification of cholesterol analogues were performed as method of the group Navakova (2004) with some modification (Navakova et al., 2004). HPLC analysis of estron (E1), estradiol (E2), testosterone (T) and progesterone (P) was carried out by using Thermo Hypersil Gold 150x4.6mm, 5µ column. Acetonitrile:methanol:acetic acid 1% (40:30:30) was used as mobile phase. Flow rate was 1.2 mL/min at 30°C. E1, E2, T and P were specified at 225 nm at 2.5, 2.7, 3.0 and 4.8 min, respectively. HPLC chromatogram, belongs to cholesterol analogues, was given in Figure 2.5.

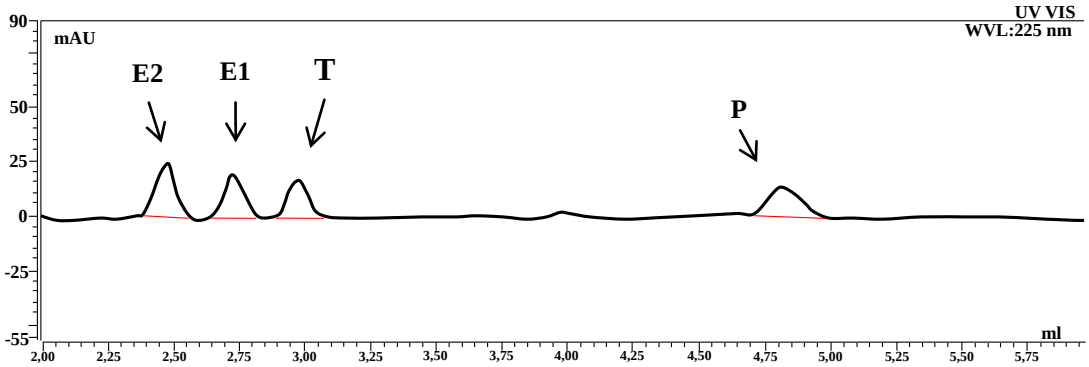

Figure 2.5 HPLC chromatogram of E1, E2, T and P

Selectivity coefficient and relative selectivity must be calculated to determine the specifity of imprinted nanospheres. The distribution coefficient (K_d) for progesterone, testosterone, estrone and estradiol with respect to cholesterol will be calculated by:

$$K_d = (Ci - Cf) / Cf \; x \; V/m = Q/Cf \qquad (2.18)$$

Where K_d represents the distribution coefficient (ml/g); Ci and Cf are initial and final concentrations of cholesterol (mg/ml), respectively. V is the sample volume (mL) and m is the nanostructure weight (g). The selectivity coefficient (k) for the binding of bilirubin in the presence of other competitive molecules can be obtained from binding data according to:

$$k = K_d\,(\text{cholesterol})/K_d\,(X)\ (X: \text{cholesterol analogues}) \qquad (2.19)$$

CHAPTER THREE
RESULTS AND DISCUSSION

3.1 Characterization of Pre-Polymerization Complexes

Complexation between monomers and template molecules or their analogues has been observed by changes in spectroscopic properties of the mixtures. UV spectrums of cholesterol solution in methanol, MAPA and pre-polymerization complexes were taken by dilution. Maximum absorption wavelengths for cholesterol, MAPA and CHO-MAPA pre-polymerization complexes are given in Table 3.1.

Table 3.1 Maximum absorption wavelengths for cholesterol, MAPA and CHO-MAPA pre-polymerization complexes

UV-absorption	λ_{max}
CHO	210 nm
MAPA	318 nm
CP (CHO-MAPA (1:1))	310 nm
CP3 (CHO-MAPA (1:3))	310 nm
C3P (CHO-MAPA (3:1))	310 nm

As seen from Table 3.1, pre-polymerization complexes have UV absorption peaks at 310 nm. This demonstrates contribution of MAPA into pre-polymerization complexes. Shifts at the maximum wavelengths of pre-polymerization complexes were observed and these results demonstrate the complexation of cholesterol with MAPA.

FTIR spectrums of cholesterol and MAPA were recorded to compare FTIR bands of these with the FTIR bands of pre-polymerization complexes and given in Figure 3.1.

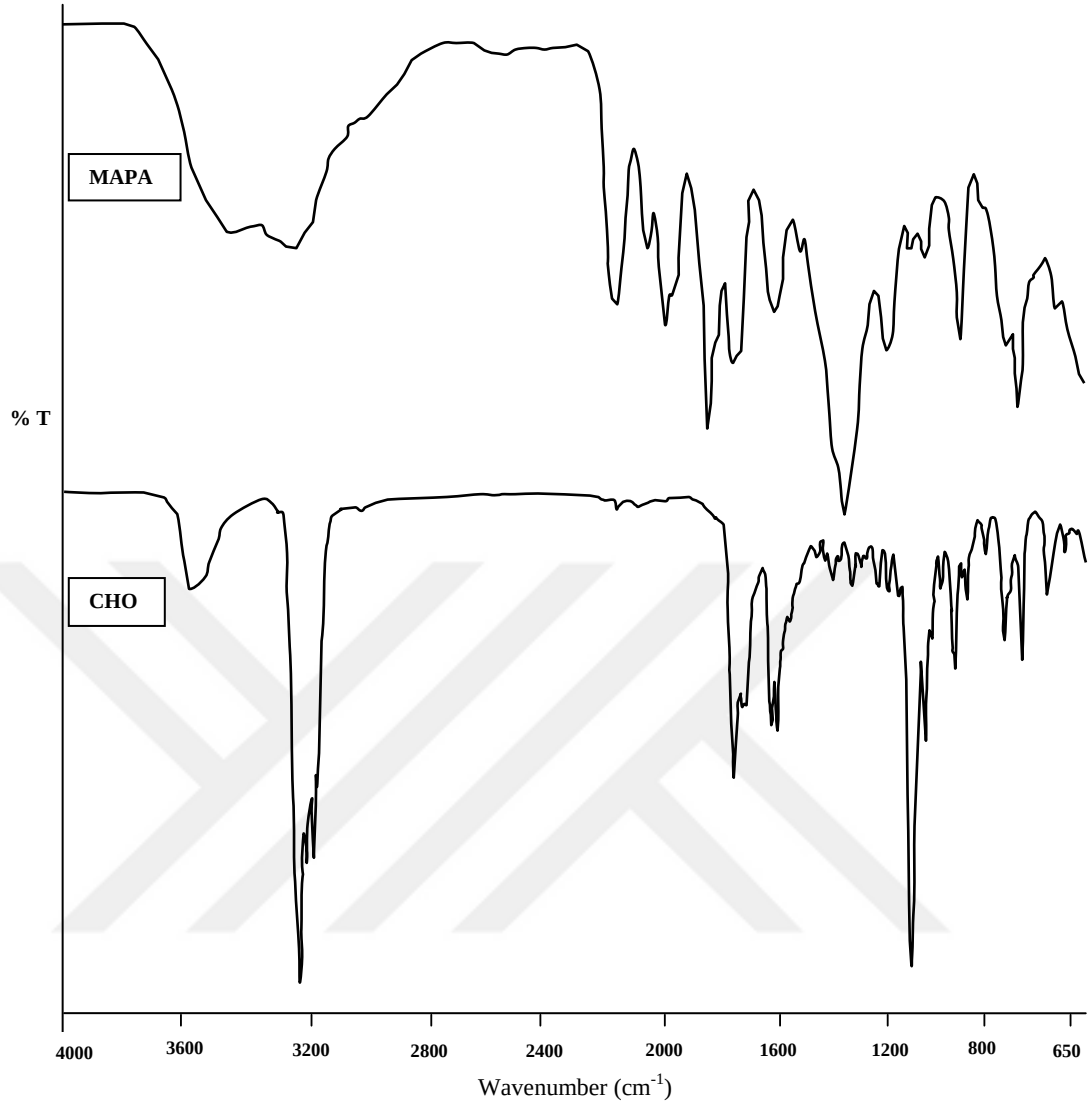

Figure 3.1 FTIR spectrums of MAPA and cholesterol

Stretching vibration of hydroxyl group of cholesterol was observed at 3530 cm^{-1}. The intensive peak at 1053 cm^{-1} corresponds to C-O stretching of cholesterol. As seen in the FTIR spectrum of MAPA; the intensive peak at 1740 cm^{-1} corresponds to C=O stretching. The adsorption band at 1020 cm^{-1} corresponds to C-O stretching. The peak observed at 750 cm^{-1} was due to aromatic character in MAPA.

FTIR spectrums of CP, C3P and CP3 pre-polymerization complexes were given in Figure 3.2.

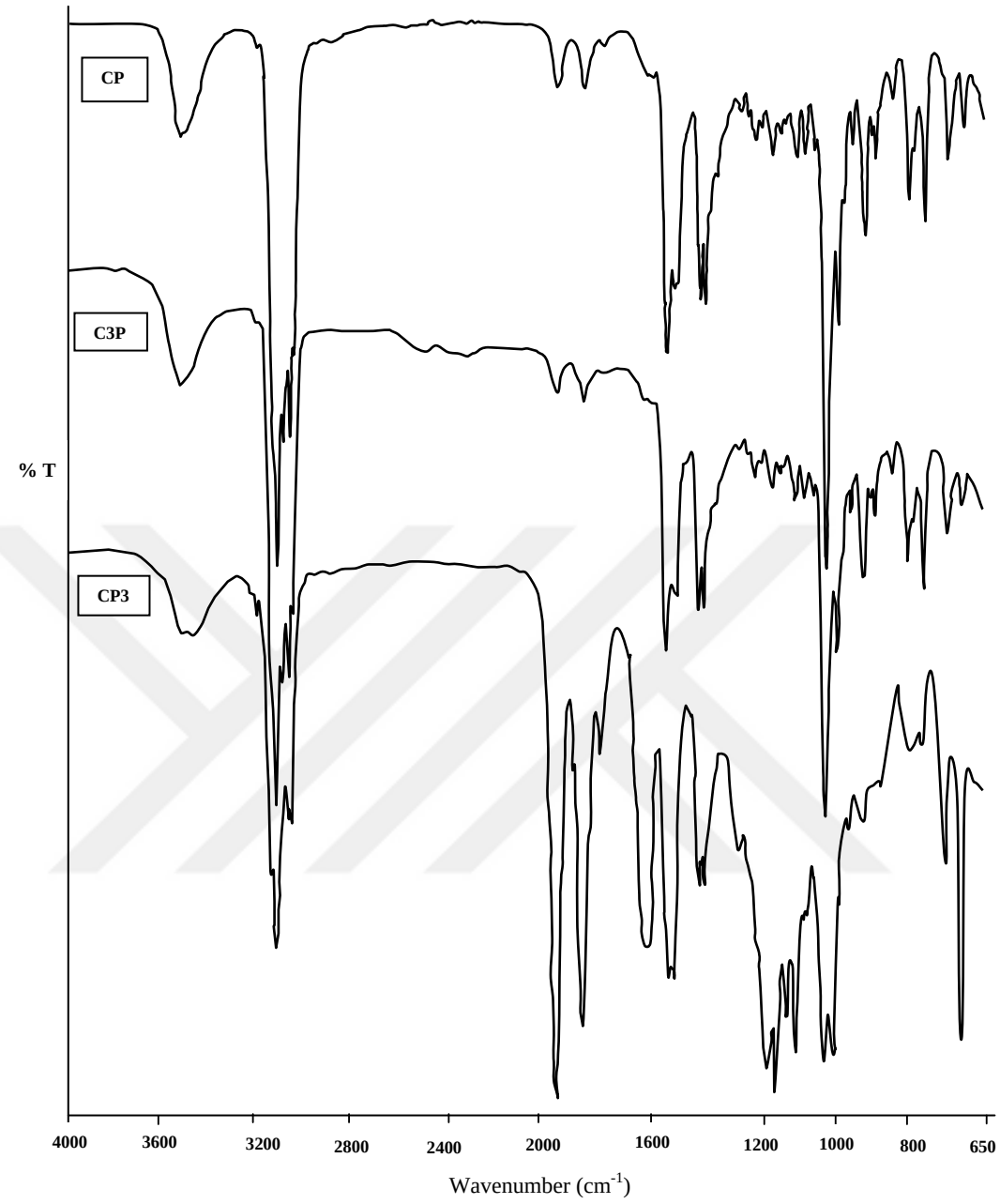

Figure 3.2 FTIR polymerization complexes spectrums of pre-polymerization complexes

O-H and C-H stretching (3400 and 2900 cm^{-1}) and C-H bending (1100 cm^{-1}) vibrations of cholesterol were seen in pre-polymerization complexes. Asymmetric C=O stretching vibration (1750 cm^{-1}) of MAPA was also seen in pre-polymerization complexes. On the other hand, the intensities of N-H stretching vibrations of MAPA (3400-3500 cm^{-1}) and O-H stretching vibrations of cholesterol (3400 cm^{-1}) decreased in pre-polymerization complexes. These findings demonstrate the complexation of cholesterol with MAPA. O-H and C-H stretching and C-H bending vibrations were

sharper in C3P than the others because of the higher incorporation of cholesterol into pre-polymerization complex structure. Aromatic C=C stretching vibration, seen in both cholesterol and MAPA (sharper), were detected in all pre-polymerization complexes but sharper in CP3. Also, asymmetric C=O stretching vibrations are sharper in CP3 than the others. These findings can be resulted from higher incorporation of MAPA into CP3 pre-polymerization structure.

H-NMR chemical shift ranges for CP pre-polymerization complex were specified as:

^{1}H NMR ($CDCl_3$) ppm= 0.86 (d, 6H, 2xCH_3, J= 6.4 Hz); 0.91 (d, 3H, CH_3, J= 6.8 Hz); 1.00 (s, 3H, CH_3); 1.07-1.22 (m, 8H, 4xCH_2), 1.25 (s, 3H, CH_3); 1.32-1.60 (m, 17H), 1.65 (d, 1H, CH, J= 10.4 Hz), 1.92 (s, 3H, CH_3); 1.95-2.08 (m, 2H, CH_2); 2.23-2.30 (m, 2H, CH_2); 3.49-3.55 (m, 1H, CH); 3.71 (t, 1H, CH, J=5.2 Hz); 3.73 (d, 2H, CH_2, J=5.6 Hz); 5.34 (m, 1H, =CH); 7.08-7.12 (m, 2H, 2xArH); 7.23-7.31 (m, 3H, 3xArH)

H-NMR spectrum of CP pre-polymerization complex was given in Figure 3.3.

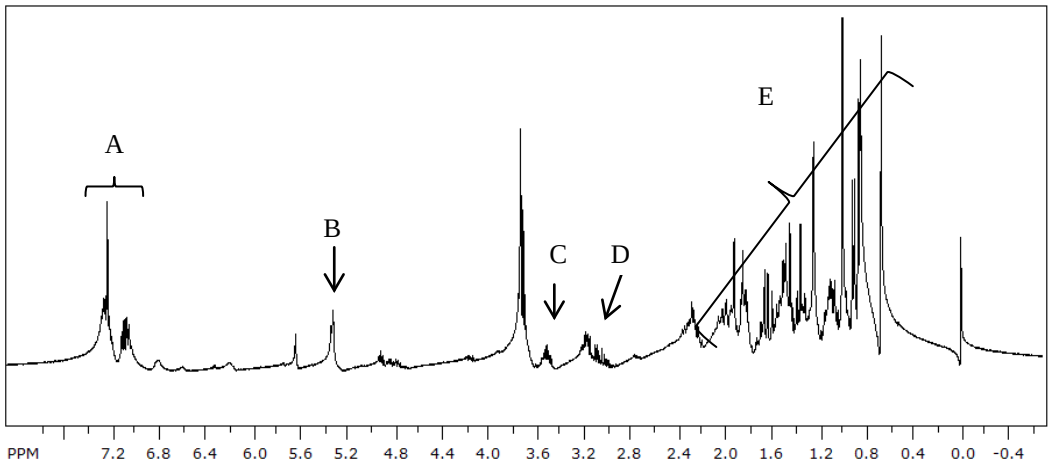

Figure 3.3 H-NMR spectrum of CP pre-polymerization complex

In Figure 3.3, A belongs to aromatic CH protons of MAPA. Shifts belong to C=C of cholesterol was seen in B. Shifts shown as C belong to CH and CH_2 protons of MAPA. CH proton of polar head of cholesterol was seen in D. Shifts seen as E in

Figure 3.3 were belong to CH, CH_2 and CH_3 protons of cholesterol and CH_3 protons of MAPA.

OH proton of cholesterol and NH proton of MAPA are not seen in H-NMR spectrum of pre-polymerization complex. Theoretically, chemical shift of OH proton of cholesterol must be seen at 3.6 ppm and chemical shift of NH proton of MAPA must be seen at 8.0 ppm. The absence of these chemical shifts makes us think that interactions between cholesterol and MAPA in pre-polymerization complex occur at these regions.

The very few interactions for cholesterol binding are either H-bonding or hydrophobic interactions (Gore et al., 2004). Possible interactions between cholesterol and MAPA functional monomer can be demonstrated as in Figure 3.4.

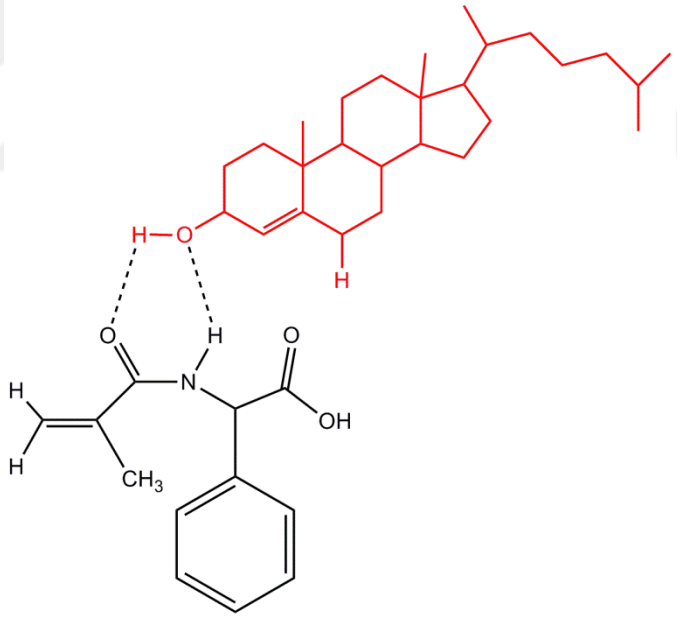

Figure 3.4 Possible interactions between cholesterol and MAPA

Polar chemical groups, such as -OH group in methanol do not cause the hydrophobic effect. H-bonding interactions occur in methanol. Thus, it may be concluded that interactions at cholesterol binding to imprinted nanospheres will be H-bonding. It was believed that the recognition of MIP towards various steroids is mainly based on a mechanism of hydrogen bonding formation (Tong et al., 2011).

3.2 Template Removal Studies

It was observed from the HPLC analysis that 1% of cholesterol included in the polymerization media was not imprinted to the polymer. Furthermore, 70% of imprinted cholesterol was removed during the washing process with methanol. A cationic (CTAB), an anionic (SDS) and a non-ionic (triton X-100) surfactant and an inorganic salt (ammonium sulphate) and an organic solvent (THF) were used to remove 30% rest of template in the nanospheres. Cholesterol concentrations in the removal solutions were determined with HPLC. Template removal percentages of various agents for the residual cholesterol after washing with methanol were given in Table 3.2.

Table 3.2 Template removal percentages of various agents

Template Removal Agent	Template Removal %
0.1 M $(NH_4)_2SO_4$	1.06
0.00001 % Triton X-100	22.43
0.00001 % SDS	15.73
0.00001 % CTAB	19.09
THF	72.48

As seen in Table 3.2, the most efficient template removal agent was determined as THF. 84% of total imprinted cholesterol was removed with methanol and THF, approximately. All imprinted polymeric nanospheres were removed from cholesterol and washed with water several times to avoid from solvent remnant. HPLC chromatogram of THF removal solution was given in Figure 3.5.

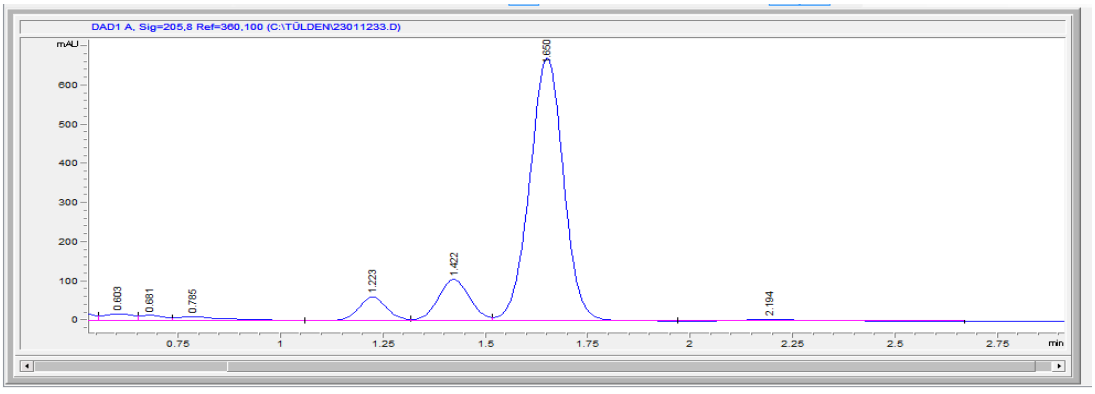

Figure 3.5 HPLC chromatogram of THF removal solution

THF including template after removal period was evaporated under N_2 stream for FTIR analysis to prove that the removed molecule is cholesterol. FTIR spectrums of removal solution and cholesterol standard were given in Figure 3.6.

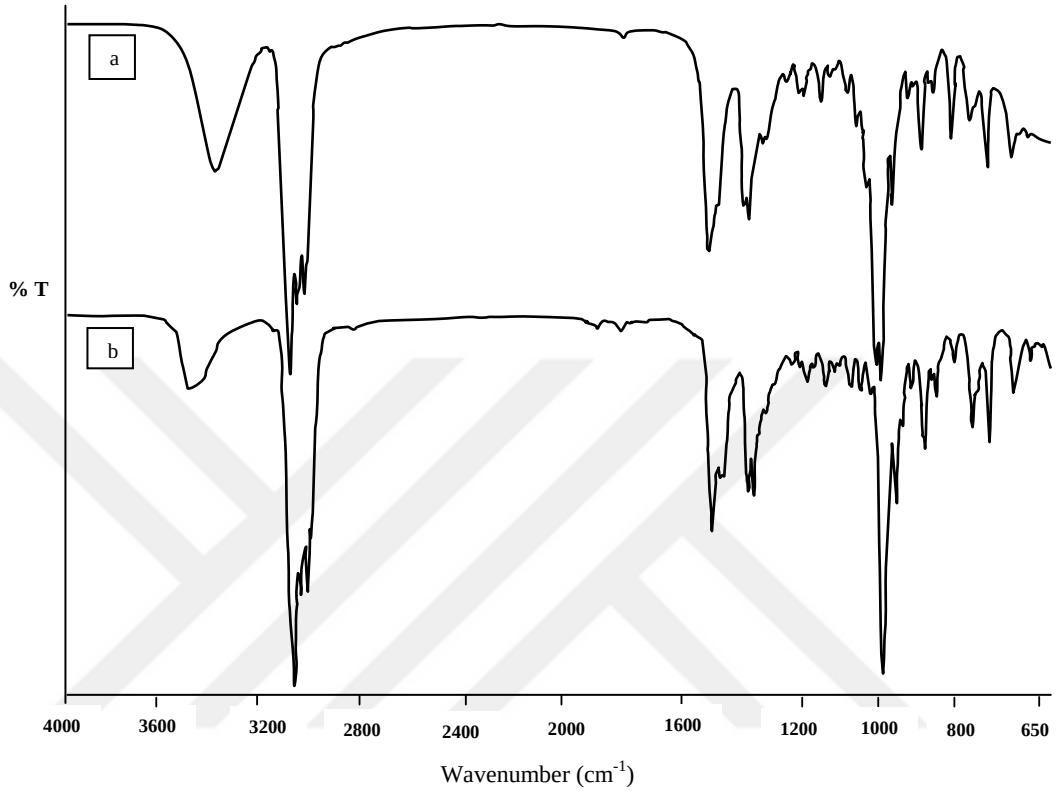

Figure 3.6 FTIR spectrums of removal solution[(a)] and cholesterol standard[(b)]

All the bands found in standard cholesterol spectrum were determined in the spectrum of removal solution. Shifts were seen at some bands and also intensities of some bands changed. These might be some conformational changes at cholesterol in the synthesis of pre-polymerization complexes or imprinted polymer.

3.3 Characterization of Cholesterol-Imprinted and Non-Imprinted Polymers

Mass of imprinted polymeric nanospheres and non-imprinted nanospheres per 1 mL must be identified with the average of 10 measurements. Mass of CP, CP3 and C3P imprinted nanospheres and non-imprinted polymeric nanospheres per 1 mL were determined as 0.0100, 0.0089, 0.0094 and 0.0113 g, respectively.

FTIR spectrum of HEMA monomer was recorded to investigate the incorporation of monomer into polymerization. FTIR spectrum of HEMA monomer was given in Figure 3.7.

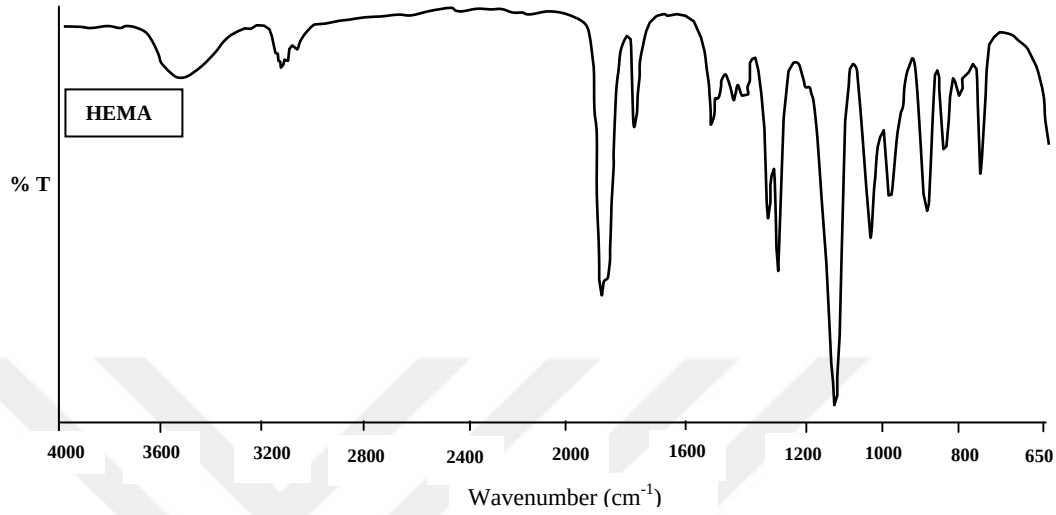

Figure 3.7 FTIR spectrum of HEMA monomer

Stretching vibration of hydroxyl group of HEMA was observed around 3420 cm^{-1}. The intensive peak at 1715 cm^{-1} corresponds to C=C stretching. The absorption peaks at 1640 cm^{-1} and 1160 cm^{-1} corresponds to C=O stretching and C-O stretching of ester group, respectively.

FTIR spectrums of CP, CP3 and C3P imprinted nanospheres and NIP were seen in Figure 3.8.

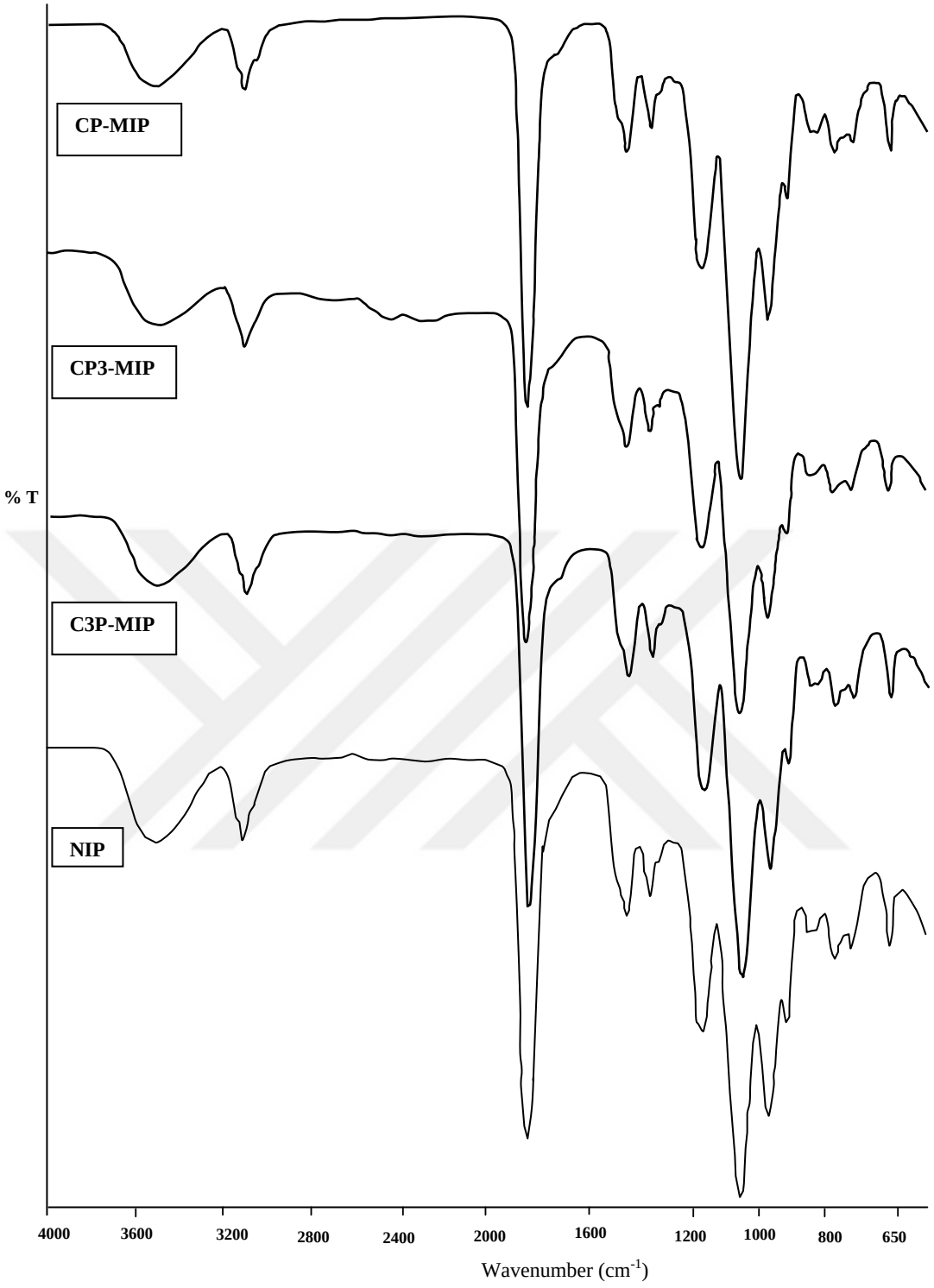

Figure 3.8 FTIR spectrums of CP, CP3, C3P imprinted and NIP nanospheres

C=C streching of HEMA (1640 cm^{-1}) was not seen in the spectrum of imprinted polymeric nanospheres. It may be due to polymerization of HEMA with pre-polymerization complex from C=C bonds. The intensive peak at 1740 cm^{-1}

corresponds to C=O stretching. The absorption bands at 1140 cm^{-1} and 1070 cm^{-1} correspond to C-O stretching of ester group and C-O stretching of carboxylic acid, respectively. This showed the polymerization of pre-polymerization complexes with HEMA. Also, the absorption peak at 750 cm^{-1} of aromatic ring of MAPA was seen in the spectrum of imprinted polymeric nanospheres. This showed polymerization of HEMA with pre-polymerization complex.

SEM micrographs of cholesterol imprinted and non-imprinted polymeric nanospheres were given in Figure 3.9.

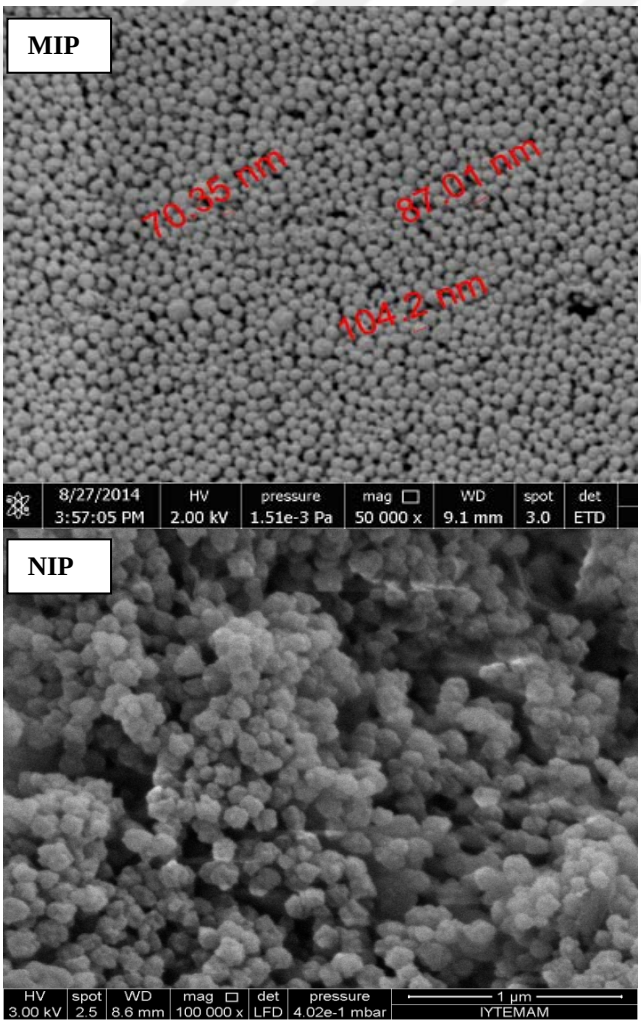

Figure 3.9 SEM micrographs of cholesterol imprinted and non-imprinted polymeric nanospheres

The spherical and monosize character of MIPs were shown in Figure 3.9. Average particle size of MIPs was detected as 87±17 nm. Average particle size of MIPs was detected as 116 nm by Zeta sizer analysis. Average particle size of NIPs was detected as 125 nm by Zeta sizer analysis. Specific surface areas of imprinted and non-imprinted polymeric nanospheres were calculated using equations that give particle count/ml and surface area of sphere. Specific surface areas were calculated as 541.5 m^2/g for MIP and 458.3 m^2/g for NIP, respectively.

DTG curves of CP (green), CP3 (black), C3P (blue) and NIP (red) nanospheres were given in Figure 3.10.

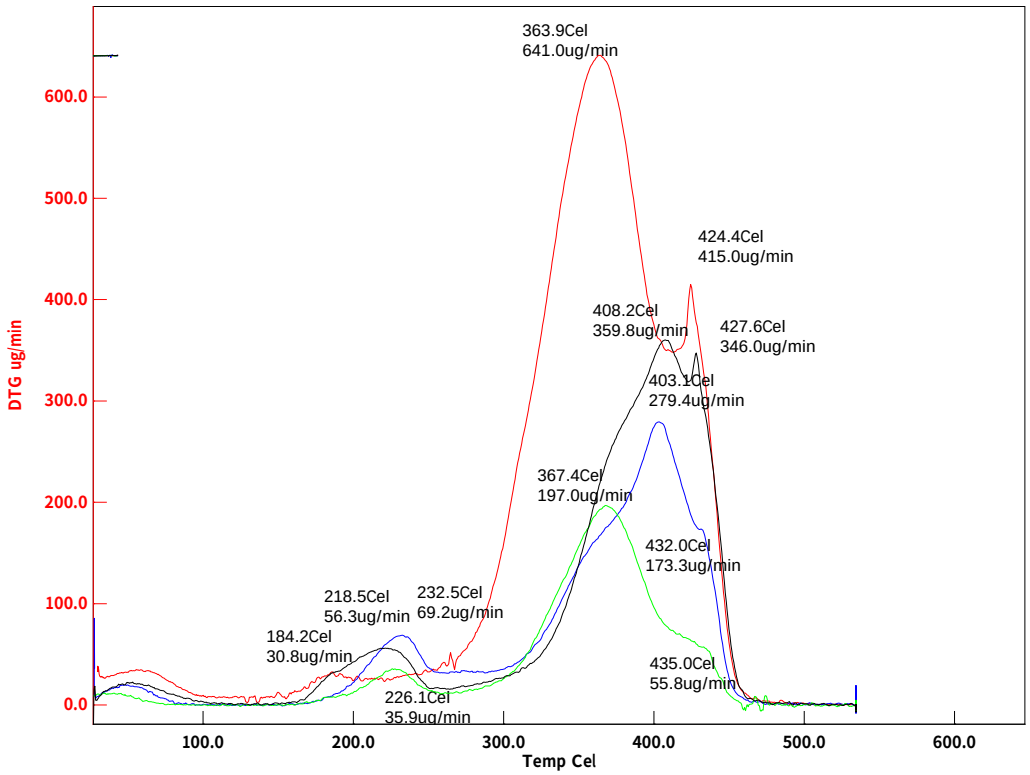

Figure 3.10 DTG curves of CP, CP3, C3P and NIP nanospheres

As seen from Figure 3.10, CP, CP3, C3P and NIP nanospheres were resistant to high temperatures. Degradation rates of polymeric nanospheres followed the order NIP > CP3 > C3P > CP. At about 200 °C, the polymers exhibited an obvious weight loss because of the loss of water or solvent molecules captured in the polymeric

nanospheres. Therefore, this temperature was the initial decomposition temperature. Based on the curve of DTG, the temperature point for the maximum weight loss was 367, 408, 403 and 364°C for CP, CP3, C3P and NIP nanospheres, respectively. In the range of 300-460 °C, polymeric nanosheres had two processes of weight loss, which was due to the production of co-polymers between HEMA and MAPA. The results showed that the prepared polymeric nanospheres had good thermal stability (Li et al., 2014).

3.4 Adsorption Studies onto Molecularly Imprinted and Non-Imprinted Polymeric Nanospheres

3.4.1 Comparison of Adsorption Capacities of Imprinted Polymeric Nanospheres with Different Template:Monomer Ratio

Adsorption capacities of CP, CP3, C3P nanospheres and NIP nanospheres at 100 ppm cholesterol concentration in methanol were shown in Figure 3.11.

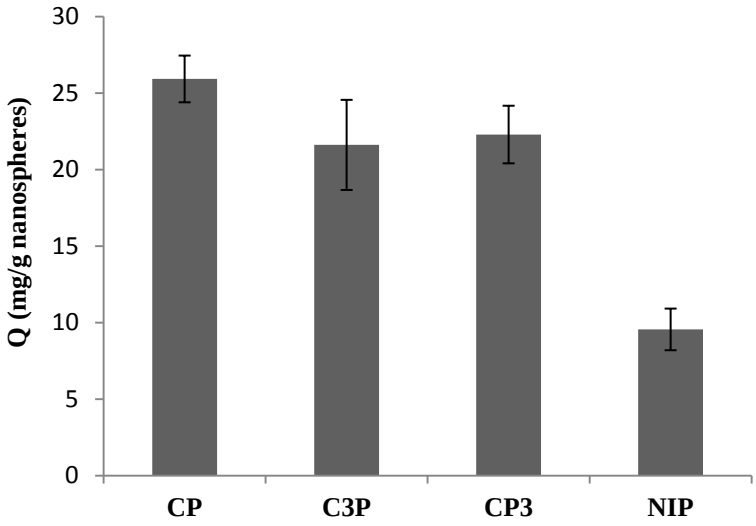

Figure 3.11 Adsorption capacities of CP, CP3, C3P and NIP nanospheres (t: 30 min, c:100 ppm, $V_{nanospheres}$:100µL, T:25°C)

Adsorption capacities of cholesterol imprinted polymeric nanospheres were detected as similar to each other. Adsorption capacity of CP nanospheres is 1.2 and

1.16-fold of C3P and CP3 nanospheres, respectively. This result can be concluded that monomer:template ratio 1:1 is more convenient for cholesterol imprinting. Non-imprinted polymers adsorbed less than the half adsorption capacity of CP nanospheres. This demonstrates that imprinting process increased the adsorption capacity of nanospheres. Consequently, CP nanospheres were used for optimization of cholesterol adsorption in methanol.

3.4.2 Effect of Time

Adsorption experiments were performed for different time periods to specify the effective contact time. Adsorption experiments were performed for 2, 4, 6, 10, 15, 20, 25, and 30 minutes in separate micro-tubes to show short-time effect on adsorption capacity. Also, adsorption experiments were performed for 45, 60, 90, 120, 150, 180, 210, and 240 minutes in separate micro-tubes to show stability of adsorption capacity with time. Effect of time on adsorption capacity was shown in Figure 3.12.

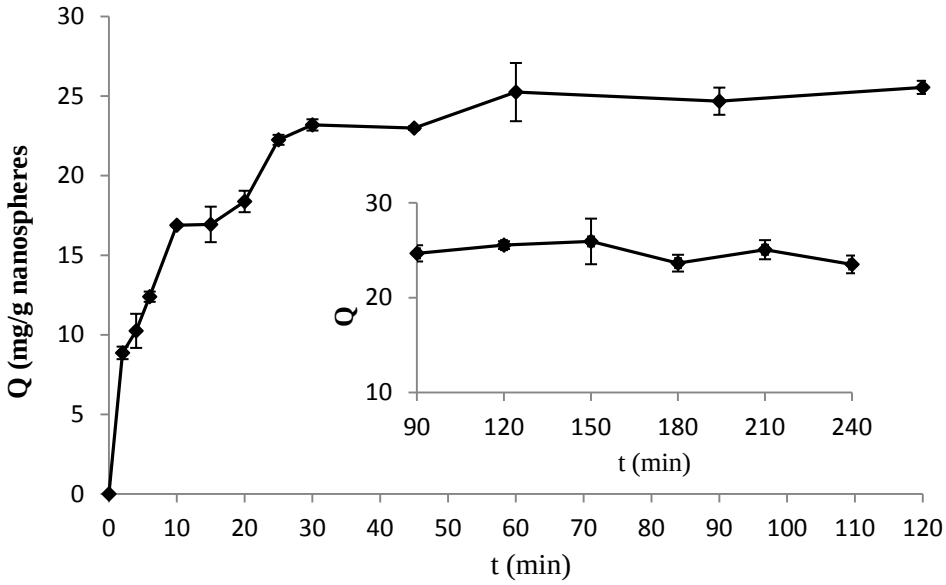

Figure 3.12 Effect of contact time on the adsorption capacity of CP nanospheres (c:100 ppm, $V_{nanospheres}$:100µL, T:25°C)

As seen in Figure 3.12, adsorption capacity reached the plateau at 30 minutes and did not change significantly after 30 min. For this reason, all other adsorption experiments were carried out for 30 minutes.

Data obtained from these experiments were used to identify adsorption kinetics. All the correlation coefficient, R^2 values and constants obtained from pseudo-first- and pseudo-second-order model, Elovich equation and intraparticle diffusion model were given in Table 3.3.

Table 3.3. Adsorption kinetics values for cholesterol adsorption onto CP nanospheres at 25°C

Pseudo-first-order kinetic model				
$q_{e,exp}$ **(mg/g)**	$q_{e,cal}$ **(mg/g)**	k_1 **(1/h)**	R^2	
23.19	16.51	2.87	0.9543	
Pseudo-second-order kinetic model				
$q_{e,cal}$ **(mg/g)**	k_2 **(g/mg h)**	$t_{½}$ **(min)**	$h_{0.2}$ **(mg/g min)**	R^2
25.64	0.42	5.54	4.63	0.9929
Elovich equation				
1/β ln(αβ) (mg/g)	**α (mg/g h)**	**β (g/mg)**	R^2	
24.66	732.66	0.20	0.9688	
Intra particle diffusion model				
k_{pi} **(mg/g h^{½})**	C_i	R^2		
2.81	5.68	0.9417		

As seen from Table 3.3, correlation constant of pseudo-second-order is higher than of the others. This shows pseudo-second-order kinetic model fits best to cholesterol adsorption. Also, experimental q_e and calculated q_e values from pseudo-second-order kinetic order for cholesterol adsorption is very similar. Initial adsorption rate of cholesterol imprinted polymeric nanospheres were calculated as 4.63 mg/g min. Half sorption time, t½, was determined as short as 5.54 min.

3.4.3 Effect of Polymer Amount

Effect of polymer amount on adsorption capacity of cholesterol imprinted polymeric nanospheres was given in Figure 3.13.

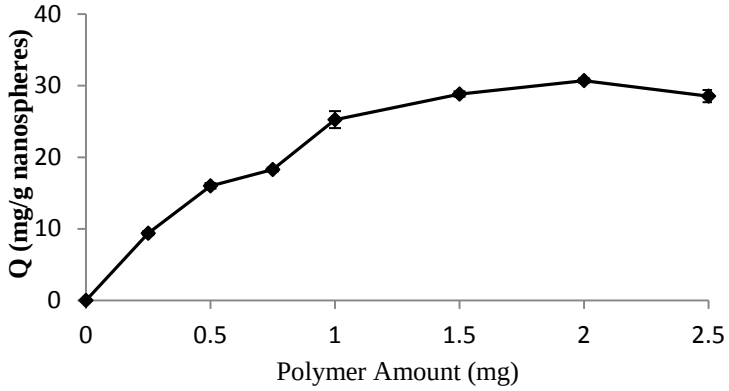

Figure 3.13 Effect of polymer amount on the adsorption capacity of CP nanospheres (t:30 min, c:100 ppm, T:25°C)

As shown in Figure 3.13, adsorption capacity increased with increasing polymer amount. After 1 mg of polymer amount, adsorption capacity came near to plateau of saturation. For this reason, all other adsorption experiments were carried out with 1 mg of polymer amount.

3.4.4 Effect of Initial Cholesterol Concentration

So as to determine maximum cholesterol adsorption capacity, initial cholesterol concentration was increased up to 3000 ppm cholesterol concentration. Effect of initial cholesterol concentration was shown in Figure 3.14.

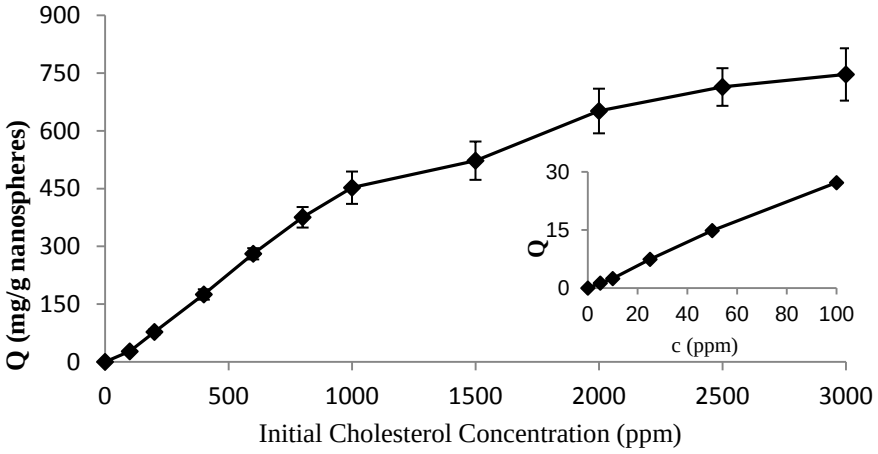

Figure 3.14 Effect of initial cholesterol concentration on the adsorption capacity of CP nanospheres (t:30 min, $V_{nanospheres}$:100µL, T:25°C)

As shown in Figure 3.14, adsorption capacity of cholesterol imprinted polymeric nanospheres increased with increasing cholesterol concentration until 2500 ppm cholesterol concentration. At the concentration above 2500 ppm, adsorption capacity did not increase with increasing concentration significantly. Consequently, maximum adsorption capacity of CP nanospheres was detected as 714.17 mg/g nanospheres. Adsorption experiment was performed at least 0.5 ppm cholesterol concentration. At this condition, 1 g CP imprinted nanospheres adsorbed 0.212 mg cholesterol.

The adsorption isotherm is the most important information which indicates how the adsorbate molecules distribute between liquid and solid when the adsorption process reaches an equilibrium state. It is important to create the most appropriate correlation for the equilibrium curves for optimizing the design of an adsorption system.

All the correlation coefficients and the constants obtained from the Langmuir, Freundlich, Temkin and Dubinin-Radushkevich isotherm models applied for cholesterol adsorption are given in Table 3.4.

Table 3.4 Adsorption isotherm model values for cholesterol adsorption onto CP nanospheres at 25°C

Langmuir Isotherm				
q_e **(mg/g)**	L **(L/mg)**	q_m**(mg/g)**	R_L	R^2
714.17	0.0006	714.29	0.248	0.9725
Freundlich Isotherm				
	n_f	K_f **(mg/g)**		R^2
	0.3118	82.376		0.8458
Temkin Isotherm				
	A (L/g)	**B**		R^2
	27.14	202.81		0.8093
Dubinin-Redushkevich Isotherm				
B **(mol^2/J^2)**	X_m**(mg/g)**	E **(kJ/mol)**		R^2
1×10^{-7}	415.34	2.24		0.9369

In this work, the correlation obtained from the fitting of the Langmuir model was better than the fit using either the Freundlich or Temkin models. The experimental q_e values are almost same with the calculated q_m values. The result of the modeling

therefore indicates monolayer adsorption. Energy values ranging between 1 and 8 kJ/mol indicate that the adsorption is due to physical interactions between adsorbent and adsorbate (Smith, 1981). The *E* values calculated from Dubinin–Radushkevich isotherm indicate that physisorption due to weak van der Waals forces plays a significant role in the adsorption process.

3.4.5 Effect of Temperature

Temperature is an important impact on adsorption. For this reason, adsorption studies were performed over a range of temperatures from 5 to 35°C. Effect of temperature was shown in Figure 3.15.

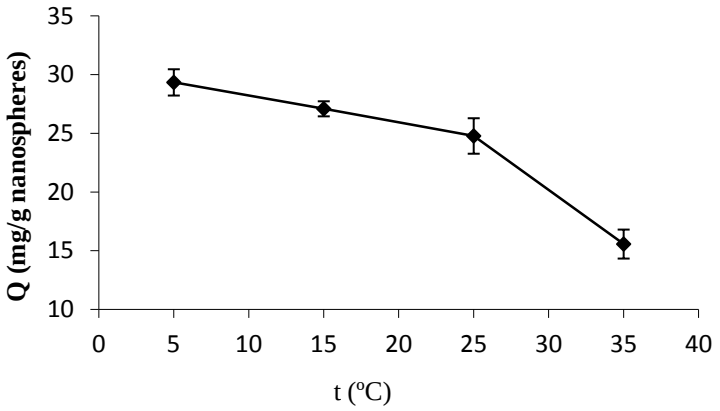

Figure 3.15 Effect of temperature on adsorption capacity of CP nanospheres (t: 30 min, $V_{nanospheres}$: 100µL, c:100 ppm)

As shown in Figure 3.15, adsorption capacity of cholesterol imprinted polymeric nanospheres decreased with increasing temperature. The van der Waals attraction forces, which operate in hydrophobic interactions, increase with increase in temperature. However, an opposite effect was reported indicating that the role of temperature in hydrophobic interaction chromatography is of a complex nature (Builder, 1993). This apparent discrepancy is probably due to the differential effects exerted by temperature on the conformational state of different biomolecules and their solubilities in aqueous solutions. Also, since physical adsorption is an exothermic process, it occurs more readily at lower temperatures and decreases with

increase in temperature. The decrease in adsorption capacity of cholesterol imprinted polymeric nanospheres might be due to physisorption.

Using the data obtained from temperature effect studies, thermodynamic parameters such as Gibbs free energy change (ΔG°), enthalpy change (ΔH°), and entropy change (ΔS°) were estimated for cholesterol adsorption. Calculated ΔH° and ΔS° values and ΔG° values at different temperatures were presented in Table 3.5.

Table 3.5 Thermodynamic parameters for cholesterol adsorption onto CP nanospheres

Δ*H*° (kJ/mol)	**Δ*S*° (J/mol)**	**Δ*G*° (kJ/mol)**			
		278 K	**288 K**	**298 K**	**308 K**
-21.45	-82.50	-14.23	-14.31	-14.68	-13.21

As seen in Table 3.5, adsorption presented favorable ΔG° values. On the other hand, all interactions presented exothermic enthalpy changes which suggest that cholesterol adsorption onto cholesterol imprinted polymeric nanospheres was enthalpically favorable. It was supported by the decreasing adsorption of cholesterol with the increase in temperature. The negative enthalpy values obtained with this study also shows that cholesterol adsorption was a physisorption process. However, the adsorption was accompanied by a decrease of entropy. The negative entropy indicated a decrease in the randomness in the system polymer/solution interface during the adsorption process. So the adsorption was favorable at low temperatures.

3.4.6 Effect of Ionic Strength

Effect of ionic strength on adsorption experiments were repeated with different salt concentrations ranging from 0 to 3000 ppm both in methanol and in GIMS. Effect of ionic strength on cholesterol adsorption was shown in Figure 3.16.

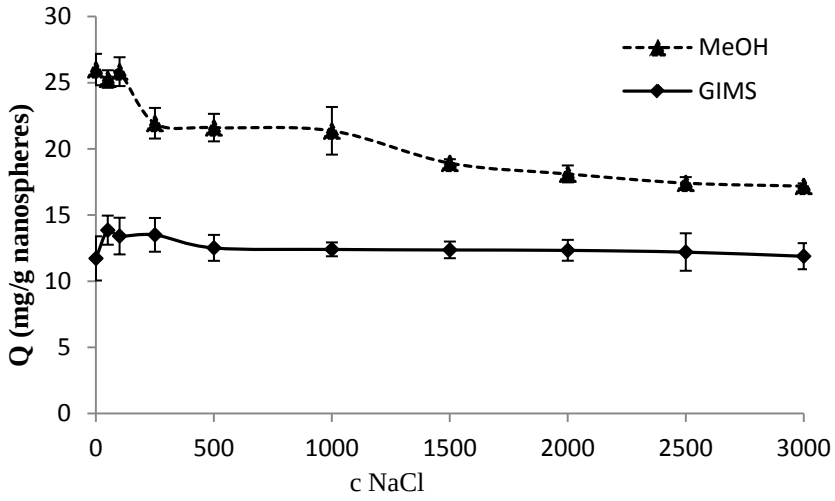

Figure 3.16 Effect of ionic strength on adsorption capacity of CP nanospheres (t: 30min, $V_{nanospheres}$:100µL, c:100 ppm)

As seen in Figure 3.16, adsorption capacity of imprinted polymeric nanospheres (CP) was decreased with increasing ionic strength in methanol while increased with increasing ionic strength in GIMS. Adsorption capacity was decreased by 18 % in methanol but increased by 15 % in GIMS when compared at 250 ppm NaCl concentration. This result shows that adsorption occurs with different interaction types explained as follows in methanol and in GIMS.

Non-polar molecules disturb the highly dynamic H-bonding interactions in water and are excluded by water. Thus, hydrophobic interactions occur in water. Hydrophobic interactions are also dominant in GIMS. So, effect of ionic strength in GIMS supports these hydrophobic interactions.

Polar chemical groups, such as OH group in methanol do not cause the hydrophobic effect. H-bonding interactions occur in methanol. Ions disturb the H-bonding interactions and, thus adsorption capacity decreases with increasing ionic strength.

3.4.7 Effect of Salt Type

Effect of salt type was studied with using NaCl, NH_4Cl, $CaCl_2$ and $AlCl_3$ at 100 ppm concentrations. Other salts could not be studied due to solubility problems in methanol. Effect of salt type on adsorption was seen in Figure 3.17.

Monovalent monoatomic, monovalent polyatomic, divalent and trivalent salts affected the adsorption capacity of cholesterol imprinted polymers. Adsorption capacity of nanospheres decreased 15.6 % when trivalent salt was added to adsorption media.

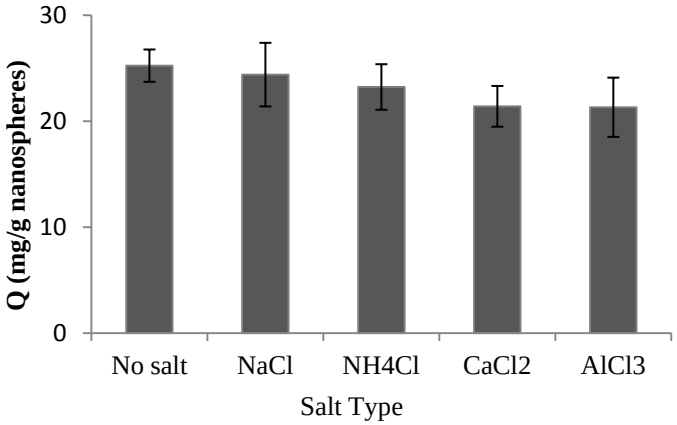

Figure 3.17 effect of salt type on cholesterol adsorption of CP nanospheres (t: 30 min, $V_{nanospheres}$:100µL, c:100 ppm cholesterol and 100 ppm salt)

3.5 Desorption and Repeated Usage

Cholesterol concentrations in desorption media were determined with Zak method spectrophotometrically with 0.9991 regression coefficient. MeOH:HAc (80:20) and THF:MeOH (70:30) were tested for determination of the most efficient desorption solution. It was detected that 86.14 % and 71.56 % of adsorbed cholesterol onto CP nanospheres was desorbed with MeOH:HAc (80:20) and THF:MeOH (70:30), respectively. Thus, MeOH:HAc (80:20) was used as the desorption agent in the repeated usage studies.

Adsorption-desorption cycle was repeated five times to show the reusability of CP nanospheres. Adsorption capacities and desorption percentages obtained from adsorption-desorption cycles performed with CP nanospheres were given in Figure 3.18.

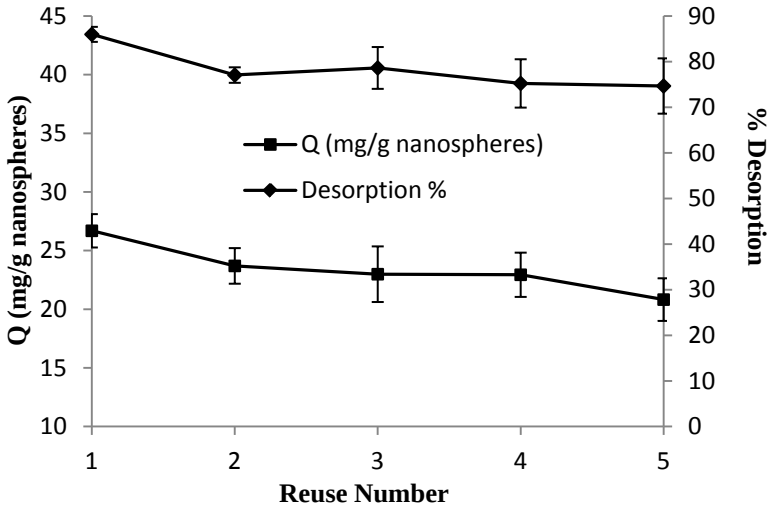

Figure 3.18 Reusability and % desorption of CP nanospheres

As seen in Figure 3.18, adsorption capacity of CP nanospheres were decreased by 21.95 % at the end of the five adsorption-desorption cycle. It can be concluded that cholesterol can be efficiently desorbed from CP nanospheres with a desorption range of 75-85 % and that CP nanospheres can be effectively used for many times.

3.6 Cholesterol Adsorption Studies from Gastrointestinal Mimicking Solution (GIMS)

Cholesterol adsorption from GIMS was studied with cholesterol imprinted polymeric nanospheres and NIP. Adsorption capacities of nanospheres from GIMS were compared with adsorption capacities in methanol. Cholesterol adsorption from GIMS and comparison of the adsorption capacities with those in methanol was given in Figure 3.19.

Adsorption capacity of CP nanospheres was determined as 11.72 mg/g in GIMS. Cholesterol adsorption capacity of imprinted polymeric nanospheres in GIMS is the half of the adsorption capacity in methanol. This also promotes the different interactions in different media in accordance with the result from ionic strength effect.

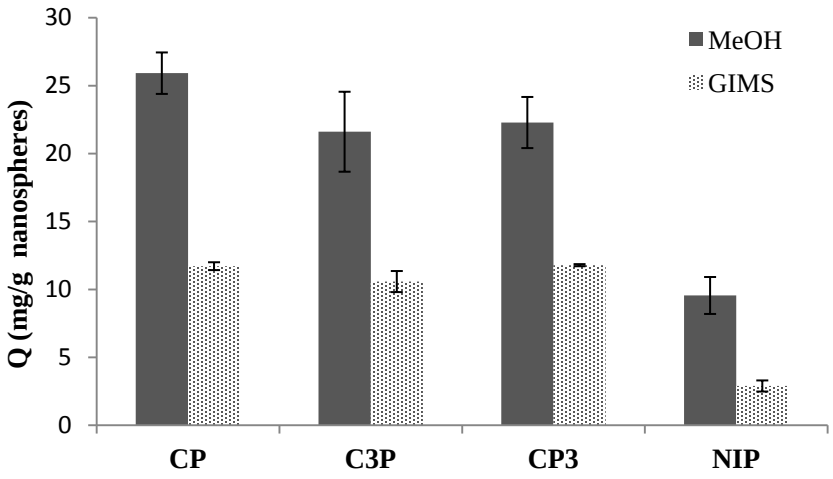

Figure 3.19 Cholesterol adsorption from GIMS and comparison of the adsorption capacities with those in methanol

3.7 Cholesterol Adsorption Studies from Healthy Plasma and Hypercholesterolemic Plasma

Cholesterol adsorption studies were performed with CP nanospheres with several dilutions with methanol and pH 7.4 buffer. Effect of dilution ratios and dilution solution on the adsorption capacity of CP nanospheres was given in Figure 3.20.

As seen in Figure 3.20, adsorption capacity of CP nanospheres was higher in methanol than in pH 7.4 buffer and 1:5 dilution ratio was the most favorable one for cholesterol adsorption. 1:5 dilution ratio was used for further cholesterol adsorption studies.

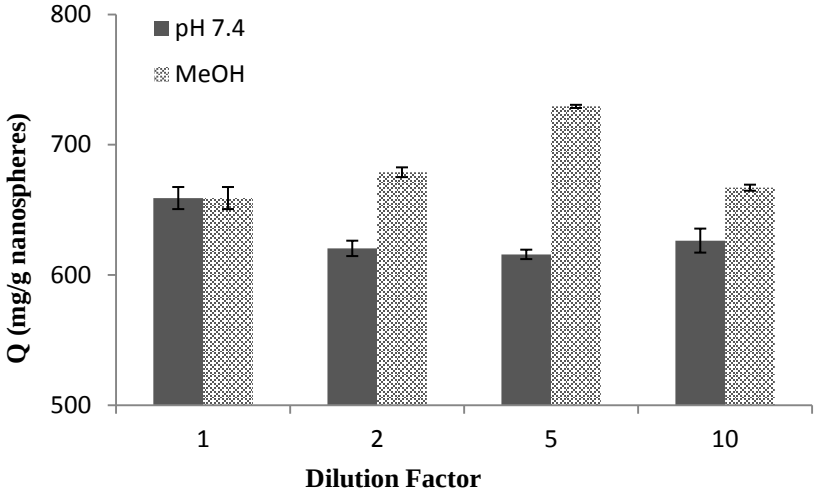

Figure 3.20 Effect of dilution ratio and solvent onto the adsorption capacity of CP nanospheres

Initial cholesterol concentration of plasma was determined as 150 mg/dL with HPLC method and 170 mg/dL by Trinder reaction with autoanalyzer equipment. Then, cholesterol adsorption studies were performed with imprinted and non-imprinted nanospheres using diluted plasma at 1:5 ratio with methanol. Adsorption capacities of cholesterol imprinted polymeric nanospheres were given in Figure 3.21.

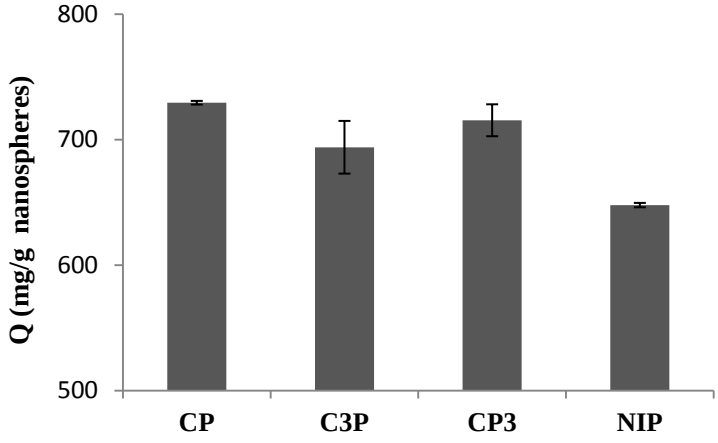

Figure 3.21 Comparison of cholesterol adsorption from human plasma with imprinted and non-imprinted nanospheres

Cholesterol adsorption capacities of imprinted polymeric nanospheres were detected as 729.4, 693.9 and 715.4 mg/g nanospheres for CP, C3P and CP3 nanospheres and 647.8 mg/g nanospheres for NIP, respectively.

For cholesterol adsorption from hypercholesterolemic plasma, plasma was diluted with methanol including high concentration of cholesterol and then, performed adsorption experiment. Initial cholesterol concentration of hypercholesterolemic plasma was determined as 265 mg/dL. Cholesterol removal % of CP nanospheres from hypercholesterolemic plasma was calculated as high as 95.33 %. This result clearly shows that these CP nanospheres can be used effectively for cholesterol removal from human plasma.

3.8 Selectivity Experiments

Selectivity experiments were performed with using estrone, estradiol, progesterone, and testosterone to determine specifity of cholesterol imprinted polymeric nanospheres. Adsorption of cholesterol and its analogues was performed as cholesterol-estrone, cholesterol-estradiol, cholesterol-progesteron, cholesterol-testosteron pairs at the same concentration. Adsorption capacities of CP, C3P, CP3 and NIP for cholesterol and its analogues in methanol were given in Figure 3.22.

As seen in Figure 3.22, imprinted polymeric nanospheres adsorbed higher cholesterol than its analogues. Imprinted polymeric nanospheres adsorbed only progesterone as the similar amount with cholesterol. It may be due to so similar molecule structure and polarity. Non-imprinted polymeric nanospheres adsorbed testosterone and progesterone more than cholesterol. This can be explained by the hydrophobic interactions between NIP and these molecules.

K_d values were calculated from results in methanol media and used to calculate selectivity coefficient (k). Relative selectivities (k') were calculated using selectivity coefficients of MIP and NIP. These values were given in Table 3.6.

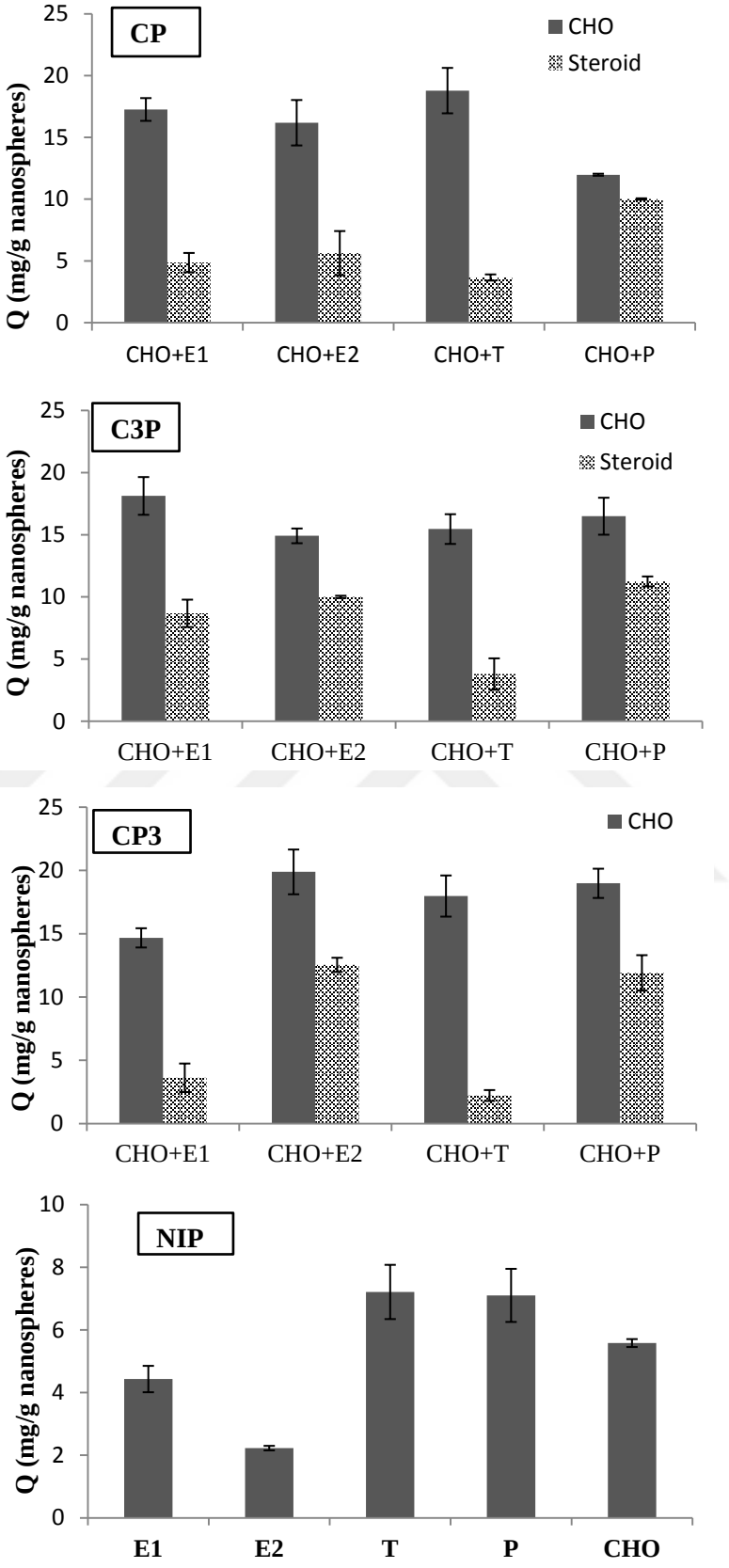

Figure 3.22 Adsorption capacities of CP,C3P, CP3 and NIP for cholesterol and its analogues

Table 3.6 Selectivity coefficients and relative selectivities for imprinted polymeric nanospheres in methanol

MeOH	k= K_d(CHO)/K_d(x)			k'= k (MIP)/k(NIP)
	CP	C3P	CP3	
CHO-E1	4.89	2.65	5.13	3.84
CHO-E2	3.86	1.68	1.91	1.44
CHO-T	7.63	5.31	11.73	10.47
CHO-P	1.26	1.67	1.95	1.69

All selectivity coefficients values in Table 3.6 are biger than 1. can be examined like that cholesterol was adsorbed selectively onto cholesterol imprinted polymeric nanospheres compared to its analogues. Relative selectivity coefficient is higher than 1; thus MIP adsorbed very selectively cholesterol compared to its analogues as far as NIP.

Selectivity experiments were also carried out in GIMS. Adsorption capacities of CP for cholesterol and its analogues were given in Figure 3.23.

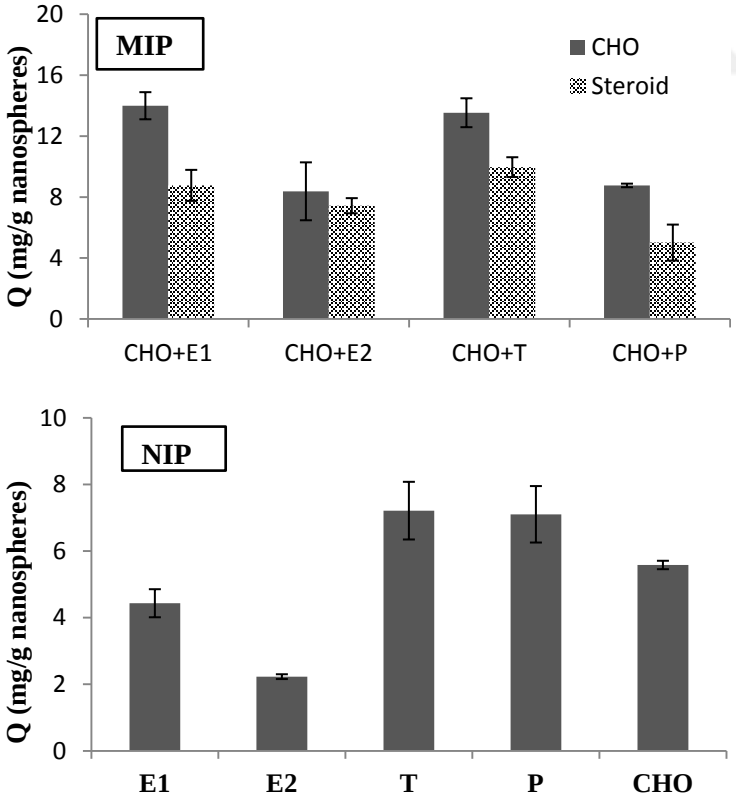

Figure 3.23 Adsorption capacities of CP for cholesterol and its analogues in GIMS

Selectivity coefficients and relative selectivities for CP nanospheres were given in Table 3.7.

Table 3.7 Selectivity coefficients and relative selectivities for CP nanospheres in GIMS

GIMS	$k= K_d(CHO)/K_d(x)$	$k'= k (MIP)/k(NIP)$
CHO-E1	1.83	0.87
CHO-E2	1.15	1.66
CHO-T	1.49	1.79
CHO-P	1.91	0.90

The values in Table 3.7 can be examined like that cholesterol is adsorbed selectively in comparison with all cholesterol analogues. Relative selectivity values are higher than for 1 for estradiol and testosterone. This demonstrates that cholesterol imprinted polymeric nanospheres adsorbs cholesterol selectively compared to estradiol and testosterone as far as non-imprinted polymeric nanospheres.

CHAPTER FOUR
CONCLUSIONS

Cholesterol is one of the most important physiological biomolecules and used in the synthesis of membranes, bile salts, steroids and vitamin D. Hypercholesterolemia, high cholesterol, occurs when cholesterol is present more than the requirement. Familial hypercholesterolemia is a well-established modifiable cardiovascular risk factor and its treatment is an essential aim in preventing cardiovascular disease. There are several methods therapeutically and extracorporeally applied for the treatment of familial hypercholesterolemia.

Molecular imprinting technology provides favored affinity to the target molecule than the other molecules when compared to other polymerization techniques. This property is the essential driving force for the applications of this technique. Biomolecules have been imprinted in different-sized polymers by using several polymerization methods. Molecularly imprinted nanopolymers combine the selective binding advantage of MIPs and high surface area advantage of nanostructures.

In this study, cholesterol imprinted polymeric nanospheres were prepared with surfactant free emulsion polymerization of HEMA. Specific surface areas of nanospheres with almost 120 nm average particle size were calculated as high as 450-550 m^2/g. Cholesterol imprinted polymeric nanospheres were synthesized with 1:1, 1:3, and 3:1 monomer:template ratios for comparison of adsorption capacities. Adsorption capacity of CP nanospheres is 1.20 and 1.16-fold of C3P and CP3 nanospheres, respectively. This result can be concluded that monomer:template ratio 1:1 is more convenient for cholesterol imprinting. These nanospheres with monomer:template ratio 1:1 were used for the optimization of cholesterol adsorption. Optimization studies showed that adsorption was completed in a short time as 30 minutes. It was detected that polymer amounts above 1 mg did not change adsorption capacity statistically.

Maximum cholesterol adsorption was determined as high as 714.17 mg/g at 2500 ppm cholesterol concentration. It was detected that CP nanospheres adsorbed notably higher cholesterol than the MIPs used in the studies in the literature. Adsorption capacities of several cholesterol imprinted polymers were summarized in Table 4.1.

Table 4.1 Summary for adsorption capacities of cholesterol imprinted polymers

Monomer or Polymer	**Q (mg/g)**	**Medium**	**Reference**
Cyclodextrin (CD)/toluene diisocyanate (TDI)	0.70	H_2O/THF	Asanuma et al., 1997
CD-coupled hydoxyethyl methacrylate (HEMA)	46.8	MeOH	Sreenivasan, 1998
p(GMA*-MAT) embedded p(HEMA) cryogel	42.7	GIMS**	Çaktü et al., 2014
Cholesteryl 2-HEMA carbonate	112	Hexane	Wang et al., 2005
HEMA and N-Vinyl Pyrrolidone (NVP)	6.25 & 9.36	MeOH	Sreenivasan, 1997
(Cholesteryl propylcarbamate)triexhoxysilane	2.03	95 % MeOH	Hsu and Yang, 2008
Cholestryl acrylate/Acryloyl-6-amino-6-deoxy-γ-CD	19.33	2-PrOH	Zhong et al., 2001
Acrylic acid	2.98	Dichloromethane	Sreenivasan, 2001
Methacrylic acid (MAA)	17.0	GIMS	Sellergen et al., 1998
B-CD-silica powder	76.5	95 % EtOH	Soares et al., 2007
Methylmethacrylate-*co*-acrylic acid based membrane	115.4/57.0	Buffer/EtOH	Ciardelli Et al., 2006
HEMA/*N*-Methacryloyl-(L)-tyrosine (MAT)	16.23/8	MeOH/GIMS	Yavuz et al., 2007
Methymethacrylate/EGDMA***	7.35	Isohexane	Perez et al., 2000
EGDMA/monocholesteryl itaconate glycerol methacrylate	43.7	GIMS	Gore et al., 2004
(MAA)/tetraethoxysilane (TEOS) (6:1 and 1:5)	214.8 & 166.4	Chloroform	Clausen et al., 2014
HEMA/ *N*-Methacryloyl-(L)-phenylalanine (MAPA)	714.17	MeOH	This work

*GMA: Glycidyl methacrylate, **GIMS: Gastrointestinal Mimicking Solution, ***EGDMA: Ethylene glycol dimethacrylate

Adsorbed cholesterol onto imprinted polymeric nanospheres desorbed with methanol:acetic acid (80:20) mixture with a desorption ratio of 86.14. Desorbed nanospheres were regenerated with several washings and used in re-use experiments. It was determined that adsorption capacity of CP nanospheres was decreased at 21.95 % at the end of the five adsorption-desorption cycle. This result show that imprinted nanospheres can be used more than one, effectively. Thus, cholesterol adsorption studies can be performed with lower cost.

Cholesterol adsorption studies were performed from GIMS and human plasma. Cholesterol adsorption capacity of imprinted polymeric nanospheres in GIMS is the half of the adsorption capacity in methanol. Results from GIMS studies and effect of salt promote different interactions in different media. Plasma cholesterol adsorption studies were performed with 5 time dilution with methanol. Cholesterol removal percentages of CP nanospheres were determined approximately 95 % from healthy

and hypercholesterolemic plasma, respectively. These results are promising for the trial use of cholesterol imprinted polymeric nanospheres for the treatment studies of hypercholesterolemia.

Selectivity experiments were performed with steroids derivated from cholesterol in methanol and GIMS. Selectivity coefficient and relative selectivity were calculated to determine the specifity of imprinted nanospheres. Imprinted polymeric nanospheres adsorbed cholesterol more than its sterol derivates while non-imprinted nanospheres adsorbed testosterone and progesterone more than cholesterol in methanol. This result showed that cholesterol and its derivates interact from different regions with NIP and MIP. All relative selectivity coefficients were higher than 1 for methanol; thus MIP adsorbed very selectively cholesterol in methanol compared to its analogues as far as NIP. Selectivity coefficients were higher than 1 for estron, progesterone and testosterone in GIMS. Relative selectivity values were higher than 1 for estradiol and progesterone in GIMS. As a result, cholesterol imprinting process was successfully performed and imprinted nanospheres adsorbed cholesterol selectively compare to its derivates in methanol and GIMS.

REFERENCES

Aghaeia, A., Hosseini, M.R.M., & Najafi, M. (2010). A novel capacitive biosensor for cholesterol assay that uses an electropolymerized molecularly imprinted polymer. *Electrochimica Acta, 55,* 1503–1508.

Akgöl, S., Öztürk, N., & Denizli A. (2009). New generation polymeric nanospheres for lysozyme adsorption. *Journal of Applied Polymer Science, 115,* 1608–1615.

Alexander, C., Andersson, H.S., Andersson, L.I., Ansell, R.J., Kirsch, N., Nicholls, I.A., O'Mahony, J., & Whitcombe, M.J. (2006). Molecular imprinting science and technology: a survey of the literature for the years up to and including 2003. *Journal of Molecular Recognition, 19,* 106–180.

Altınışık, A., Gür, E., & Seki, Y. (2010). A natural sorbent, Luffa cylindrica for the removal of a model basic dye. *Journal of Hazardous Materials, 179,* 658–664.

Andersson, H.S., Koch-Schmidt, A.C., Ohlson, A., & Mosbach, K. (1996). Study of the nature of recognition in molecularly imprinted polymers. *Journal of Molecular Recognition, 9,* 675-682.

Andersson, L.A., O'Shannessy, D.J., & Mosbach, K. (1990). Molecular recognition in synthetic polymers: preparation of chiral stationary phases by molecular imprinting of amino acid amides. *Journal of Chromatography A, 513,* 167–169.

Andersson, L.I. (2000). Molecular imprinting for drug bioanalysis: A review on the application of imprinted polymers to solid-phase extraction and binding assay. *Journal of Chromatography B, 739,* 163–173.

Andersson, L.I., Paprica, A., & Arvidsson, T. (1997). A highly selective solid phase extraction sorbent for pre-concentration of sameridine made by molecular imprinting. *Chromatographia, 46,* 57-62.

Asanuma, H., Kakazu, M., Shibata, M., Hishiya, T., & Komiyama, M, (1997). Molecularly imprinted polymer of b-cyclodextrin for the efficient recognition of cholesterol. *Chemical Communications, 20*, 1971-1972.

Asanuma, H., Kakazu, M., Shibata, M., Hishiya, T., & Komiyama, M. (1998). Synthesis of molecularly imprinted polymers of β-cyclodextrin for the efficient recognition of cholesterol. *Supramolecular Science, 5*, 417–421.

Bangs, L.B. (1987). *Uniform latex particles*, (3th ed.). Indianapolis: Seragen Diagnostics Inc.

Berg, J.M., Tymoczko, J.L., Stryer, L., & Gatto G.J. (2011). Lipids and cell membranes. In A.P. Radislav, M.M. Vladimir, (Ed.), *Biochemistry* (7th ed.) (345-370). New York: W. H. Freeman and Company.

Berg, J.M., Tymoczko, J.L., Stryer, L., & Gatto G.J. (2011). The Synthesis of Membrane Lipids and Steroids. In A.P. Radislav, M.M. Vladimir, (Ed.), *Biochemistry* (7th ed.) (759-790). New York: W. H. Freeman and Company.

Blessing, F., Wang, Y., Walli, A.K., & Seidel, D. (2004). Heparin-mediated extracorporeal low-density lipoprotein precipitation: rationale for a specific adjuvant therapy in cardiovascular disease. *Transfusion and Apheresis Science, 30*, 255–266.

Boonpangrak, S., Prachayasittikul, V., Bülow, L., & Ye, L. (2006). Molecularly Imprinted Polymer Microspheres Prepared by Precipitation Polymerization Using a Sacrificial Covalent Bond. *Journal of Applied Polymer Science*, *99*, 1390–1398.

Boonpangrak, S., Whitcombe, M.J., Prachayasittikul, V., Mosbach, K., & Ye, L. (2006). Preparation of molecularly imprinted polymers using nitroxide-mediated living radical polymerization. *Biosensors and Bioelectronics*, *22* (3), 349-54.

Bosch, T., Schmidt, B., Kleophas, W., Gillen, C., Otto, V., Passlick-Deetjen, J., & Gurland, H.J. (1997). LDL hemoperfusion-a new procedure for LDL apheresis: first clinical application of an LDL adsorber compatible with human whole blood. *Artificial Organs, 21,* 977-982.

Bossi, A., Bonini, F., Turner, A.P.F., & Piletsky, S.A. (2007). Molecularly imprinted polymers for the recognition of proteins: The state of the art. *Biosensors and Bioelectronics, 22,* 1131–1137.

Barter, P., & Ginsberg, H.N. (2008). Effectiveness of combined statin plus omega-3fatty acid therapy for mixed dyslipidemia. *American Journal of Cardiology, 102,* 1040–1045.

Brautbar, A., & Ballantyne, C.M. (2011). Pharmacological strategies for lowering LDL cholesterol: statins and beyond. *Nature Reviews Cardiology, 8,* 253–265.

Bruchez, M., Moronne, M., Gin, P., Weiss, S., & Alivisatos, A.P. (1998). Semiconductor nanocrystals as fluorescent biological labels. *Science, 281,* 2013-2016.

Builder, S.E. (1993). *Hydrophobic interaction chromatography: principles and methods* (1st ed.). Amersham Pharmacia Biotech: Piscataway NJ.

Bui, B.T.S., & Haupt, K. (2010). Molecularly imprinted polymers: synthetic receptors in bioanalysis. *Analytical and Bioanalytical Chemistry, 398,* 2481-2492.

Cao, Y.C., Jin, R., Nam, J.M., Thaxton, C.S., & Mirkin, C.A. (2003). Raman dye labeled nanoparticle probes for proteins. *Journal of American Chemical Society, 125,* 14676-14677.

Chan, W.C.W., & Nie, S.M. (1998). Quantum dot bioconjugates for ultrasensitive nonisotopic detection. *Science, 281,* 2016-2018.

Chen, L., Xu, S., & Li, J. (2011). Recent advances in molecular imprinting technology: current status, challenges and highlighted applications. *Chemical Society Reviews, 40*, 2922–2942.

Choeng, W.J., Yang, S.H., & Fiaz, A. (2013). Molecular imprinted polymers for separation science: A review of reviews. *Journal of Seperation Science, 36*, 609–628.

Ciardelli G., Borrelli C., Silvestri D., Cristallini C., Barbani N., & Giusti P. (2006). Supported imprinted nanospheres for the selective recognition of cholesterol. *Biosensors and Bioelectronics, 21*, 2329-2338.

Clausen, D.N., Pires, I.M.R., & Tarley, C.R.T. (2014). Improved selective cholesterol adsorption by molecularly imprinted poly(methacrylic acid)/silica (PMAA–SiO2) hybrid material synthesized with different molar ratios. *Materials Science and Engineering C, 44*, 99–108.

Cormark, P.A.G., & Elorza, A.Z. (2004). Molecularly imprinted polymers: synthesis and characterisation. *Journal of Chromatography B, 804*, 173–182.

Çaktü, K., Baydemir, G., Ergün, B., & Yavuz, H. (2014). Cholesterol removal from various samples by cholesterol-imprinted monosize microsphere-embedded cryogels. *Artificial Cells, Nanomedicine, and Biotechnology, 42*, 365–375.

Dickert, F.L., Hayden, O., Lieberzeit, P., Haderspoeck, C., Bindeus, R., & Palfinder, C., et al. (2003). Nano- and micro-structuring of sensor materials—from molecule to cell detection. *Synthetic Metals, 138*, 65-69.

Dickert, F.L., Lieberzeit, P., & Hayden, O. (2003). Sensor strategies for microorganism detection--from physical principles to imprinting procedures. *Analytical and Bioanalytical Chemistry, 377*, 540-549.

Dubinin, M.M., & Radushkevich, L.V. (1947). Equation of the characteristic curve of activated charcoal. *Proceedings of the USSR Academy of Sciences, 55*, 331–333.

Edelstein, R.L., Tamanaha, C.R., Sheehan, P.E., Miller, M.M., Baselt, D.R., & Whitman, L.J., et al. (2000). The BARC biosensor applied to the detection of biological warfare agents. *Biosensors and Bioelectronics, 14*, 805-813.

Eisenhauer, T., Armstrong, V.W., Wieland, H., Fuchs, C., Scheler, F., & Seidel, D. (1987). Selective removal of low density lipoproteins (LDL) by precipitation at low pH; first clinical application of the HELP system. *Klinische Wochenschrift, 65*, 161–168.

Ellwanger, A., Berggren, C., Bayoudh, S., Crecenzi, C., Karlsson, L., & Owens, P.K. et al. (2001). Evaluation of methods aimed at complete removal of template from molecularly imprinted polymers. *Analyst, 126*, 784–792.

Freundlich, H.M.F. (1906). Over the adsorption in solution. *Journal of Physical Chemistry, 57*, 385–470.

Goldstein, J.L., & Brown, M.S. (2009). The LDL receptor. *Arteriosclerosis, Thrombosis, and Vascular Biology, 29* (4), 431–438.

Gore, M.A., Karmalkar, R.N., Kulkarni, M.G. (2004). Enhanced capacities and selectivities for cholesterol in aqueous media by molecular imprinting: role of novel cross-linkers. *Journal of Chromatography B, 804*, 211–221.

Gupta, R., & Kumar, A. (2011). Synthesis and characterization of sol–gel-derived molecular imprinted polymeric materials for cholesterol recognition. *Journal of Sol-Gel Science and Technology, 58*, 182–194.

Guz, A.N., & Rushchitskii, Y. Y. (2003). Nanomaterıals: on the mechanics of nanomaterials. *International Applied Mechanics, 39* (11), 1271-1293.

Haines, T.H. (2001). Do sterols reduce proton and sodium leaks through lipid bilayers. *Progress in Lipid Research, 40* (4), 299–324.

Han, M., Gao, X., Su, J.Z., & Nie, S. (2001). Quantum-dot-tagged microbeads for multiplexed optical coding of biomolecules. *Nature Biotechnology, 19*, 631-635.

Hanukoglu, I. (1992). Steroidogenic enzymes: structure, function, and role in regulation of steroid hormone biosynthesis. *Journal of Steroid Biochemistry and Molecular Biology, 43* (8), 779–804.

Harada-Shiba, M., Arai, H., Oikawa, S., Ohta, T., Okada, T., & Okamura, T., et al. (2012). Guidelines for the management of familial hypercholesterolemia. *Journal of Atherosclerosis Thrombosis, 19* (12), 1043–1060.

Hayden, O., & Dickert, F.L. (2001). Selective Microorganism Detection with Cell Surface Imprinted Polymers. *Advanced Materials, 13*, 1480-1483.

Hayden, O., Bindeus, R., & Dickert, F.L. (2003). Combining atomic force microscope and quarz crystal microbalance studies for cell detection. *Measurement Science and Technology, 14*, 1876-1881.

Ho, Y.S., & McKay, G. (1998). The kinetics of sorption of basic dyes from aqueous solutions by sphagnum moss peat. *The Canadian Journal of Chemical Engineering, 76*, 822–826.

Hsu, C.W., & Yang, M.C. (2008). Enhancement of the imprinting effect in cholesterol-imprinted microporous silica. *Journal of Non-Crystalline Solids, 354*, 4037–4042.

Hwang, C.C., & Lee, W.C. (2002). Chromatographic characteristics of cholestrol-imprinted polymers prepared by covalent and non-covalent imprinting methods. *Journal of Chromatography A, 962*, 69-78.

Incardona, J.P., & Eaton, S. (2000). Cholesterol in signal transduction. *Current Opinion in Cell Biology, 12* (2), 193–203.

Isla, A., Brostow, W., Bujard, B., Estevez, M., Rodriguez, J.R., & Vargas, S., et al. (2003). Nanohybrid scratch resistant coating for teeth and bone viscoelasticity manifested in tribology. *Materials Research Innovations, 7*, 110-114.

Ito, M.K., McGowan, M.P., & Moriarty, P.M. (2011). Management of familial hypercholesterolemias in adult patients: recommendations from the National Lipid Association Expert Panel on familial hypercholesterolemia. *Journal of Clinical Lipidology, 5* (3 Suppl.), S38–45.

Ji, H.S., McNiven, S., Kyong-Hoon, L., Saito, T., Ikebukuro, K., & Karube, I. (2000). Increasing the sensitivity of piezoelectric odour sensors based on molecularly imprinted polymers. *Biosensors and Bioelectronics, 15*, 403-409.

Kandimalla, V.B., & Ju, H. (2004). Molecular imprinting: a dynamic technique for diverse applications in analytical chemistry. *Analytical and Bioanalytical Chemistry, 380*, 587–605.

Kempe, M. (1996). Antibody-Mimicking Polymers as Chiral Stationary Phases in HPLC. *Analytical Chemistry, 68*, 1948–1953.

Kempe, M., & Mosbach, K. (1995). Molecular imprinting used for chiral seperations. *Journal of Chromatography A, 694*, 3–13.

Khachadurian, A.K., & Uthman, S.M. (1973). Experiences with the homozygous cases of familial hypercholesterolemia. A report of 52 patients. *Nutrition Metabolism, 15* (1), 132–40.

Kitahara, K.I., Yoshihama, I., Hanada, T., Kokuba, H., & Arai, S. (2010). Synthesis of monodispersed molecularly imprinted polymer particles for high-performance liquid chromatographic separation of cholesterol using templating polymerization in porous silica gel bound with cholesterol molecules on its surface. *Journal of Chromatography A, 1217*, 7249–7254.

Kröger, S., Turner, A.P.F., Mosbach, K., & Haupt, K. (1999). Imprinted Polymer-Based Sensor System for Herbicides Using Differential-Pulse Voltammetry on Screen-Printed Electrodes. *Analytical Chemistry, 71*, 3698-3702.

Kryscio, D.R., & Peppas, N.A. (2012). Critical review and perspective of macromolecularly imprinted polymers. *Acta Biomaterialia, 8*, 461–473.

Kugimiya, A., Kuwada, Y., & Takeuchi, T. (2001). Preparation of sterol-imprinted polymers with the use of 2-(methacryloyloxy)ethyl phosphate. *Journal of Chromatography A, 938*, 131–135.

Lane, D.M., McConathy, W.J., Laughlin, L.O., Comp, P.C., von Albertini, B., Bricker, L.A., et al. (1995). Selective removal of plasma low-density lipoprotein with the HELP system: biweekly versus weekly therapy. *Atherosclerosis, 114*, 203–211.

Langergren, S., & Svenska, B.K. (1898). Zur theorie der sogenannten adsorption geloester stoffe. *Veternskapsakad Handlingar, 24* (4), 1–39.

Leydecker, S. (2008). What is nanotechnology? In *Nanomaterials in Architecture, Interior Architecture and Design* (1st ed.) (12-19). Basel: Birkhäuser.

Li, J., Xu, S., & Chen, L. (2011). Recent advances in molecular imprinting technology: current status, challenges and highlighted applications. *Chemical Society Reviews, 40*, 2922–2942.

Li, J., Zhang, X., Liu, Y., Tong, H., Xu, Y., & Liu, S. (2013). Preparation of a hollow porous molecularly imprinted polymer using tetrabromobisphenol A as a dummy template and its application as SPE sorbent for determination of bisphenol A in tap water. *Talanta, 117*, 281–287.

Li, X., Li, M., Li, J., Lei, F., Su, X., Liu, M., Li, P., & Tan, X. (2014). Synthesis and characterization of molecularly imprinted polymers with modified rosin as a crosslinker and selective SPE-HPLC detection of basic orange II in foods. *Analytical Methods, 6*, 6397-6406.

Lupien, P-J., Moorjani, S., & Awad, J. (1976). A new approach to the management of familial hypercholesterolaemia: removal of plasma cholesterol based on the principle of affinity chromatography. *The Lancet, 1*, 1261-1265.

Ma, J., Wong, H., Kong, L.B., & Peng, K.W. (2003). Biomimetic processing of nanocrystallite bioactive apatite coating on titanium. *Nanotechnology, 14*, 619-623.

Mabuchi, H., Koizumi, J., Shimizu, M., Kajinami, K., Miyamoto, S., & Ueda, K., et al. (1998). Long-term efficacy of low-density lipoprotein apheresis on coronary heart disease in familial hypercholesterolemia. Hokuriku-FH-LDL-Apheresis Study Group. *American Journal of Cardiology, 82*, 1489–1495.

Mah, C., Zolotukhin, I., Fraites, T.J., Dobson, J., Batich, C., & Byrne, B.J. (2000). Microsphere-mediated delivery of recombinant AAV vectors *in vitro* and *in vivo*. *Molecular Therapy, 1*, S239.

Mahtab, R., Rogers, J.P., & Murphy, C.J. (1995). Protein-sized quantum dot luminescence can distinguish between "straight", "bent", and "kinked" oligonucleotides. *Journal of American Chemical Society, 117*, 9099-9100.

Marks, D., Thorogood, M., Neil, H.A., & Humphries, S.E. (2003). A review on the diagnosis, natural history, and treatment of familial hypercholesterolaemia. *Atherosclerosis,168* (1), 1–14

Martin-Esteban, A. (2001). Molecularly imprinted polymers: new molecular recognition materials for selective solid-phase extraction of organic compounds. *Fresenius Journal of Analytical Chemistry, 370*, 795–802.

Martin-Esteban, A., Turiel, E., & Stevenson, D. (2001). Effect of template size on the selectivity of molecularly imprinted polymers for phenylurea herbicides. *Chromatographia Supplement, 53*, 434-437.

Mayes, A.G., & Whitcombe M.J. (2005). Synthetic strategies for the generation of molecularly imprinted organic polymers. *Advanced Drug Delivery Reviews, 57*, 1742– 1778.

Molday, R.S., & MacKenzie, D. (1982). Immunospecific ferromagnetic iron dextran reagents for the labeling and magnetic separation of cells. *Journal of Immunological Methods, 52*, 353-367.

Mosbach, K., Yu, Y., Andersch, J., & Ye, L. (2001). Generation of new enzyme inhibitors using imprinted binding sites: The anti-idiotypic approach, a step toward the next generation of molecular imprinting. *Journal of American Chemical Society, 123*, 12420–1242.

Nam, J.M., Thaxton, C.C., & Mirkin, C.A. (2003). Nanoparticles-based bio-barcodes for the ultrasensitive detection of proteins. *Science, 301*, 1884-1886.

Navakova, L., Solich, P., Matysova, L., & Sıcha, J. (2004). HPLC determination of estradiol, its degradation product, and preservatives in new topical formulation estrogel HBF. *Analytical and Bioanalytical Chemistry, 379,* 781-787.

Nelson, D.L., & Cox, M.M. (2004). Lipids In *Lehninger Principles of Biochemistry* (4th ed.) (340-368). New York: W. H. Freeman.

Nelson, D.L., & Cox, M.M. (2004). Biosynthesis of Cholesterol, Steroids, and Isoprenoids. In *Lehninger Principles of Biochemistry* (4th ed.) (816-832). New York: W. H. Freeman.

Nicholls, I.A. (1995). Thermodynamic considerations for the design of and ligand recognition by molecularly imprinted polymers. *Chemical Letters,* 1035-1036.

Ozacar, M., & Sengil, I.A. (2005). A kinetic study of metal complex dye sorption onto pine sawdust. *Process Biochemistry, 40,* 565–572.

Page, M.M., Bell, D.A., Hooper, A.J., Watts, G.F., & Burnett, J.R. (2014). Lipoprotein apheresis and new therapies for severe familial hypercholesterolemia in adults and children. *Best Practice & Research Clinical Endocrinology & Metabolism, 28,* 387–403.

Panatarotto, D., Prtidos, C.D., Hoebeke, J., Brown, F., Kramer, E., & Briand, J.P., et al. (2003). Immunization with peptide-functionalized carbon nanotubes enhances virus-specific neutralizing antibody responses. *Chemistry & Biology, 10,* 961-966.

Pankhurst, Q.A., Connolly, J., Jones, S.K., & Dobson, J. (2003). Applications of magnetic nanoparticles in biomedicine. *Journal of Physics D: Applied Physsics, 36,* R167-R181.

Parak, W.J., Boudreau, R., Gros, M.L., Gerion, D., Zanchet, D., & Micheel, C.M., et al. (2002). Cell motility and metastatic potential studies based on quantum dot imaging of phagokinetic tracks. *Advanced Materials, 14*, 882-885.

Parak, W.J., Gerion, D., Pellegrino, T., Zanchet, D., Micheel, C., & Williams, C.S., et al. (2003). Biological applications of colloidal nanocrystals. *Nanotechnology, 14*, R15-R27.

Pawlina, W., & Ross, M.W. (2005). *Histology: A Text and Atlas: With Correlated Cell and Molecular Biology* (5th ad.). Philadelphia: Lippincott Wiliams & Wilkins.

Perez-Moral, N., & Mayes, A.G. (2002). Novel MIP formats. *Bioseparation, 10*, 287–299.

Perez, N., Whitcombe, M.J., & Vulfson, E.N. (2000). Molecularly imprinted nanoparticles prepared by core-shell emulsion polymerization. *Journal of Applied Polymer Science, 77*, 1851-1859.

Piletsky, S. A., Piletskaya, E. V., Sergeeva, T. A., & Panasyuk, T. L. (1999). Molecularly imprinted self-assembled films with specificity to cholesterol. *Sensors Actuators B, 60*, 216-??.

Piletsky, S.A., Piletska, E.V., Bossi, A., Karim, K., Lowe, P., & Turner, A.P.F. (2001). Subsitutation of antibodies and receptors with molecular imprinted polymers in enzyme-linked and fluorescent assays. *Biosensors and Bioelectronics, 16*, 701–707.

Poma, A., Turner, A.P.F., & Piletsky, S.A. (2010). Advances in the manufacture of MIP nanoparticles. *Trends in Biotechnology, 28* (12), 629-637.

Prasad, B.B., Srivastava, S., Tiwari, K., & Sharma, K.S. (2009). Trace-level sensing of dopamine in real samples using molecularly imprinted polymer-sensor. *Biochemical Engineering Journal, 44*, 232–239.

Raal, F.J., & Santos, R.D. (2012). Homozygous familial hypercholesterolemia: current perspectives on diagnosis and treatment. *Atherosclerosis, 223* (2), 262–268.

Rachkov, A. & Minoura, N. (2000). Recognition of oxytocin and oxytocin-related peptides in aqueous media using a molecularly imprinted polymer synthesized by the epitope approach. *Journal of Chromatography A, 889* (1-2), 111–118.

Rachkov, A., & Minoura, N. (2001). Towards molecularly imprinted polymers selective to peptides and proteins. The epitope approach. *Biochimica et Biophysica Acta, 1544* (1/2), 255–266.

Reich, D.H., Tanase, M., Hultgren, A., Bauer, L.A., Chen, C.S., & Meyer, G.J. (2003). Biological applications of multifunctional magnetic nanowires. *Journal of Applied Physics, 93*, 7275-7280.

Remcho, V.T., & Tan, Z.J. (1999). MIPs as chromatographic stationary phases for molecular recognition. *Analytical Chemistry, 71*, A248–A255.

Richter, W.O., Jacob, B.G., Ritter, M.M., Sühler, K., Vierneisel, K., & Schwandt, P. (1993). Three-year treatment of familial heterozygous hypercholesterolemia by extracorporeal low-density lipoprotein immunoadsorption with polyclonal apolipoprotein B antibodies. *Metabolism, 42*, 888-894.

Ruckert, B., Hall, A.J., & Sellergren, B. (2002). Molecularly imprinted composite materials via iniferter modified supports. *Journal of Material Chemistry, 12*, 2275-2280.

Sadava, D., Hillis, D.M., Heller, H.C., & Berenbaum, M.R. (2011). *Life: the science of biology* (9th ed.). San Francisco: Freeman.

Salata, O.V. (2004). Applications of nanoparticles in biology and medicine. *Journal of Nanobiotechnology, 2:3*, 1-6.

Sánchez-Machado, D.I., López-Hernández, J., Paseiro-Losada, P., & López-Cervantes, J. (2004). An HPLC method for the quantification of sterols in edible seaweeds. *Journal of Biomedical Engineering, 18* (3), 183 – 190.

Say, R., Emir, S., Garipcan, B., Patır, S., & Denizli, A. (2003). Novel Methacryloylamidophenylalanine functionalized porous chelating beads for adsorption of heavy metal ions. *Advances in Polymer Technology, 22* (4), 355–364.

Say, R., Gültekin, A., Özcan, A.A., Denizli, A., & Ersöz, A. (2009). Preparation of new molecularly imprinted quartz crystal microbalance hybride sensor system for 8-hydroxy-2'-deoxyguanosine determination. *Analytica Chimica Acta, 640*, 82–86.

Schmaldienst, S., Banyai, S., Stulnig, T.M., Heinz, G., Jansen, M., & Hörl, W.H., et al. (2000). Prospective randomised cross-over comparison of three LDL-apheresis systems in statin pretreated patients with familial hypercholesterolaemia. *Atherosclerosis, 151*, 493-499.

Schweitz, L., Andersson, L.I., & Nilsson, S. (1998). Molecular imprint-based stationary phases for capillary electrochromatography. *Journal of Chromatography A, 817*, 5–13.

Sellergen, B. (2003). A historical perspective of the development of molecular imprinting. In *Molecularly Imprinted Polymers: Man-made mimics of antibodies*

and their applications in analytical chemistry (Sellergren B. ed.) (1-19). Amsterdam: Elsevier.

Sellergren, B., Ruckert, B., & Hall, A.J. (2002). Layer-by-layer grafting of molecularly imprinted polymers via iniferter modified supports. *Advanced Materials, 14*, 1204-1208.

Sellergren, B., Schillinger, E., & Lanza, F. (2009). Experimental combinatorial methods. R.A. Potyrallo, V.M. Mirsky, (Ed.) C*ombinatorial methods for chemical and biological sensors* (1st ed.) (173-198). New York: Integrated Analytical Systems.

Sellergren, B., Wieschemeyer, J., Boos, K.S., & Seidel, D. (1998). Imprinted polymers for selective adsorption of cholesterol from gastrointestinal fluids. *Chemical Materials, 10*, 4037-4046.

Sinani, V.A., Koktysh, D.S., Yun, B.G., Matts, R.L., Pappas, T.C., & Motamedi, M., et al. (2003). Collagen coating promotes biocompatibility of semiconductor nanoparticles in stratified LBL films. *Nano Letters*, *3*, 1177-1182.

Smith, J.M. (1981). *Chemical engineering kinetics* (3th ed.), New York: McGraw-Hill.

Soares, C.M.F., Zanin, G.M., Moraes, F.F., Santos, O.A.A., Castro, H.F. (2007). Molecular imprinting of *b*-cyclodextrin/cholesterol template into a silica polymer for cholesterol separation. *Journal of Inclusion Phenomena and Macrocyclic Chemistry*, *57*, 79–82.

Soutar, A.K., & Naoumova, R.P. (2007). Mechanisms of disease: genetic causes of familial hypercholesterolemia. *Nature Clinical Practice Cardiovascular Medicine*, *4* (4), 214–225.

Spivak, D.A. (2005). Optimization, evaluation, and characterization of molecularly imprinted polymers. *Advanced Drug Delivery Reviews, 57*, 1779– 1794.

Sreenivasan K. (1997). Imparting cholesterol recognition sites in radiation polymerised poly(2-hydroxyethyl methacrylate) by molecular imprinting. *Polymer International, 42*, 189-172.

Sreenivasan, K. (1998). Synthesis and evaluation of a beta cyclodextrin-based molecularly imprinted copolymer. *Journal of Applied Polymer Science, 70*, 15-18.

Sreenivasan, K. (2001). Molecularly imprinted polyacrylic acid containing multiple recognition sites for steroids. *Journal of Applied Polymer Science, 82*, 889-893.

Sreenivasan, K. (2006). Surface imprinted polyurethane film as a chiral discriminator. *Talanta, 68*, 1037–1039.

Stoffel, W., Borberg, H., & Greve, V. (1981). Application of specific extracorporeal removal of low density lipoprotein in familial hypercholesterolaemia. *The Lancet, 2*, 1005–1007.

Tamayo, F.G., Turiel, E., & Martin-Esteban, A. (2007). Molecularly imprinted polymers for solid-phase extraction and solid-phase microextraction: recent developments and future trends. *Journal of Chromatography A, 1152*, 32–40.

Temkin, M.T., & Pyzhev, V. (1940). Kinetics of ammonia synthesis on promoted iron catalyst. *Acta Physiochimica URSS, 12*, 327–356.

Thompsen, J., & Thompson, P.D. (2006). Systematic review of LDL apheresis in the treatment of cardiovascular disease. *Atherosclerosis, 189*, 31–38.

Thompson, G.R. (2003). LDL apheresis. *Atherosclerosis, 167*, 1-13.

Thompson, G.R. (2008). Recommendations for the use of LDL apheresis. *Atherosclerosis, 198*, 247–255.

Thompson, G.R., Lowenthal, R., & Myant, R. (1975). Plasma exchange in the management of homozygous familial hypercholesterolaemia. *The Lancet, 1*,1208-1211.

Tiwari, V., & Khokhar, M. (2014). Mechanism of action of anti-hypercholesterolemia drugs and their resistance. *European JournalofPharmacology*, *741*, 156–170.

Tong, Y., Guan, H., Wang, S., Xu, J., & He, C. (2011). Syntheses of chitin-based imprinting polymers and their binding properties for cholesterol. *Carbohydrate Research, 346*, 495–500.

Trinder, P., & Webster, D. (1984). Determination of HDL-cholesterol using 2,4,6-tribromo-3-hydroxybenzoic acid with a commercial CHOD-PAP reagent. *Annals of Clinical Biochemistry, 21*, 1430-1433.

Tseng, R.L. (2006). Mesopore control of high surface area NaOH-activated carbon. *Journal of Colloid Interface Science, 303*, 494–502.

Usifo, E., Leigh, S.E., Whittall, R.A., Lench, N., Taylor, A., & Yeats, C., et al. (2012). Low-density lipoprotein receptor gene familial hypercholesterolemia variant database: update and pathological assessment. *Annals of Human Genetics, 76* (5), 387–401.

Verheyen, E., Schillemans, J.P., Wijk, M., Demeniex, M.A., Hennink, W.E., & Nostrum C.F. (2011). Challenges for the effective molecular imprinting of proteins. *Biomaterials, 32*, 3008-3020.

Wang, S., Mamedova, N., Kotov, N.A., Chen, W., & Studer, J. (2002). Antigen/antibody immunocomplex from CdTe nanoparticle bioconjugates. *Nano Letters, 2*, 817-822.

Wang, S., Xu, J., Tong, Y., Wang, L., & He, C. (2005). Cholesterol-imprinted polymer receptor prepared by a hybrid imprinting method. *Polymer International, 54*, 1268–1274.

Watts, G.F., Sullivan, D.R., Poplawski, N., van Bockxmeer, F., Hamilton-Craig, I., & Clifton, P.M., et al. (2011). Familial hypercholesterolaemia: a model of care for Australasia. *Atherosclerosis Supplements, 12* (2), 221–263.

Weber, T.W., & Chakkravorti, R.K. (1974). Pore and solid diffusion models for fixed-bed adsorbers. *American lnstitute of Chemical Engineers, 20*, 228–238.

Weber, W.J., & Morris, J.C. (1962). Advances in water pollution research: Removal of biologically-resistant pollutants from waste waters by adsorption. In *Proceedings of Second International Conference on Water Pollution Symposium* (1st ed.) (231-266) Oxford: Pergamon Press.

Weissleder, R., Elizondo, G., Wittenburg, J., Rabito, C.A., Bengele, H.H., & Josephson, L. (1990). Ultrasmall superparamagnetic iron oxide: characterization of a new class of contrast agents for MR imaging. *Radiology, 175*, 489-493.

Whitcombe, M.J., Rodriguez, M.E., Villar, P., & Vulfson E.N. (1995). A New Method for the Introduction of Recognition Site Functionality into Polymers Prepared by Molecular Imprinting: Synthesis and Characterization of Polymeric Receptors for Cholesterol. *Journal American Chemical Society, 117*, 7105-7111.

Whitesides, G.M. (2003). The 'right' size in Nanobiotechnology. *Nature Biotechnology, 21*, 1161-1165.

Wulff, G., & Akelah, A. (1978). Enzyme-analogue built polymers, 6) Synthesis of 5-vinylsalicaldehyde and a simplified synthesis of some divinyl derivatives. *Makromolecular Chemistry, 179*, 2647–2651.

Wulff, G., Kemmerer, R., Vietmeier, J., & Poll, H.G. (1982). Chirality of vinyl-polymers-the preparation of chiral cavities in synthetic-polymers. *New Journal of Chemistry, 6*, 681–687.

Wulff, G., Vietmeier, J., & Poll, H.G. (1987). Enzyme-analog built polymers-22: influence of the nature of the cross-linking agent on the performance of imprinted polymers in racemic-resolution. *Macromolecular Chemistry, 188*, 731–740.

Yan, H., & Row, K.H. (2006). Characteristic and synthetic approach of molecularly imprinted polymer. *International Journal of Molecular Science, 7,* 155-178.

Yavuz, H., Karakoç¸ V., Türkmen, V., Say, R., & Denizli, A. (2007). Synthesis of cholesterol imprinted polymeric particles. *International Journal of Biological Macromolecules, 41*, 8–15.

Yeagle, P.L. (1991). Modulation of membrane function by cholesterol. *Biochimie, 73* (10), 1303–1310.

Yilmaz, E., Mosbach, K., & Haupt, K. (1999). Influence of functional and cross-linking monomers and the amount of template on the performance of molecularly imprinted polymers in binding assays. *Analytical Communications, 36*, 167–170.

Yoshida, J., & Kobayashi, T. (1999). Intracellular hyperthermia for cancer using magnetite cationic liposomes. *Journal of Magnetism and Magnetic Materials*, 194, 176-184.

Zhang T., Liu F., Chen W., Wang J., & Li K. (2001). Influence of intramolecular hydrogen bond of templates on molecular recognition of molecularly imprinted polymers. *Analytica Chimica Acta, 450*, 53–61.

Zhang, Y., Kohler, N., & Zhang, M. (2002). Surface modification of superparamagnetic magnetite nanoparticles and their intracellular uptake. *Biomaterials, 23*, 1553-1561.

Zhong, N., Byun, H.S., & Bittman, R. (2001). Hydrophilic cholesterol-binding molecular imprinted polymers. *Teterahedron Letters, 42*, 1839-1841.

Zhu, L., & Xu, X. (2003). Selective separation of active inhibitors of epidermal growth factor receptor from Caragana Jubata by molecularly imprinted solid-phase extraction. *Journal Chromatography A, 991*, 151-158.

Zhu, L., Chen, L., & Xu, X. (2003). Application of a molecularly imprinted polymer for the effective recognition of different anti-epidermal growth factor receptor inhibitors. *Analytical Chemistry, 75*, 6381–6387.

Zlatkis, A., Zak B., & Boyle, A.J. (1953). A new method for the direct determination of serum cholesterol. *Journal of Laboratory Clinical Medicine, 41* (3), 486–492.